Interactions of the cannabinoid CB1 and dopamine D2 receptors

Morag Rose Hunter

A thesis submitted in fulfilment of the requirements for the degree of Doctor of Philosophy in Pharmacology, the University of Auckland, 2015.

Abstract

The effects of cannabinoids in the nervous system are predominantly mediated by cannabinoid receptor 1 (CB1), a G protein-coupled receptor (GPCR). GPCRs are known to form homodimeric and heterodimeric structures, which affect the signalling and regulation of each constituent receptor. CB1 has been shown to have functional interactions with the dopamine D2 receptor (D2). This thesis explores the structure, regulation and function of the CB1-D2 heterodimer.

A bioluminescence resonance energy transfer (BRET) assay was utilised to detect constitutive CB1-D2 heterodimer, which was not detectibly altered by receptor agonists. BRET was also utilised to test a proposed heterodimer interface containing four key residues on transmembrane helix 1 of each receptor, however mutation of these residues did not significantly disrupt detection of heterodimer.

Previous studies on GPCR heterodimers have suggested that interactions may occur throughout the protein synthesis and ligand-mediated trafficking pathways. Immunocytochemistry-based receptor trafficking and expression assays were used to determine whether CB1 and D2 interact in their regulation. Subtle differences were found in CB1 agonist-driven internalisation in the presence of a D2 agonist. Co-expression of CB1 and a flag-tagged D2 resulted in changes to flag-D2 processing, perhaps by the addition of a post-translational modification, although it is not clear if this is solely a modification of the flag-tag.

When activated concurrently, CB1 and D2 have been shown to “switch” signalling phenotype from Gαi-like to Gαs-like activity, resulting in accumulation of cAMP. When this signalling interaction was first observed by Glass *et al*. (1997), it was hypothesised that this may be a result of the receptors competing for a limited pool of Gαi proteins. If this were the case, this mechanism would also be in effect when CB1 was expressed alone. In order to test this, a mixed population of cells was created and sorted by flow cytometry on the basis of CB1 surface expression. cAMP assays performed on these cells showed that cells with low to moderate expression of CB1 inhibit cAMP production, while cells with high CB1 expression increase cAMP accumulation.

In conclusion, while it is likely that CB1 and D2 form a constitutive heterodimer, this does not affect ligand-mediated receptor trafficking. CB1 expression does, however, change the synthesis and processing of flag-tagged D2 in a manner that has yet to be determined. Since CB1 expression alone is sufficient to change the predominant cAMP phenotype to Gαs, presumably by competition of G proteins, this work suggests that CB1-D2 heterodimerisation may function simply to increase the local competition for G proteins, rather than the dimer itself mediating the functional signalling switch.

Acknowledgements

The work described in this thesis would not have been possible without the following contributions:

First, I would like to thank my supervisors: Associate Professor Michelle Glass, for her excellent supervision and support throughout this project, as well as her unwavering optimism, that has driven this project through countless challenges. Also Dr Natasha Grimsey, for leading by example with her meticulous nature and perceptive insight into both the specific and general aspects of her work.

Next, I would like to thank the past and present members of the Receptor Signalling Laboratory for sharing their ideas and technical skills. This group has provided steadfast support and friendship, and I really appreciate the fantastic team dynamic. In particular I'd like to thank Dr Erin Cawston, for her constant encouragement, and David Finlay for our constructive discussions and his wise insights. For their technical assistance and camaraderie, I wish to thank Christa Macdonald and Davanea Forbes.

Beyond the Lab, I'd like to thank Stephen Edgar for his extensive technical assistance in flow cytometry experiments, the majority of which were ultimately not included in this thesis. And my extended scientific support network: particularly Sheryl Tan, Duneeshya Gunasekara, Dr Emma Scotter, and Dr Scott Graham. I really appreciate you all sharing your knowledge and experience.

The research for this thesis has benefitted from contributions of many people. Within the Receptor Signalling Laboratory, Dr Natasha Grimsey made the majority of the plasmids and cell lines for use throughout this project, David Finlay also developed a cell line and provided preliminary data, and Aanchal Bakshi (nee Sharma) developed several BRET constructs used in this project. I'd also like to thank Professor Patti Reggio (University of North Carolina, Greensboro) for providing the homology model of the CB1-D2 heterodimer.

I gratefully acknowledge the Marsden Fund of New Zealand for funding this research.

And lastly, I'd like to thank my parents, extended family and friends for their continued support and patience. And of course Ben, for thought-provoking discussions, and providing abundant practical and moral support.

Table of Contents

List of figures

List of tables

Abbreviations

ANOVA, analysis of variance

AU, arbitrary units

BiFC, bimolecular fluorescence complementation

Bmax, maximal occupancy

BRET, bioluminescence resonance energy transfer

BSA, bovine serum albumin

cAMP, cyclic adenosine monophosphate

CAMYEL, cAMP sensor using YFP-Epac-Rluc

CB1, cannabinoid receptor 1

CB2, cannabinoid receptor 2

D2, dopamine receptor 2

DMEM, Dulbecco's modified Eagle medium

EC50, half maximal effective concentration

EL, extracellular loop

Emax, maximum effect

ERK, extracellular signal-regulated kinases

FBS, foetal bovine serum

FRET, Förster/fluorescence resonance energy transfer

FUEL, fluorescence by unbound excitation from luminescence

GFP, green fluorescent protein

GPCR, G protein-coupled receptor

GRK, G protein-coupled receptor kinase

HA, haemagglutinin

HBSS, Hank's balanced salt solution

HEK, human embryonic kidney

IL, intracellular loop

JNK, Jun amino-terminal kinases

MAPK, mitogen-activated protein kinase

ns, not significant

PACAP, pituitary adenylate cyclase-activating polypeptide

PBS, phosphate buffer saline

PCR, polymerase chain reaction

PDE, phosphodiesterase

PFA, paraformaldehyde

PKA, protein kinase A

PPLSS, preprolactin signal sequence

RET, resonance energy transfer

Rluc, Renilla luciferase

Rluc8, Renilla luciferase variant

SEM, standard error of the mean

THC, Δ9-tetrahydrocannabinol

TM, transmembrane region

V8-CAMYEL, Venus-Rluc8 variant of CAMYEL

wt, wildtype

YFP, yellow fluorescent protein

1. Introduction

The psychoactive properties of cannabis have been known for thousands of years. Since the identification of the active compound in cannabis (Gaoni *et al.*, 1964), the endocannabinoid system has been investigated extensively, and research has accelerated rapidly upon the identification of the specific proteins which mediate these effects (Matsuda *et al.*, 1990; Munro *et al.*, 1993). Compounds which modulate the endocannabinoid system fall into three overarching categories: the endogenously-present endocannabinoids; the plant-derived phytocannabinoids; and the synthetic cannabinoids. The latter two are used as recreational drugs, however, both agonists and antagonists also have demonstrable therapeutic applications.

The effects of cannabinoid ligands are mediated through at least two G protein coupled receptors (GPCRs). Cannabinoid receptor 1 (CB1) is most abundant in the central nervous system (Howlett *et al.*, 2004), although it is also expressed in the gastrointestinal tract (Croci *et al.*, 1998; Massa *et al.*, 2005), adipose tissue (Bensaid *et al.*, 2003; Gary-Bobo *et al.*, 2006), male and female reproductive systems (Gye *et al.*, 2005; Horne *et al.*, 2008; Park *et al.*, 2003; Ruiz-Llorente *et al.*, 2003), and the cardiovascular system (Szabo *et al.*, 2001; Wagner *et al.*, 2001). Cannabinoid receptor 2 (CB2) is found predominantly in cells of the immune system, including lymphocytes, monocytes, and microglia (Howlett *et al.*, 2004; Klein *et al.*, 2003). Furthermore, there is evidence for at least one more cannabinoid receptor, as the known actions of CB1 and CB2 are not sufficient to explain the full range of effects cannabinoids have been observed as having *in vivo* (Pertwee *et al.*, 2010). Candidate receptors for “CB3” include GPR18 and GPR55 (Pertwee *et al.*, 2010), but there is currently insufficient evidence to reclassify these GPCRs as cannabinoid receptors.

Both CB1 and CB2 have many reported functional interactions with other GPCRs, which could be exploited for therapeutic advantage. One such interaction is between CB1 and the dopamine D2 receptor, which are co-expressed in the medium spiny neurons of the striatum. This review will first cover the general features of GPCRs, before focusing on the nature of the CB1-D2 interaction.

GPCR signalling

General structure of GPCRs

G protein-coupled receptors (GPCRs) are a large family of proteins which are found embedded into cellular membranes, typically on the cell surface. The general structure of GPCRs is well-conserved, with an extracellular N-terminal tail, seven transmembrane (TM) alpha-helices joined by intra- and extra-cellular loops (IL, EL), an intracellular eighth helix, and an intracellular C-terminal tail (Venkatakrishnan *et al.*, 2013). As their name suggests, GPCRs activate G proteins, by acting as a cofactor for the exchange of GDP, which is bound to the Gα subunit, to GTP (Dupré *et al.*, 2009). The intracellular loops, and perhaps helix 8, provide the contact points for G protein coupling (Venkatakrishnan *et al.*, 2013).

G proteins

Meanwhile, G proteins are heterotrimeric structures (Dupré *et al.*, 2009). An activated G protein was traditionally thought to separate into two functional subunits, the Gα and Gβγ, (Brandt *et al.*, 1985; Higashijima *et al.*, 1987; Janetopoulos *et al.*, 2002), allowing them to interact with their effectors. However, it is possible that the activated G protein can be functional while still fully-associated (discussed in Rebois *et al.*, 1997). Once separated, these G protein subunits have a variety of cellular effects, depending on the G protein subtype and cellular environment of the receptor/G protein system. There are four groups of G proteins, defined by their Gα subunit: Gαs, which stimulates adenylate cyclase, increasing cAMP production; Gαi, which inhibits adenylate cyclase, reducing cAMP production; Gαq, which activates phospholipase C; $G\alpha_{12/13}$, which alters Rho-GTPase signalling pathways (Neves *et al.*, 2002). The signalling profiles of the various Gβγ subunits are less well-characterised, but these also affect a wide range of effectors, including GPCR kinases (GRKs), mitogen-activated kinase (MAPK) phosphorylation, phosphatidylinositol-3-kinase (PI3K), and adenylate cyclases (Dupré *et al.*, 2009). Gβγ also affects ion channels: selectively activating inwardly rectifying potassium channels; and inhibiting N-, P/Q-, and R-type voltage-gated Ca2+ channels (Altier, 2012; Currie, 2010; Doupnik, 2008; Huang *et al.*, 1995).

Non-G protein mediated GPCR signalling

Activated GPCRs can recruit arrestins, a step which has previously been considered as a stage in the desensitisation sequence (Magalhaes *et al.*, 2012). However, arrestins have been demonstrated to initiate some signalling, including activation of multiple MAPK pathways (Luttrell *et al.*, 2002; Zhan *et al.*, 2014). This provides a second complement of GPCR signalling cascades beyond canonical G protein effects.

Key processes affected by GPCR signalling

GPCR signalling can activate a wide variety of cellular processes, depending on the particular G protein and/or arrestin which is activated, and the available pathways in the particular cell type. Adenylate cyclase and mitogen-activated kinase (MAPK) pathways are the most commonly-used measures of GPCR signalling, although GPCRs can also modify many other pathways, as mentioned above.

Adenylate cyclases catalyse the formation of cyclic adenosine monophosphate (cAMP), and are stimulated by Gαs and inhibited by Gαi. In addition, different adenylate cyclase subtypes are regulated by Gβγ and Ca^{2+} (Hanoune *et al.*, 2001; Kamenetsky *et al.*, 2006). cAMP is a key regulator of cellular metabolism, and modulates several cellular processes differentially depending on cAMP concentration. Protein kinase A (PKA) activity is saturated by low cAMP concentrations (1 μM) (Antoni, 2012). PKA phosphorylates a wide variety of protein targets, including other protein kinases and ion channels, as determined by the co-expression of various PKA-anchoring proteins, leading to cell-type specific phenotypes (Logue *et al.*, 2010; Taylor *et al.*, 2004). Two types of ion channel are activated by cAMP: hyperpolarization-activated and cyclic nucleotide-modulated channels, and channels directly modulated by cyclic nucleotides. These channels are maximally responsive to 10 μM cAMP, and when activated they increase the electrical activity of the cell (Antoni, 2012). Exchange proteins activated by cAMP (Epac) require high levels of cAMP (40 μM), and in turn activate Rap pathways, which can affect processes including phospholipase activity and cytoskeletal changes (Gloerich *et al.*, 2010; Raaijmakers

et al., 2009). Phosphodiesterases (PDEs) reduce cellular cAMP concentrations by hydrolysing it into 5'AMP. Some PDEs are also regulated by cAMP, with the cAMP binding sensitivity varying significantly between PDE subtypes (Keravis *et al.*, 2010).

GPCRs also activate the MAPK pathways: extracellular signal-regulated kinases 1/2 (ERK1/2), ERK5, Jun amino-terminal kinases (JNK), and p38 pathways (Chang *et al.*, 2001; Fukuhara *et al.*, 2000; Trejo, 2014). This signalling can be initiated through either activated G proteins or arrestins (Chavkin *et al.*, 2014; Fukuhara *et al.*, 2000; Kolch, 2005). The MAPK pathways modify a large range of processes, including gene transcription, protein synthesis, cell proliferation and differentiation (Chang *et al.*, 2001; Kyriakis *et al.*, 2012). Generally, activation of the ERK1/2 and ERK5 pathways increase cell survival, whereas JNK induces apoptosis, although this depends on cell type and signal duration (Chang *et al.*, 2001; Tatake *et al.*, 2008; Xia *et al.*, 1995). For example, low level activation of p38 promotes cell survival, while higher levels result in apoptosis (Dolado *et al.*, 2008).

GPCR dimerisation

GPCRs are able to function both as monomers, and in groups of two (dimers) or more (oligomers). Currently, much effort is being put into developing experimental methods to determine the stoichiometry of GPCRs in dimers and higher-order oligomers (Ferré *et al.*, 2014). Dimers and higher order oligomers may be composed of several copies of the same receptor (homodimers) or different GPCRs (heterodimers). Large groupings of receptors, containing several different GPCRs, have been termed "mosaics" (Agnati *et al.*, 2010b; Fuxe *et al.*, 2008). The interactions within such mosaics may affect the pathology and therapeutic strategies for complex disease states (Fuxe *et al.*, 2009), however this is beyond the scope of this review. For most Class A GPCRs, it is unknown whether dimerisation is required for normal function. However, there is extensive description of heterodimer formation and function in mammalian cell systems (reviewed in Fuxe *et al.*, 2012, Pin *et al.*, 2007).

Function

Both ligand binding and signalling can be influenced by dimerisation, providing a unique functional character to the dimer when compared to the receptor monomer/homodimer. These functions are defined by the conformation of the receptors, which is altered by heterodimerisation interactions. Once defined *in vitro*, the unique function of a GPCR dimer can be used to test for the presence of dimer in isolated primary cells and *in vivo*.

A good example of heterodimerisation affecting ligand binding is the adenosine A2A receptor. When expressed in the medium spiny neurons of the striatum, this receptor has been described to dimerise with both the adenosine A1 receptor and dopamine D2 receptor, in pre-synaptic and post-synaptic locations respectively (Azdad *et al.*, 2008; Ciruela *et al.*, 2006; Orru *et al.*, 2011). Rationally, there must be a function for A1-A2A interactions in the same cellular domain, since both have the same endogenous ligand, but opposing G protein coupling (Gαi and Gαs, respectively). Selective activation of A2A has been demonstrated to reduce the affinity of agonists at the A1 receptor (Ciruela *et al.*, 2006). Since A1 receptors have an intrinsically higher affinity for adenosine than A2A receptors, this cross-talk creates a biphasic response to adenosine, with A1 receptors being activated at low concentrations, and the A2A-

mediated response becoming active at high adenosine concentrations (Ciruela *et al.*, 2006). In addition, although KW-6002, an A2A antagonist, binds with the same affinity for A2A receptors in homodimers or in the A1-A2A heterodimer, this ligand has a significantly increased affinity for the A2A-D2 heterodimer. Therefore, when KW-6002 is given to rats systemically, the antagonist preferentially blocks post-synaptic receptors and gives a corresponding behavioural response in rats (Orru *et al.*, 2011). Findings such as these demonstrate that heterodimerisation interactions change the receptor's activity state, which can be demonstrated by altered ligand affinities.

In terms of dimer signalling, the current predominant theory is that receptors in a dimer share a G protein, likely at a ratio of one G protein per two receptors (Maurice *et al.*, 2011). This stoichiometry was first noted for the GABAB receptor, which, as a Class C GPCR, is an obligate dimer (Duthey *et al.*, 2002; Kniazeff *et al.*, 2011; Zhang *et al.*, 2014). The theory that this is applicable to other GPCR heterodimers is based on the observation that a single G protein requires two contact points in order to be activated, and that these are too far apart to allow one receptor to activate the G protein (Maurice *et al.*, 2011; Oldham *et al.*, 2008). This interpretation has been used to model the interactions of rhodopsin (Filipek *et al.*, 2004); and experimentally defined by functional studies of dopamine D2 (Han *et al.*, 2009), and reconstitution studies using leukotriene BLT1 (Banères *et al.*, 2003) and serotonin 5-HT4 (Pellissier *et al.*, 2011) receptors. If this theory is correct, it is unsurprising that some GPCR heterodimers have been shown to "switch" G protein coupling when compared to each receptor expressed alone (Chandrasekera *et al.*, 2013; Kearn *et al.*, 2005; Lee *et al.*, 2004). However, although this is an appealing theory, there are also many studies using isolated monomeric GPCRs which have shown results consistent with a 1:1 GPCR to G protein ratio (Arcemisbéhère *et al.*, 2010; Damian *et al.*, 2012; Kuszak *et al.*, 2009; Whorton *et al.*, 2007; Whorton *et al.*, 2008).

Ways to measure dimerisation

Once functional interactions were found between pairs of GPCRs, there was a requirement to determine whether these features occurred as a physical interaction between the receptors, or whether the interaction occurred during convergent signalling cascades. A range of biophysical methods have been developed which aid in the identification of physical interactions. Co-immunoprecipitation allows the detection of dimers in cell lysates. Antibodies are used to precipitate one receptor of interest (the "bait"), then an immunoblot on the precipitated proteins is probed for the second receptor of interest (the "prey"). Co-immunoprecipitation is able to pull down whole signalosomes, so the presence of the prey protein doesn't necessarily indicate a direct contact between the two receptors of interest. Using this technique, serotonin 5-HT1A, 5-HT1B and 5-HT1D receptors were shown to co-immunoprecipitate with all other GPCRs they were co-expressed with (EDG1, EDG3, GPR26 and GABA2B), even though the authors could not identify native cell types which would co-express some of these pairings (Salim *et al.*, 2002).

Resonance energy transfer (RET) techniques are a well-established and frequently utilised method of measuring dimer formation. Both Förster/fluorescent RET (FRET) and bioluminescence RET (BRET) have been used extensively for GPCR interaction studies, differing only in the source of the energy required to trigger the reaction. In either assay format, one receptor is tagged with a "donor" protein and the other to an "acceptor" protein. The donor and acceptor tags are chosen such that the emission wavelength for the donor overlaps with the excitation spectrum of the acceptor, allowing the transfer of

energy (Stryer, 1978). During the interaction assay, the energy donor is excited with either an external light source (for FRET) or a chemical substrate (for BRET) (Pfleger *et al.*, 2006b). A RET interaction can only occur over short distances, of approximately 10 nm in the case of standard BRET donor-acceptor pairs (Pfleger *et al.*, 2006b). Provided the donor and acceptor tags are close enough, the excited state of the donor transfers its energy to the acceptor by a non-radiative mechanism, through dipole-dipole interactions, and without the emission/absorption of a photon (Stryer, 1978; Wolber *et al.*, 1979; Wu *et al.*, 1994). Since a RET interaction can only occur over very short distances, the presence of donor fluorophore emission is likely to be due to a physical association between the two proteins of interest.

A key limitation of both FRET and BRET are the large protein tags which need to be added to the receptors, which can hinder normal function. Bimolecular fluorescence complementation (BiFC) somewhat overcomes this, with each receptor being tagged with half of a fluorescent protein. When these tags are brought into close proximity, the two halves are able to fold together to form one functional fluorescent protein, resulting in fluorescent emission. However, while BRET and FRET interactions can be monitored in real time, BiFC has significant kinetic limitations with full protein folding and emission taking several hours after the initial protein interaction occurs, and producing an irreversible interaction (Demidov *et al.*, 2006; Kerppola, 2006; Reid *et al.*, 1997). All of these methods (BRET, FRET and BiFC) require the overexpression of transgenes in a transfectable host cell line. As such, they are unable to measure the interactions of endogenously-expressed receptors, which requires either co-immunoprecipitation (for example, Chakrabarti *et al.*, 2010, Chandrasekera *et al.*, 2013), or heterodimer-specific antibodies (Gomes *et al.*, 2014). More recently FRET between fluorescent ligands has been utilised, an approach which has the advantage of enabling dimer formation in native expressing tissue to be probed (as described below), but is limited by the availability of appropriate ligands.

GPCR dimer interfaces

Advances in protein crystallography have allowed the structures of GPCRs to be resolved increasingly frequently (Audet *et al.*, 2012; Venkatakrishnan *et al.*, 2013). The crystal packing of these receptors has been interpreted as indicating potential homodimer interaction sites. For example, crystal structures of the chemokine CXCR4 receptor homodimer (Wu *et al.*, 2010) and μ-opioid receptor homodimer (Manglik *et al.*, 2012) have been interpreted as having primary interfaces at TM5 and TM6. However, it has been discussed that a TM5-TM6 interface may prevent normal G protein coupling, as conformational changes in this region are generally required during receptor activation (Ferré *et al.*, 2014; Manglik *et al.*, 2012; Rasmussen *et al.*, 2011). This highlights the importance of critical analysis of crystal structure determination of dimerisation interfaces. Secondary interfaces, which may be more physiologically-relevant, were also identified for these homodimers: TM3 and TM4 for CXCR4 (Wu *et al.*, 2010); and TM1, TM2 and helix 8 for the μ-opioid receptor (Manglik *et al.*, 2012). Considering the limitations of protein crystallography, more traditional experimental techniques need to be employed to validate any identified dimer interfaces. For example, the β1-adrenergic receptor crystal structure demonstrated two interfaces: TM1-TM2-EC1-helix8 and TM4-TM5-IL2 (Huang *et al.*, 2013). The authors then verified the relevance of these interfaces using cysteine crosslinking experiments and demonstrated both interaction sites were physiologically-relevant.

While crystallisation can aid in the identification of putative dimerisation sites, it cannot compete with the ability of traditional experimental approaches to replicate the complex biological environment of cell membranes. One such method is to introduce peptide sequences which are identical to a known segment of the receptor of interest. If this peptide contains the dimerisation interface, then it will compete with the full-length receptors, thus preventing normal dimerisation. This approach has been used for studies of the β2-adrenergic receptor (Hebert *et al.*, 1996) and leukotriene BLT1 receptor (Banères *et al.*, 2003), both of which found peptides homologous to TM6 disrupted homodimerisation. The second method alters the full-length receptor, by mutating putative dimer interaction sites in an attempt to either increase or decrease dimerisation. This strategy was used to elucidate the interfaces of the A2A-CB1-D2 oligomer, demonstrating that the cytoplasmic end of TM5 in A2A interacts with the C-terminus of CB1, the IL3 of CB1 interacts with the IL3 of D2, and the cytoplasmic end in TM5 of D2 interacts with the C-terminus of A2A (Navarro *et al.*, 2010). Another method is to use cysteine cross-linking, generally by substituting cysteine residues through mutagenesis. The homodimer interface of the muscarinic M3 receptor homodimer was identified this way, with cysteine substitutions in TM5 and IL3 stabilising this interaction (Hu *et al.*, 2012).The dopamine D2 homodimer was found, through crosslinking experiments, to have an interface at TM4. While some residues in this helix cross-linked under all conditions, some were sensitive to receptor activation state, as controlled by agonist and inverse agonist application (Guo *et al.*, 2005). The serotonin 5-HT2C receptor homodimer was shown using cysteine crosslinking to have several interfaces. Crosslinking between TM4 and TM5 was found to be sensitive to receptor activation state, with agonist promoting more interaction at this location, while the TM1 interface was insensitive to receptor activation (Mancia *et al.*, 2008).

Evidence for GPCR heterodimers *in vivo*

It is considerably easier to demonstrate the existence of oligomers *in vitro* than it is to prove their existence *in vivo*. However, several techniques have been used to successfully determine the presence and location of GPCR heterodimers *in vivo*.

Bivalent ligands are drugs which have been designed to bind to two receptors simultaneously. Two pharmacophores, one specific to each receptor in the heterodimer, are separated by a linker sequence (Shonberg *et al.*, 2011). The intention is that each pharmacophore will bind to its receptor, with the linker acting as a tether to stabilise the dimer-ligand assembly (Berque-Bestel *et al.*, 2008). As the ligand binds in two locations, it would have an increased apparent affinity for the heterodimer compared to each receptor alone. This technique was used to identify and characterise δ-κ opioid receptor dimers in a transgenic cell line (Xie *et al.*, 2005) and the spinal cord of mice (Bhushan *et al.*, 2004). This provided evidence that the δ1- and κ2-opioid receptor subtypes were, in fact, simply the phenotypes of δ- and κ-opioid receptors in the heterodimeric state (Bhushan *et al.*, 2004). Indeed, if specific bivalent ligands can be developed, they can be used as pharmacological tools, labelled as fluorescent or radiographic probes, or as a therapeutic agent.

Ligand-FRET has also been used to visualise GPCR oligomers, using two receptor ligands tagged with an energy donor and acceptor, analogous to the FRET assays described above. Thus ligand-FRET can be performed without the addition of fluorescent tags to the receptors. This approach has been used to demonstrate dopamine D1-D3 heterodimers in a transfected cell line, albeit still requiring genetic fusion

tags (Hounsou *et al.*, 2015). But, more importantly, ligand-FRET has also been used to demonstrate oxytocin homodimers in endogenously-expressing tissues (Albizu *et al.*, 2010). Labelled ligands were applied to tissue sections, and then visualised to detect a FRET interaction. This approach gave similar results to the oligomers observed in transgenic cell lines (Albizu *et al.*, 2010). Another method, which relies on the availability of specific antibodies, is the proximity ligation assay. In this assay, antibodies to each receptor are labelled with a short single-stranded DNA tag, which form complimentary double-stranded DNA structures that can then be amplified for visualisation. This has been used to show dopamine D2-adenosine A2A heterodimers in mouse striatum slices (Trifilieff *et al.*, 2011).

Application to therapeutics

GPCR heterodimers generally have a more restricted tissue distribution than their component receptors. Thus, therapeutics focusing on heterodimers may offer the opportunity to selectively target a specific subset of receptors within the body and exploit dimer-specific signalling pathways. For example, the adenosine A2A-dopamine D2 heterodimer is being pursued as a target in Parkinson's disease, with the combination of an A2A antagonism and D2 agonism being suggested as particularly useful (Beggiato *et al.*, 2014; Jörg *et al.*, 2014a; Jörg *et al.*, 2014b).

Cannabinoid receptor 1 signalling and therapeutic indications

CB1 is a GPCR which is found throughout the central nervous system and responds to endogenously-produced cannabinoids (endocannabinoids). In neurons, CB1 is predominantly located presynaptically (Katona *et al.*, 1999). These receptors are activated when endocannabinoids, such as anandamide and 2-arachidonoylglycerol, are primarily released during retrograde neurotransmission (i.e. are released from the postsynaptic cell to act on the presynaptic cell) (Castillo *et al.*, 2012). This results in an inhibition of presynaptic neurotransmitter release, thus suppressing anterograde synaptic transmission (Diana *et al.*, 2002; Kreitzer *et al.*, 2001; Ohno-Shosaku *et al.*, 2001; Wilson *et al.*, 2001; Yoshida *et al.*, 2002).

CB1 Gαi signalling

CB1 is primarily classified as a Gαi-coupled receptor (Felder *et al.*, 1995; Howlett *et al.*, 1986; Matsuda *et al.*, 1990), with a signalling profile which, on the whole, reflects the canonical Gαi pathways. The traditional test for Gαi-dependence in a cell signalling assay is to pre-treat cells with pertussis toxin. This ADP-ribosylates the Gαi subunit, preventing Gαi turnover (Milligan, 1988). Using this approach, CB1 has been shown to inhibit the activity of adenylate cyclases, thus reducing cAMP production, via activation of Gαi proteins (Matsuda *et al.*, 1990). cAMP modulates the activity of cAMP-dependent protein kinase A, phosphodiesterases, and ion channels (Antoni, 2012), therefore making it a key molecule in the control of cellular metabolism.

CB1 also increases ERK phosphorylation (pERK). In most cells, CB1-mediated pERK stimulation is sensitive to PTX, but mediated by the Gβγ subunit (Bouaboula *et al.*, 1995). The specific mechanisms and consequences of CB1's pERK response likely vary by cell type. For example, in cultured cortical neurons, an early wave of pERK is reportedly Gαq-derived, with a second, Gαi-derived pERK signal after 15 minutes (Asimaki *et al.*, 2011). In hippocampal slices pERK is downstream of cAMP inhibition and unaffected by blockade of phosphoinositol-3-kinase (Derkinderen *et al.*, 2003), while in other cell types

this is not the case (Bouaboula *et al.*, 1997; Bouaboula *et al.*, 1995). There have also been studies which suggest CB1 may induce ERK phosphorylation through activation of receptor tyrosine kinases. CB1 activation of Gαi resulted in transactivation of vascular endothelial growth factor receptor, inducing pERK (Rubovitch *et al.*, 2004). Further complicating matters, Fyn (a tyrosine kinase from the Src family) appears to mediate the CB1 pERK signal in the hippocampus, as Fyn knock out mice do not show a CB1-mediated pERK response (Derkinderen et al., 2003), and contributes to the Gαi-mediated pERK signal seen in hippocampal neurons (Asimaki et al., 2011). Other kinase cascades are also mediated by CB1 signalling through Gαi, namely the activation of JNK (Rueda *et al.*, 2000) and protein kinase B/Akt (Gómez *et al.*, 2000).

Receptor activation inhibits N-type (Mackie *et al.*, 1992; Pan *et al.*, 1996), L-type (Gebremedhin *et al.*, 1999), P/Q-type (Twitchell *et al.*, 1997), and T-type (Chemin *et al.*, 2001) calcium channels, and activate potassium channels (Ho *et al.*, 1999; Mackie *et al.*, 1995; McAllister *et al.*, 1999). Since presynaptic neurotransmitter release is calcium-dependent, inhibition of calcium channels (either directly, or indirectly following potassium channel activation) reduces anterograde neurotransmission (Daniel *et al.*, 2004; de Jong *et al.*, 2009). CB1 Gαi signalling inhibits N-type calcium channels in neuronal cell lines (Mackie *et al.*, 1992; Pan *et al.*, 1996); L-type in arterial smooth muscle and nucleus tractus solitarius neurons (Endoh, 2006; Gebremedhin *et al.*, 1999); and P/Q-type in hippocampal and Purkinje neurons (Fisyunov *et al.*, 2006; Twitchell *et al.*, 1997). Pertussis toxin abolishes CB1's effects on potassium ion channels, specifically G protein-coupled Inwardly Rectifying K^+ (GIRK) channels, although this appears to be mediated by Gβγ and cAMP signalling (Ho *et al.*, 1999; Mackie *et al.*, 1995; McAllister *et al.*, 1999; Yamada *et al.*, 1998). In nonpigmented ciliary epithelial cells (which endogenously express CB1), Gβγ-mediated pERK leads to activation of Cl^- currents (Shi *et al.*, 2003).

CB1 alternative signalling – Gαs, Gαq, Gα12/13, Gαz

Although CB1 is typically described as a Gαi-linked GPCR, there is a strong body of literature suggesting that this is not the case in all cell types and pharmacological conditions. There is robust evidence that CB1 is capable of activating non-Gαi-type signalling pathways. The most frequently reported "secondary" signalling pathway of CB1 is through Gαs, first reported in medium spiny neurons (Glass *et al.*, 1997). This signalling pathway can be unmasked by either pharmacological treatment with D2 receptor agonists (discussed below), or use of pertussis toxin, which prevents Gαi signalling (Glass *et al.*, 1997; Kearn *et al.*, 2005). Alternatively, the Gαs component can be removed by treatment with anti-Gαs antibodies (Bash *et al.*, 2003).

Gαq coupling by the CB_1 receptor has also been reported. Activation of this G protein subtype activates phospholipase C and its downstream signalling cascade, resulting in Ca^{2+} release from the endoplasmic reticulum into the cytoplasm. One CB1 agonist is particularly efficient in eliciting this functional effect – WIN55,212-2. Application of relatively high (5 μM) concentrations of this agonist to hippocampal neurons or transfected HEK293 cells has been shown to cause a large increase of cytosolic Ca^{2+} (Lauckner *et al.*, 2005). This effect was abolished by co-application of SR141716A, a specific CB1 inhibitor, and was significantly reduced by the expression of a dominant-negative Gαq construct (Lauckner *et al.*, 2005).

CB1 might also signal through $G\alpha_{12/13}$ pathways. This signalling pathway is the least characterised G protein pathway, but is known to primarily act as a regulator of actin cytoskeleton, thereby controlling cell

morphology, through the small GTPase RhoA (Suzuki *et al.*, 2003). Anandamide was shown to induce rounding of B103 rat neuroblastoma cells, in a manner consistent with $G\alpha_{12/13}$ protein coupling (insensitive to PTX-treatment, but sensitive to treatment with a Rho inhibitor (Ishii *et al.*, 2002)). Lastly, there is *in vivo* data suggesting that CB1 may also couple to Gαz (a $G\alpha_{i/o}$-related G protein) in neurons (Garzon *et al.*, 2009). Gαz knockdown mice showed attenuated cannabinoid-mediated tolerance to analgesia compared to wildtype animals (Garzon *et al.*, 2009).

Arrestin interactions

Arrestin recruitment by CB1 is still relatively uncharacterised. In cultured cells, CB1 is generally observed to weakly interact with β-arrestin1 (Jin *et al.*, 1999) and β-arrestin2 (Daigle *et al.*, 2008; Gyombolai *et al.*, 2013), and these interactions can be altered by the allosteric modulator ORG27569 (Ahn *et al.*, 2013). β-arrestin1 has been found to couple CB1 to ERK and Src pathways, while β-arrestin2 is associated with receptor internalisation (Ahn *et al.*, 2013). In smooth muscle cells, activation of ERK and Src pathways may be solely arrestin-dependent (Mahavadi *et al.*, 2014), but these have been reported as G protein-mediated in other cell types (Bouaboula *et al.*, 1995; He *et al.*, 2005).

There is some evidence from animal studies that CB1-arrestin interactions are physiologically-relevant. β-arrestin2 knockout mice show an increased behavioural response to acute doses of Δ9-tetrahydrocannabinol (THC) (Breivogel *et al.*, 2008; Nguyen *et al.*, 2012). Upon chronic systemic THC treatment, these β-arrestin2 knockout mice show changes in the development of tolerance, with an increase in the globus pallidus, but a decreased development of tolerance in the spinal cord (Nguyen *et al.*, 2012). However, these knockout mice only have altered responses to THC, and not synthetic cannabinoids (including synthetic partial agonists) or endocannabinoids (Breivogel *et al.*, 2008). Further evidence for cell-type specific arrestin interactions is the observation that chronic THC increases β-arrestin1 protein expression only in specific regions of the mouse brain (the striatum, cerebellum and hippocampus) (Rubino *et al.*, 2006).

Therapeutic applications of cannabinoids at CB1

Cannabis, containing phytocannabinoids, has a long history of use as a traditional remedy, but pharmaceutical formulations have also been tested and regulated. The pharmaceutical formulation of THC is called dronabinol, and has been studied and used extensively as a treatment for a wide range of disease states, including anorexia related to human immunodeficiency virus/acquired immune deficiency syndrome (Lutge *et al.*, 2012), cancer chemotherapy-related nausea and vomiting (Machado Rocha *et al.*, 2008), and chronic pain (de Vries *et al.*, 2014). Similar effects have been seen with nabilone, a synthetic cannabinoid (Campbell *et al.*, 2001; Ware *et al.*, 2008). Phytocannabinoid mixes, such as the THC-cannabidiol formulation nabiximols (trade name “Sativex”), have gained regulatory approval, and have been shown to be useful in the management of neuropathic pain (Nurmikko *et al.*, 2007), spasticity in multiple sclerosis (Barnes, 2006; Novotna *et al.*, 2011; Wade *et al.*, 2010), and rheumatoid arthritis (Blake *et al.*, 2006). A CB1 antagonist, rimonabant (also known as SR141716A), also reached the market, being approved for the treatment of obesity (Christensen *et al.*, 2007; Gray *et al.*, 2012), and undergoing clinical trials as an aid smoking cessation (Cahill *et al.*, 2012). However, due to psychiatric adverse reactions, it was withdrawn from the market (Gray *et al.*, 2012; Jones, 2008; Le Foll *et al.*, 2009).

In general, the side effects of both agonists and antagonists appear to be due to general activation/inactivation of CB1 and other as-yet unidentified cannabinoid receptors (Howlett *et al.*, 2004).

Nevertheless, there is still interest in developing cannabinoid drugs which target CB1 to treat many disease states. There is also some accumulated evidence that cannabinoids may have therapeutic benefits in movement disorders, including tic disorders (Müller-Vahl *et al.*, 1998; Müller-Vahl *et al.*, 2002; Müller-Vahl *et al.*, 2003); dystonia in animals (Richter *et al.*, 2002; Richter *et al.*, 1994) (but not humans (Fox *et al.*, 2002; Zadikoff *et al.*, 2011)); and tremor and spasticity in multiple sclerosis (Baker *et al.*, 2000; Clifford, 1983; Collin *et al.*, 2010; de Lago *et al.*, 2006; Zajicek *et al.*, 2003) (although not in all human studies (Fox *et al.*, 2004)).There is also mixed evidence for a therapeutic role of CB1 in Parkinson's disease, where CB1 mRNA is reduced in the human caudate nucleus, and parts of the putamen and globus pallidus (Hurley *et al.*, 2003), with increased CB1 receptor-mediated G protein turnover in these areas and the substantia nigra (Lastres-Becker *et al.*, 2001). CB1 protein expression is increased in the caudate nucleus and the putamen (Lastres-Becker *et al.*, 2001). In rat models CB1 mRNA and expression is either unchanged or slightly increased (Romero *et al.*, 2000). In cell culture model, the protective effect of THC was not mediated by CB1 (Carroll *et al.*, 2012; Lastres-Becker *et al.*, 2005). In a mouse model of Parkinson's disease, WIN55,212-2 did improve pathogenesis, but this was not mediated through CB1 receptors (Price *et al.*, 2009). Meanwhile, in a rat model of the disease, concurrent treatment with a D2 receptor agonist and a CB1 receptor inverse agonist improved symptoms (Di Marzo *et al.*, 2000), as did CB1 inverse agonist alone (Garcia-Arencibia *et al.*, 2008). Controlled studies in humans have not shown that cannabinoids offer much benefit for the motor symptoms of Parkinson's disease, or levodopa-induced dyskinesias (Carroll *et al.*, 2004; Chagas *et al.*, 2014; Mesnage *et al.*, 2004), with one exception (Sieradzan *et al.*, 2001).

Huntington's disease has been a key focus for cannabinoid research. CB1 levels decline very early in the pathogenesis of Huntington's disease (Glass *et al.*, 2000; Van Laere *et al.*, 2010), an effect replicated in experimental animal models of the disease (Chiodi *et al.*, 2012; Lastres-Becker *et al.*, 2002). CB1 knockout mice have an accelerated pathogenesis, in a toxin-induced model of Huntington's disease (Mievis *et al.*, 2011). In a cell line model, CB1 signalling through Gαs proteins was found to increase cell death, while Gαi was found to be protective (Scotter *et al.*, 2010). Consistent with this finding, SR141716A, a selective CB1 inverse agonist, was found to increase neurodegeneration (Lastres-Becker *et al.*, 2003), presumably through preventing the Gαi coupling of CB1. Other animal studies suggest there may be some benefit to cannabinoid-targeted treatment, for example by endocannabinoid uptake inhibitors (de Lago *et al.*, 2006; Lastres-Becker *et al.*, 2002) or inhibiting endocannabinoid degradation (Dowie *et al.*, 2010), which would be expected to increase the concentration of endocannabinoids. However, exogenous agonist application provide mixed results in some animal models, with reports of no effect (Dowie *et al.*, 2010), or moderate effect (Lastres-Becker *et al.*, 2003; Pintor *et al.*, 2006; Valdeolivas *et al.*, 2012), depending on the ligand. In human patient populations (albeit with small sample sizes), some benefits were found for nabilone treatment (Curtis *et al.*, 2009), but not cannabidiol (Consroe *et al.*, 1991), although it is unclear which receptors these ligands are acting through.

CB1 homodimers and heterodimerisation partners

CB1 can form both homodimers (Wager-Miller *et al.*, 2002), and heterodimers with a number of other GPCRs. These heterodimers include the β2-adrenergic (Hudson *et al.*, 2010b), μ-opioid (Hojo *et al.*, 2008; Rios *et al.*, 2006), and orexin OX1 (Ellis *et al.*, 2006) receptors. CB1 can also heterodimerise with the dopamine D2 receptor, with a distinct functional phenotype. Here, we will focus on this interaction.

Interactions between the cannabinoid and the dopamine systems

There is considerable behavioural evidence that the cannabinoid and dopamine systems interact in the rodent and human brain, affecting motor functioning and the reward pathway. Dopamine receptors are either D1-like or D2-like, with D1-like receptors increasing, and D2-like decreasing adenylate cyclase activity. Behavioural responses to activation of D1 and D2 receptors differ, and CB1 is capable of modulating both D1- and D2-derived motor responses (Martín *et al.*, 2008), however this review will focus on the CB1-D2 interaction. CB1 and D2 are co-localised in GABAergic synapses in the prefrontal cortex (Chiu *et al.*, 2010) and the nucleus accumbens (Pickel *et al.*, 2006).

Dopamine D2 receptors

Dopamine D2 receptors come in two splice variants, the short and long isoforms, which vary by the length of IL3 (Castro *et al.*, 1993; De Mei *et al.*, 2009; Tan *et al.*, 2003). This review will focus on D2L, which is the primary isoform in the striatum (Wang *et al.*, 2000). D2 receptors are Gαi-linked, thereby inhibiting adenylate cyclase activity and reducing cAMP through both Gα and Gβγ subunits (Albert *et al.*, 1990; Neve *et al.*, 2004; Sidhu *et al.*, 2000). These receptors can also couple to Gαz, although Gαi/o coupling is predominant in the mouse brain and cell lines (Jiang *et al.*, 2001; Neve *et al.*, 2004; Watts *et al.*, 1998). These receptors also activate pERK (Faure *et al.*, 1994; Kim *et al.*, 2004), JNK (Luo *et al.*, 1998), and inwardly rectifying potassium channels (Surmeier *et al.*, 1993); inhibit the activity of L, N, and P/Q-type calcium channels (Hernández-López *et al.*, 2000; Neve *et al.*, 2004; Seabrook *et al.*, 1994; Yan *et al.*, 1997); and several other effectors (Neve *et al.*, 2004). D2 signalling also leads to Gβγ-mediated phospholipase C activation, leading to calcium mobilisation and arachidonic acid release (Kanterman *et al.*, 1991; Neve *et al.*, 2004).

As well as D2 homodimer (Guo *et al.*, 2003; Guo *et al.*, 2008), D2 has been shown to heterodimerise with dopamine D1 (Dziedzicka-Wasylewska *et al.*, 2006; George *et al.*, 2007), adenosine A2A (Fuxe *et al.*, 2005),and CB1 receptors (Kearn *et al.*, 2005).

CB1-D2 interactions *in vivo*

CB1 and D2 primarily interact in the movement pathways. In the striatum, D2 receptors are expressed on neurons of the indirect pathway, providing inhibitory connections to the external globus pallidus (Svenningsson *et al.*, 2000). In rodents, activation of D2 produces oral stereotypies and horizontal locomotion, while more complex behaviours, such as grooming, are controlled by D1 receptors on neurons of the direct pathway (Giuffrida *et al.*, 1999).

Treatment with cannabinoids increases the production of dopamine in the striatum (Bossong *et al.*, 2009), and activation of D2 receptors increases endocannabinoid release (Giuffrida *et al.*, 1999). Activation of either receptor inhibits neurotransmission (Robbe *et al.*, 2001; Robbe *et al.*, 2002; Ronesi *et al.*, 2005), presumably because CB1 and D2 signal through very similar pathways.

In general, exogenous cannabinoids reduce dopamine-mediated behaviour (Rodriguez de Fonseca *et al.*, 1998), as does blocking the endocannabinoid uptake transporter (Beltramo *et al.*, 2000). Although the opposite has also been reported, where an increase in motor activity seen upon application of cannabinoid agonists to the striatum (Sanudo-Pena *et al.*, 1998). When administered systemically, the D2-selective agonist quinpirole increases movement (Eilam *et al.*, 1989a; Eilam *et al.*, 1989b). As CB1 activation results in dopamine release, it is unsurprising that pretreatment with or co-administration of CB1 agonists exacerbates the increased motor activity which is induced by D2 agonists (Ferre *et al.*, 2009; Giuffrida *et al.*, 1999; Martín *et al.*, 2008).

Apart from the control of movement, CB1 and D2 interact in other pathways. For example, CB1 activation impairs working memory, and this impairment is increased by concurrent treatment with D2 agonists, and reduced by D2 antagonists (Nava *et al.*, 2000). These receptors also interact in the reward pathways, as demonstrated in a rat model of alcohol addiction. In this model, CB1 and D2 activation by exogenous agonists have opposing effects, with CB1 agonists increasing relapse and D2 preventing it. The effect of CB1 agonism can be counteracted by concurrent antagonism of D2 (Alen *et al.*, 2008).

CB1 and D2 signalling have been found to be concurrently dysfunctional in a number of disease states. For example, schizophrenia is treated with antipsychotic drugs which target D2 receptors as antagonists (Geyer *et al.*, 1993). D2 receptor expression has been found to be aberrant in patients with schizophrenia, with increased expression in the striatum in some patients (Hietala *et al.*, 1994; Seeman *et al.*, 1987), and decreased in anterior cingulate cortex and sub-regions of the thalamus (Takahashi *et al.*, 2006; Yasuno *et al.*, 2014). CB1 has been implicated in the pathology of schizophrenia, initially through observations that acute cannabinoid administration in healthy volunteers mimics some symptoms of schizophrenia (Emrich *et al.*, 1997; Leweke *et al.*, 1999b; Schneider *et al.*, 1998; Skosnik *et al.*, 2001), and that cannabinoid administration to schizophrenic patients worsens symptoms (Caspari, 1999; Voruganti *et al.*, 2001). The endocannabinoid system, and specifically CB1 expression, is also altered in schizophrenia (Dean *et al.*, 2001; Leweke *et al.*, 1999a; Zamberletti *et al.*, 2012). In the rat social isolation model of schizophrenia, adolescent rats are raised in isolation, resulting in neurodevelopmental and behavioural changes similar to schizophrenia in humans (Fitzgerald *et al.*, 2013; Geyer *et al.*, 1993; Malone *et al.*, 2006; Zamberletti *et al.*, 2012). Administration of cannabinoid agonists during the isolation phase exacerbates this pathological phenotype (Malone *et al.*, 2006; Schneider *et al.*, 2003), while CB1 antagonists improve outcomes (Zamberletti *et al.*, 2012). Following isolation, administration of D2 antagonists counters the effect of adolescent cannabinoid exposure (Schneider *et al.*, 2003). In this model, CB1 and D2 expression has been found to be unchanged in presynaptic terminals, although dendritic/postsynaptic D2 is selectively decreased when there is no presynaptic CB1 expression (Fitzgerald *et al.*, 2013). In female mice (not modelling schizophrenia), subchronic treatment with antipsychotic drugs leads to a decrease in agonist-induced CB1 G protein activation without changing receptor number, although this is not observed in males (Wiley *et al.*, 2008).

As might be expected with their overlapping expression patterns, many of the movement disorders where CB1 is a therapeutic target also involve D2 dysregulation. For example, in Huntington's disease, D2 receptor expression declines alongside CB1 expression during the early stages of the pathology (Glass *et al.*, 2000). Levodopa treatment for Parkinson's disease functions to increase dopamine levels, but

often induces dyskinesias. CB1 agonists may act to counter this side effect, as has been seen in animal models (Morgese *et al.*, 2009).

CB1-D2 signalling interaction in cells

In the striatal medium spiny neurons, knockdown of either CB1 or D2 receptors reduced the expression of the other (Blume *et al.*, 2013), suggesting that protein levels are closely controlled by the activity of both receptors. As touched on earlier, the Gαs signalling phenotype of CB1 was first described in cells which endogenously express both CB1 and D2 (Glass *et al.*, 1997). When these striatal medium spiny neurons were treated concurrently with CB1 agonist (HU210) and D2 agonist (quinpirole), forskolin-induced cAMP production was increased, rather than decreased, despite both receptors being activated individually leading to a decrease in cAMP accumulation. This effect could also be replicated in HEK293 cells (Kearn *et al.*, 2005). This signalling switch has been found to be dependent on the co-expression of these two receptors (Jarrahian *et al.*, 2004), leading to the hypothesis that this was due to a direct physical interaction between the two receptors i.e. heterodimerisation.

CB1-D2 heterodimerisation

Several experimental approaches have been used to demonstrate that CB1 and D2 coexist in a heterodimer. The first demonstration that the receptors were part of a multiprotein complex came from co-immunoprecipitation experiments (Kearn *et al.*, 2005), followed by FRET (Carriba *et al.*, 2008; Marcellino *et al.*, 2008) and BiFC (Przybyla *et al.*, 2010).

The first co-immunoprecipitation experiments showed that the CB1-D2 heterodimer was predominantly transient, with a low level of basal dimer detected, which became significantly increased after short-term (7 minute) co-incubation with CB1 and D2 agonists (Kearn *et al.*, 2005). However, recently a study has used co-immunoprecipitation to detect considerable constitutive heterodimer (Khan *et al.*, 2014). As constitutive heterodimer has been reported many times using other techniques (Khan *et al.*, 2014; Marcellino *et al.*, 2008; Przybyla *et al.*, 2010), this perhaps indicates that the co-immunoprecipitation conditions in the original study were unable to efficiently pull down the constitutive heterodimer.

Longer-term drug incubations have also been tested by FRET, with no change to constitutive CB1-D2 FRET efficiency after 45 minute incubation with CB1 and/or D2 agonists (Marcellino *et al.*, 2008). FRET between CB1 and D2 was also reported as part of a study of adenosine A2A-CB1-D2 oligomers, where sequential BRET-FRET studies showed that both CB1 and D2 demonstrated a BRET interaction with A2A, and could then further transfer this energy via a FRET interaction to the third receptor (Carriba *et al.*, 2008; Navarro *et al.*, 2010). Another indication that these three receptors oligomerise comes from a BiFC-BRET study, in which A2A and CB1 had a BiFC interaction, and this fluorophore was used as the acceptor in a BRET interaction with D2 (Navarro *et al.*, 2008b). However, neither of these studies investigated the effects of drug treatment on oligomer stability. Data also suggest that CB1 and D2 can exist in mosaics, containing the adenosine A2A receptor and metabotropic glutamate receptor mGlu5, which is discussed elsewhere (Agnati *et al.*, 2010a; Navarro *et al.*, 2008b; Navarro *et al.*, 2010)

Multicolour BiFC was used to investigate competition between D2-D2 and CB1-D2 dimers, both of which were determined to be formed constitutively (Przybyla *et al.*, 2010). This study found that long-term (20

hour) treatment with either a CB1 agonist or D2 agonist drove formation of CB1-D2 heterodimer over D2-D2 homodimer. This effect was replicated with the expression of a constitutively active CB1 mutant.

Two previous studies have identified sites for the CB1-D2 heterodimer interface. These include intracellular loop 3 (residues T321 and S322) of CB1 and the intracellular loop 3 of D2 (Navarro *et al.*, 2010), as determined by a reduction in FRET efficiency; and the CB1 C terminus (C417-S431 in rat, which is identical throughout to human C415-S429) with D2 intracellular loop 3 (Khan *et al.*, 2014), as defined by peptide interference in co-immunoprecipitation.

Aims and hypotheses

Current evidence indicates that CB1 and D2 receptor interact, most likely as a heterodimer, in neurons of the striatum. Because this brain region is affected in several disease states, they offer an attractive target for drug development. However, in order to embark on rational drug design, the CB1-D2 heterodimer requires more investigation into its function. Therefore, this thesis aims to explore the functional interactions of these receptors, from the assumption that they form a physically-interacting heterodimer.

Aim 1: Optimise a BRET assay to detect CB1-D2 heterodimerisation, and use this to investigate features of the constitutive and ligand-driven dimerisation states

Several studies have demonstrated constitutive CB1-D2 heterodimerisation (Carriba *et al.*, 2008; Khan *et al.*, 2014; Marcellino *et al.*, 2008; Przybyla *et al.*, 2010), although only one study has looked for, and found, ligand-dependent dimerisation (Kearn *et al.*, 2005). BRET allows real-time measurement of protein interactions, making it a suitable method to observe dynamic changes in receptor heterodimerisation interactions. First, a BRET assay needed to be developed to determine whether constitutive heterodimer formation could be observed in the HEK293 FT cell line, using a rationalised experimental design (Chapter 3). Then the optimised method was utilised to determine whether the BRET approach could detect heterodimerisation modified by agonist co-stimulation. Finally, the BRET assay was utilised to explore a predicted CB1-D2 dimer interface through receptor mutation studies (Chapter 4).

Aim 2: Examine CB1-D2 trafficking interactions and the phenotypic changes of the D2 receptor based on co-expression with CB1

While the signalling ramifications of CB1/D2 heterodimer interactions have been extensively investigated, it has also been demonstrated for many GPCR heterodimers that dimer formation alters receptor trafficking profiles, affecting both constitutive and ligand-driven receptor trafficking. To date no studies have investigated this effect in the CB1-D2 heterodimer. Therefore, the expression and trafficking phenotypes of CB1 and D2 were investigated in transfected HEK293 cells (Chapter 5). These studies produced the unexpected finding that CB1 expression appeared to stabilise the expression of D2 receptors in the HEK cells, therefore this was further investigated (Chapter 6)

Aim 3: Explore the role of CB1 in the altered cAMP signalling of the CB1-D2 heterodimer

The initial hypothesis put forward by Glass et al (1997) suggested that the cAMP signalling profile of co-stimulated CB1 and D2 receptors was due to the receptors competing for Gαi proteins (Glass *et al.*,

1997). When Gαi proteins are limited, CB1 couples to Gαs instead, which manifests as a “switch” from inhibiting to stimulating cAMP synthesis. Thus, following this theory, co-expression of any Gαi-linked GPCR with CB1 would replicate this phenotype. However, no studies have yet tested this hypothesis. For this reason, the relationship between CB1 expression level and cAMP signalling phenotype (without D2) was explored, in an attempt to replicate the CB1-D2 signalling phenotype (Chapter 7).

2. General methods

Materials

Cells were grown in culture reagents (Dulbecco's modified Eagle medium (DMEM), foetal bovine serum (FBS), Hank's balanced salt solution (HBSS), bovine serum albumin (BSA), poly-L-lysine, G418 and zeocin) supplied by Life Technologies (CA, USA) or Sigma-Aldrich (Australia), on plasticware supplied by Corning (NY, USA). Unless otherwise stated, receptor cDNA constructs were purchased from Missouri cDNA Resource Center (MO, USA). Drugs (forskolin, CP55,940, WIN55,212-2, delta-9-tetrahydrocannabinol (THC), quinpirole, raclopride) were obtained from Tocris Bioscience (UK) and Sigma Aldrich (Australia), with the exception of human PACAP (residues 1-27; GenScript, NJ, USA). Coelenterazine h was purchased from Promega (WI, USA) and Nanolight (AZ, USA).

Molecular biology

GPCR constructs for transient and stable transfections

This thesis utilises a range of plasmid constructs encoding G protein-coupled receptors (GPCRs). With the exception of those used in Chapters 3 and 4, these plasmids were previously prepared in the Receptor Signalling Laboratory. For reference, the GPCR constructs used for transfections are described in Table 2.1. GPCR constructs used in bioluminescence resonance energy transfer (BRET) experiments are detailed in Chapters 3 and 4.

V8-CAMYEL plasmid construction

The Venus-Rluc8 variant of "cAMP sensor using YFP-Epac-Rluc" (V8-CAMYEL) plasmid was constructed by Gibson Assembly (New England Biolabs, MA, USA) using PCR products generated using KAPA HiFi polymerase (KAPA biosystems, MA, USA), following the manufacturers' protocol. Venus was amplified from Venus-pcDNA3 (Kevin Pfleger, University of Western Australia, Australia); Rluc8 from Rluc8-pcDNA3.1+ (Sanjiv Sam Gambhir, Stanford University, CA, USA); EPAC exon 1 and the pcDNA3L-His plasmid backbone were from pcDNA3L-His-CAMYEL (American Type Culture Collection (ATCC), VA, USA).

Table 2.1 Plasmid constructs for stable and transient transfection of GPCRs.

Annotation in text	Coding region	Vector	Source
3HA-hCB1	Human CB1, with three HA tags at the N-terminus	pEF4a	As described in (Cawston *et al.*, 2013; Grimsey *et al.*, 2010)
PPLSS-3HA-hCB1	3HA-hCB1 as above, with a preprolactin signal sequence at the N-terminus	pEF4a	As described in (Grimsey *et al.*, 2010)
3HA-hCB2	Human CB2, with three HA tags at the N-terminus	pEF4a	As described in (Grimsey *et al.*, 2011)
flag-hD2	Human D2, with one flag tag at the N-terminus	pcDNA3.1+	D2 in pcDNA3.1+ from Missouri cDNA (cat. #DRD0200001); flag tag (DYKDDDDK) introduced by PCR

Table 2.2 Cell lines utilised.

Annotation in text	Parental cell line	Stably-expressed transgenes[a]	Maintenance antibiotics	Source
HEK FT	HEK293 FT	n/a	G418	Kevin Pfleger, University of Western Australia, Australia
HEK wt	HEK293	n/a	n/a	ATCC (cat. CRL-1573)
HEK 3HA-hCB1	HEK293	3HA-hCB1	Zeocin 350 µg/ml	As described in (Cawston *et al.*, 2013)
HEK 3HA-hCB1 /flag-hD2	HEK 3HA-hCB1	3HA-hCB1, flag-hD2	Zeocin 350 µg/ml, G418 400 µg/ml	Generated by transfection of flag-hD2 into the HEK 3HA-hCB1 clonal cell population.
HEK 3HA-hCB2	HEK 293	3HA-hCB2	Zeocin 350 µg/ml	As described in (Grimsey *et al.*, 2011)
HEK-V8-CAMYEL	HEK293 FlpIn	V8-CAMYEL	G418 400 µg/ml	HEK293 FlpIn cells (Invitrogen, cat. R750-07), transfected with V8-CAMYEL.

[a] Refer to Table 2.1

Cell culture

All HEK wildtype (wt) cells were cultured in DMEM + 10% FBS, at 37 °C in 5% CO_2. Stable cell lines were generated utilising the constructs described in Table 2.2, by transfection with Lipofectamine 2000 (Invitrogen, CA, USA) following the manufacturer's instructions. Cells expressing the protein of interest were selected, using zeocin 350 µg/ml (for pEF4a vectors) and G418 550 µg/ml (for pcDNA3.1-derivative vectors). Clonal cell populations were isolated by the colony picking method and validated for receptor expression by immunocytochemistry and maintained in antibiotics as described in Table 2.2. Stably transfected cell lines were used in Chapters 5, 6 and 7.

HEK FlpIn cells (Invitrogen, CA, USA) were stably transfected with the V8-CAMYEL biosensor (described below), using the pcDNAL-His-V8-CAMYEL plasmid and Lipofectamine 2000 (Invitrogen, CA, USA) transfection reagent, following the manufacturer's protocol. This construct was transfected using the standard, random-integration transfection method, so that the FlpIn site remained available for future transfection. Cells were grown in DMEM + 10% FBS, with 400 µg/ml G418 as a selection antibiotic. Clonal cell populations were isolated by the colony picking method and validated for Venus expression by microscopy.

Transient transfections

Polyethylenimine transfections

HEK FT cells were transiently transfected using the polyethylenimine (PEI) method in 6-well plates. Plasmid DNA was mixed at a 1:6 ratio with PEI (Polysciences, Taiwan) in 150 mM NaCl, and after a 10 minute incubation was applied to the media of cells at approximately 50% confluency. Twenty four hours after transfection, cells were replated at a density of 30,000-60,000 cells/well in poly-L-lysine-treated white 96-well plates (Perkin Elmer, MA, USA) for BRET assays, and clear 96-well plates (Nunc, ThermoFisher Scientific, MA, USA) for immunocytochemistry. Cells were assayed (as below) 48 hours after transfection.

Lipofectamine 2000 transfections

HEK cells, stably transfected with various constructs, were transiently transfected in 96-well plates or 100 mm dishes using Lipofectamine 2000, following the manufacturer's protocol. Experiments were performed 48 hours after transfection.

cAMP assays

Cytoplasmic cAMP signalling was measured in live cells using a cAMP biosensor. The 'cAMP sensor using YFP-Epac-Rluc' ("CAMYEL") biosensor was developed by Jiang *et al.* (2007), and purchased from ATCC. In this biosensor, cytoplasmic cAMP concentration is indicated through changes in bioluminescence resonance energy transfer (BRET) signal, which can be measured in real time in live

cells (see Figure 2.1). A variant biosensor, V8-CAMYEL, was developed for use in this thesis, because cell number was limited in several of the experiments (particularly Chapter 7). V8-CAMYEL contains a modified luciferase and acceptor fluorophore, in order increase the bioluminescent output of the biosensor and better exploit the sensitivity range of standard luminescence plate readers. The luciferase was changed to the luciferase mutant "Rluc8" (Loening *et al.*, 2006) and the fluorescent acceptor was changed to Venus (Nagai *et al.*, 2002) and the resulting construct named "V8-CAMYEL" (Figure 2.1).

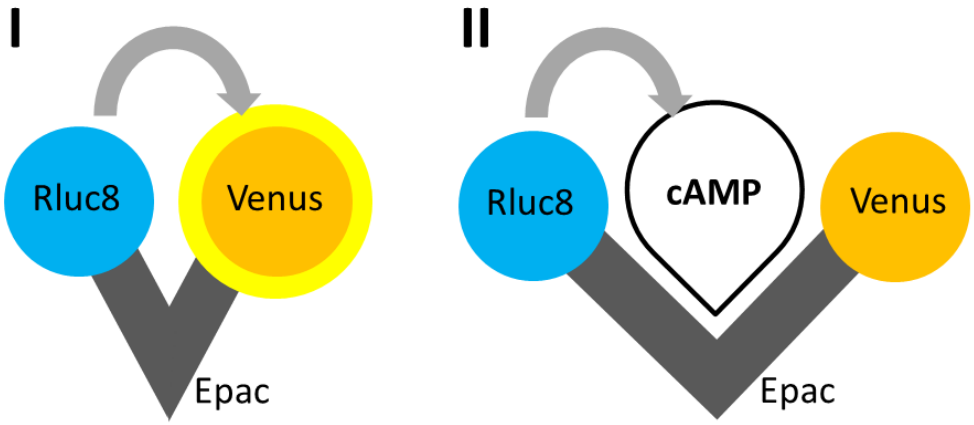

Figure 2.1 Design of the V8-CAMYEL cAMP biosensor.

The BRET pair in V8-CAMYEL is separated by the cAMP sensor 'Epac'. I.) When no cAMP is bound, resonance energy transfer can occur between Rluc8 and Venus. II.) When cAMP is present in the Epac binding site, Rluc8 and Venus are further apart, and energy transfer is reduced.

Validation of the V8 CAMYEL biosensor

To determine that the V8-CAMYEL biosensor acted equivalently to the original CAMYEL construct, cAMP assays were performed using both biosensors. The HEK 3HA-hCB1 cell line was transiently transfected with either the CAMYEL or V8-CAMYEL construct using PEI, as described above. Cells were assayed for changes in cytosolic cAMP as described below. Area under the curve measurements were taken across 20 minutes. In the case of PACAP, data were collected 5 minutes after agonist addition for 15 minutes. Signal-to-noise ratios were calculated by dividing the mean BRET ratio by the standard deviation, across all readings between 9-11 minutes after drug addition. This time point was chosen because drug responses were generally observed to be stable by this time, allowing a measurement of steady-state biosensor response. The results of these validation experiments are detailed in the Appendix.

Preparation of cells for cAMP assays

In Chapters 6 and 7, the V8-CAMYEL biosensor was used to measure changes in cytosolic cAMP. Cells were transfected using Lipofecamine 2000, as described above. In Chapter 6, cells were seeded at 20,000-30,000 cells/well, transfected, and assayed in poly-L-lysine treated white 96-well plates. In

Chapter 7, cells were seeded and transfected in 100 mm dishes. Cells were harvested and plated on Nunc plates for immuno-labelling on the day of the cAMP assay (described in Chapter 7).

Detection of cytosolic cAMP changes by BRET

All cAMP assays were performed 48 hours after transfection. Cells were equilibrated with assay buffer (HBSS + 1 mg/ml BSA) for 30 minutes, and then incubated for a further 5 minutes with the luciferase substrate coelenterazine h to a final concentration of 5 µM. Drugs were then added, and luminescence was detected immediately in a VictorXLight plate reader (Perkin Elmer, MA, USA), using 460/25 nm and 535/25 nm filter sets, with temperature control at 37°C.

An inverse BRET ratio was calculated by dividing the donor signal by the acceptor signal, such that higher BRET ratio reflects more cytoplasmic cAMP concentration. Inverse BRET ratio responses for 15-20 minutes were measured, and plotted as a function of time. The overall response over time was determined by an area under the curve calculation, representing the cumulative cAMP response. Data was processed and graphed using Prism (version 6, GraphPad, CA, USA), and agonist responses normalised to Vehicle (0%) and forskolin (100%).

General immunocytochemistry

Sample preparation

Transiently- or stably-transfected cells were seeded in poly-L-lysine treated Nunc clear 96-well plates, and grown for 24 hours at 37 °C, 5% CO_2. The various cell lines were seeded such that they were 50-80% confluent at the time of antibody application. When cells were to be labelled with more than one antibody, they were applied simultaneously to the same wells if the antibodies were from different species, or separately on replicate samples when the antibodies were sourced from the same species.

For experiments requiring specific labelling of the surface receptor population, cells were equilibrated with assay media (DMEM + 5 mg/ml BSA) for 30 minutes, then incubated with primary antibodies for 30 minutes at 37 °C to label surface receptors. Cells were then washed twice with assay media before fixation with 50% methanol + 50% acetone at 4 °C, or 4% PFA at room temperature, for 10 minutes. For experiments requiring labelling of the total cell population, primary antibodies in phosphate buffered saline containing 1% normal goat serum, 0.1% Triton X-100, and 0.4 mg/ml thiomersal were applied after fixation. Secondary antibodies were then applied in the same buffer as above. Finally, DNA was stained with Hoechst in phosphate buffered saline containing 0.1% Triton X-100.

Table 2.3 Antibodies used in immunocytochemistry experiments.

Antibody	Species raised in	Supplier (catalogue number)	Dilution, live-cell incubation	Dilution, fixed-cell incubation
anti-HA monoclonal	Mouse	Covance, NJ, USA (MMS-101P)	1:500	1:1000
anti-flag polyclonal	Rabbit	Sigma-Aldrich, MO, USA (F7425)	1:400-1:500, depending on batch	1:10,000
anti-flag monoclonal (M2)	Mouse	Sigma-Aldrich, MO, USA (F1804)	1:500-1:2000, depending on batch	n/a
anti-phospho-p44/42 MAPK (Thr202/Tyr204)	Rabbit	Cell Signaling Technology, MA, USA (4370S)	n/a	1:200
anti-mouse, Alexa 488	Goat	Molecular Probes, Life Technologies, CA, USA (A11029)	1:300	1:400
anti-mouse, Alexa 594	Goat	Molecular Probes, Life Technologies, CA, USA (A11032)	1:300	1:400
anti-rabbit, Alexa 594	Goat	Molecular Probes, Life Technologies, CA, USA (A11037)	1:300	1:400

Table 2.4 Filter sets used for Discovery-1 and ImageXpress Micro XLS microscopes.

Fluorophore(s)	Microscope	
	Discovery-1	**ImageXpress Micro XLS**
Hoechst	Excitation: 325-375 nm Emission: 450-480 nm Dichroic mirror: 435 nm	Excitation: 381-399 nm Emission: 412-455 nm Dichroic mirror: 403 nm
Alexa Fluor 488 Venus	Excitation: 453-487 nm Emission: 505-565 nm Dichroic mirror: 495-500 nm	Excitation: 461-490 nm Emission: 508-553 nm Dichroic mirror: 502 nm
Alexa Fluor 594	Excitation: 540-580 nm Emission: 625-675 nm Dichroic mirror: 580 nm	Excitation: 561-590 nm Emission: 612-643 nm Dichroic mirror: 604 nm

Image acquisition and analysis

Images were acquired using the Discovery-1 and ImageXpress Micro XLS (both Molecular Devices, CA, USA) automated microscopes, at 10x magnification, with four sites imaged per well. All data for each set of experiments was acquired using the same microscope, to minimise any variation due to different microscope camera sensitivities.

To analyse the number of cells labelled, images were analysed using the MetaXpress (version 5.3.0.4, Molecular Devices) "Multiwavelength cell scoring" function, or the MetaMorph (versions 6 and 10; Molecular Devices) "Cell scoring" functions. These functions identify each cell by nuclear Hoechst staining, followed by segmentation of one or both wavelengths of interest in a user-defined "nucleus and cytoplasm" area and provides staining intensity data for each individual cell in every image. Therefore these analyses provide data for each individual cell in each image.

To analyse the average intensity of labelling across the total population of cells, images were processed using MetaMorph software (versions 6 and 10), using the "Total Grey Value Per Cell" method previously described by Grimsey, *et al.* (2008b). This analysis paradigm measures fluorescent antibody labelling above a user-defined background, and averages it across the total number of nuclei counted per image. This analysis provides labelling intensity results as a population average.

Radioligand binding

Whole cell radioligand binding

Cells were seeded at 125,000 cells/well in 24-well plates and grown for 24-48 hours. Cells were then incubated for 30 minutes with assay buffer (DMEM + 5 mg/ml BSA), followed by 30 minutes with [^{3}H]-raclopride (Perkin Elmer, MA, USA) at 1.3 nM, with or without 20 µM unlabelled raclopride as a displacer. Assay buffer was removed and cells were washed twice in ice-cold phosphate buffer saline, then lysed in 0.1 M NaOH for 10-20 minutes. Lysate samples were then mixed with IrgaSafe scintillation fluid (PerkinElmer, MA, USA) and scintillation events were measured for 2 minutes in a Wallac 1450 MicroBeta TriLux (Perkin Elmer, MA, USA). Lysate samples were also assayed in DC protein assay (Biorad, CA, USA) to enable normalisation to protein concentration.

Calculation of receptor number

Receptor density was calculated either from the results of saturation binding assays, or from extrapolation from a single concentration of radioligand. The Kd of raclopride was determined experimentally as 2.0 nM (Hunter, 2010).

When a single concentration of radioligand was utilised, total receptor number was determined using the following equation:

$$\text{Total receptors (fmol/sample)} = \text{Bmax} = \frac{\text{B0 x (Kd + L)}}{\text{L}}$$

Where: Bmax is maximum radioligand binding, B0 is specific radioligand binding in the assay conditions, Kd is the Kd of the radioligand, and L is the ligand concentration used in the experiment.

Statistics and data presentation

Statistical analysis

GraphPad Prism (version 6, GraphPad, CA, USA) and SPSS (version 21, IBM, NY, USA) were used to test for statistical significance. The Brown-Forsythe test for equal variance was performed to ensure parametric testing was appropriate. In all experimental designs where matching was applicable, paired/repeated measures testing was performed, in order to control for any minor variation in absolute results between replicate experiments. A t-test was used when two experimental results were to be compared. When experiments contained three or more conditions, one-way analysis of variance (ANOVA) was used to compare independent experiments. Post-hoc testing (Tukey's or Dunnett's multiple comparison tests) was performed as appropriate, with the specific test described in the Methods of each Chapter. Where the interaction between two factors was of interest, repeated measures two-way ANOVA was performed with Sidak's multiple comparison post-test.

Data presentation

All graphs were generated in Prism (version 6), with the exception of Figure 7.2 which was generated using FlowJo (version 10, Tree Star, OR, USA). Data are shown as the mean and standard error of the mean (SEM) of a representative experiment, or combined data from multiple experiments (as appropriate), as indicated.

3. Validation of BRET for studying CB1-D2 dimerisation

Introduction

Interest in GPCR dimerisation has led to the use of biophysical principles for the measurement of such interactions. Resonance energy transfer (RET) techniques have considerably aided research into GPCR heterodimerisation, requiring only routine cloning techniques and relatively common instrumentation. These assays comprise two closely-related methods: Förster/fluorescent resonance energy transfer (FRET), and bioluminescent resonance energy transfer (BRET), differing only in their excitation energy source. Here, we will focus on BRET, in which two proteins of interest are fused to either a bioluminescent "donor" protein or a fluorescent "acceptor" protein. In studies of mammalian proteins, the bioluminescent donor is typically Renilla luciferase (Rluc), which produces light through enzymatic oxidation of a chemical substrate (coelenterazine) and the acceptor is typically Green Fluorescent Protein (GFP) or its yellow variant YFP (Pfleger *et al.*, 2006b). In FRET, both the donor and acceptor are fluorescent proteins, such as cyan and YFP (Qian *et al.*, 2014). In either case, the energy donor can transfer its energy to acceptor fluorophore, provided the excitation wavelength for the acceptor overlaps with the emission spectrum of the donor (Stryer, 1978). In a RET interaction, the excited state of the donor transfers its energy to the acceptor by a non-radiative mechanism, through dipole-dipole interactions, and without the emission/absorption of a photon (Stryer, 1978; Wolber *et al.*, 1979; Wu *et al.*, 1994). This "resonance" occurs only across very short distances, approximately 10 nm in the case of Rluc/YFP BRET (Pfleger *et al.*, 2006b). Because energy transfer can only occur over such short distances, the presence of a RET interaction is highly suggestive of a physical association between the two proteins of interest (Pfleger *et al.*, 2006a).

While both FRET and BRET have been used extensively to study GPCR heterodimerisation, they have differing applications. In FRET, monochromatic light is applied to the sample to excite the donor fluorophore (Boute *et al.*, 2002). This method of excitation gives a strong emission, making it appropriate for visualising protein interactions by microscopy (Padilla-Parra *et al.*, 2012). Unfortunately, the excitation light also excites the acceptor fluorophore, as all currently-available FRET pairs have overlapping excitation properties (Padilla-Parra *et al.*, 2012; Qian *et al.*, 2014), resulting in data which requires careful analysis. FRET is also unsuitable for longer time-scale measurements, as fluorophore bleaching and cell phototoxicity limit total assay time (Pfleger *et al.*, 2006a; Salahpour *et al.*, 2012). Similarly, the emission spectra in FRET overlap considerably, making it difficult to separate the RET signal from the individual fluorophores (Padilla-Parra *et al.*, 2012). In BRET, the excitation is specific to the donor luciferase, as the acceptor fluorophore cannot catalyse the oxidation of coelenterazine. This reduction in assay noise results in significantly increased sensitivity compared to FRET (Arai *et al.*, 2001). The luminescence resulting from this reaction is not as bright as the fluorescence achieved with FRET, meaning that BRET imaging requires sensitive cameras and long exposure times (up to 7 seconds) (Ayoub *et al.*, 2002;

Coulon *et al.*, 2008; Xu *et al.*, 2013). While the emission spectrum of the luciferase does overlap into the emission spectrum of the acceptor, this is to a lesser degree than FRET. BRET is well-suited for experiments requiring many samples because it can be easily measured using the sensitive detectors of a luminescence-capable plate reader (Boute *et al.*, 2002). The aim of this Chapter was to develop a system to measure heterodimerisation which could be used for screening ligand interactions and mutated receptors (see Chapter 4), thus BRET was determined to be the more appropriate option.

While observation of a positive BRET signal can represent strong evidence for dimerisation, experiments need to be designed carefully to minimise the possibility of a false-positive reading. The risk of observing nonspecific BRET interactions is thought to be increased when tagged receptor constructs are overexpressed (James *et al.*, 2006). As well as BRET interactions, energy transfer can also occur through radiative energy transfer termed "fluorescence by unbound excitation from luminescence" (FUEL), whereby the acceptor fluorophore is excited not through RET, but by light emitted by the donor (Holland *et al.*, 2014). Therefore at high expression levels, a measurable degree of FUEL can occur between proteins which are co-expressed, even if they are not in close proximity (Dragavon *et al.*, 2014; Holland *et al.*, 2014). Compounding this problem, some researchers report that unlikely heterodimerisation partners (such as those not normally found in the same cell type) will be identified in receptor overexpression systems simply as an artefact of overexpression (Ramsay *et al.*, 2002; Salim *et al.*, 2002; Vischer *et al.*, 2008). In order to control for this possibility a valid approach is to include suitable negative controls, however this experimental design is not trivial. A commonly utilised and convenient negative control is simply the unconjugated acceptor fluorophore (GFP or YFP) (Achour *et al.*, 2009; Cheng *et al.*, 2001; Gandía *et al.*, 2008; Kamiya *et al.*, 2003; Levoye *et al.*, 2009; Pfleger *et al.*, 2003; Szalai *et al.*, 2014), which is expressed in the cytoplasm as opposed to GPCRs, which are targeted to the membranous fractions of the cell. This makes it an imperfect control because a low proportion of the expressed cytoplasmic Venus is in proximity to the plasma membrane, therefore underestimating the local concentration of transmembrane proteins.

In light of these risks several authors have developed experimental paradigms which aim to expose the difference between specific and nonspecific BRET signals. These assays are executed by transiently expressing the tagged receptor constructs at various ratios, and observing the change in BRET signal between the conditions. By far the most widely-used BRET experimental paradigm is the "saturation" assay (Pfleger *et al.*, 2006b), thus there is a considerable body of literature to support this assay format. In this approach, the receptor tagged with the energy donor is expressed at a constant level, and the energy acceptor is expressed at increasing levels. This is designed to progressively fill all specific interaction sites on the donor receptor, the ability to saturate these sites being indicative of a genuine interaction. Less widely utilised is the "competition" assay, in which untagged receptors are transfected into cells containing the donor- and acceptor-tagged receptors; it is assumed that a resulting reduction in BRET represents competition for specific interaction sites (Pfleger *et al.*, 2006b). James, *et al.* (2006), also introduced the "type I" and "type II" assay designs. A type I assay is similar to a saturation assay paradigm, except controls for protein expression density by "swapping out" donors for acceptors, yielding a linear relationship between true heterodimerisation and nonlinear relationships for nonspecific interactions. A type II assay is executed by expressing both proteins at the same ratio, but changing the total protein density; in the case of specific heterodimerisation, the observed BRET efficiency should

remain constant as dimers “find” each other regardless of the expression level (Felce *et al.*, 2012; James *et al.*, 2006). However these have not been widely validated in the literature. Recently, Felce *et al.* (2014) have described a protocol for a type III assay which is based on the format of a competition assay but accounts for any changes in the ratios of protein expression which occur in co-transfection conditions.

The primary assumption of these assay paradigms is that transgene expression can be closely controlled in transient transfections. Most authors are apparently satisfied that quantity of plasmid in the transfection mix corresponds directly and linearly to quantity of transgenic protein expressed, for example see references (Bagher *et al.*, 2013; Jäntti *et al.*, 2014; Yasuda *et al.*, 2014). Unfortunately, this is not always a valid assumption since receptor constructs may differ in transcription and/or translation efficiency, and receptor expression may be aided by co-transfection in the case of obligatory dimers (Felce *et al.*, 2014; Szalai *et al.*, 2014). For example, CB1 constructs have been described as yielding low transgene expression in transient transfection conditions (Przybyla *et al.*, 2010), which has also been our observation. Mutant receptors are even more likely to exhibit problems with expression efficiency, yet these are often used in BRET assays to elucidate the dimer interface. Furthermore, the two plasmids used to carry the transgenes usually contain the same constitutive promoter (CMV), which may allow for promoter competition in assays where plasmid load is not tightly controlled (i.e. using empty vector).

To address this concern, some authors calculate protein “expression ratio” to replace the DNA “transfection ratio” in their analysis. Expression ratio is calculated by measuring the protein which is produced in the cells, rather than relying on the aforementioned assumption of equal efficiency across transfection conditions. There are many ways to measure relative receptor number, but the most common approach is to measure luminescence as a correlate to receptor-Rluc construct expression, and laser-excited fluorescence as a correlate to receptor-YFP expression (Frederick *et al.*, 2015; Guo *et al.*, 2008; James *et al.*, 2006; Navarro *et al.*, 2008b; Pfleger *et al.*, 2006b; Szalai *et al.*, 2014).

While using a luminescence measurement is a valiant attempt to ascertain receptor-Rluc expression, interpretation is complicated by the confounding factor that Rluc luminescence may be altered under some circumstances, including constitutively occurring BRET. This is because Rluc emission is reduced through the RET process itself; donor quenching is a required step in acceptor excitation (Sapsford *et al.*, 2006; Veatch *et al.*, 1977; Wolber *et al.*, 1979; Wu *et al.*, 1994). In the case of constitutive dimerisation, this donor quenching occurs whether or not the acceptor/fluorescence emission is being monitored. In a similar vein, radiative energy transfer (FUEL) can also occur when the donor and acceptor tags are co-expressed, which further decreases the apparent luminescence. Quenching in the donor wavelength has been observed in the data from multiple sources, beginning in the early literature of bioluminescent species (where BRET occurs *in vivo*) (Morin *et al.*, 1971), to FRET single-molecule imaging (Zhao *et al.*, 2010). Other factors can also affect luciferase activity, for example the concentration of the substrate (coelenterazine) needs to be equally distributed between conditions and samples read at the same time, as the luciferase enzymatic rate is dependent on substrate concentration.

The above considerations primarily apply to the study of constitutive heterodimers. BRET is well-suited for studying dynamic changes in protein interactions, such as ligand-mediated association, because the samples provide their own internal control. For example, if a BRET signal increases or decreases upon addition of a receptor agonist but not vehicle, then this is good evidence for a ligand-mediated change in

the protein interface (Pfleger *et al.*, 2006b). As the CB1-D2 interaction has previously been described as being somewhat ligand-mediated (Kearn *et al.*, 2005), this makes BRET a good approach. However, as the CB1-D2 heterodimer is also present constitutively (Carriba *et al.*, 2008; Khan *et al.*, 2014; Marcellino *et al.*, 2008; Przybyla *et al.*, 2010), it was imperative for this project to appropriately control for all the variables which could affect the interpretation of the detection of constitutive heterodimer. Therefore, in this chapter we explore an alternative technique to calculate receptor expression ratio using immunocytochemistry.

Methods

Cell culture

HEK FT cells were cultured as described in Chapter 2.

Plasmid construction

The human cannabinoid CB1 receptor ("hCB1"; GenBank Accession NM_016083) and dopamine D2 (long isoform) receptor ("hD2"; GenBank Accession NM_000795) in pcDNA3.1+, with or without three HA tags chimerised at the receptor N-terminus, were sourced from Missouri S&T cDNA Resource Centre (MO, USA); Rluc8 pcDNA3.1+ was kindly gifted by Sanjiv Sam Gambhir (Stanford University, CA, USA); and Venus pcDNA3 was sourced from Kevin Pfleger (University of Western Australia, Australia). Stop codons were removed by PCR, and 3HA-hCB1 and 3HA-hD2 were inserted with restriction digest into Rluc8 pcDNA3.1+, while untagged-hCB1 and untagged-hD2 were inserted into Venus pcDNA3, in order to create a C-terminally tagged receptor, with a four amino-acid linker sequence separating the receptor and the BRET tag. In order to increase surface expression of hCB1-Venus, the bovine preprolactin signal sequence (GenBank Accession AF426315.1) was added to the extreme N-terminus to aid protein folding.

Transient transfection

HEK FT cells were transiently transfected using the PEI method, as detailed in Chapter 2. To achieve the expression conditions for the saturation assay, hCB1 and hD2 constructs tagged with Rluc8 or Venus were co-transfected at various ratios. Empty pcDNA3.1+ plasmid was used to maintain total DNA content when required. Twenty-four hours after transfection, 40,000-60,000 cells/well were reseeded into white 96-well plates (Perkin Elmer, MA, USA).

pERK signalling assay

Cells were transfected as above with one receptor construct at a time, and seeded onto clear Nunc plates (ThermoFisher Scientific, MA, USA). Approximately 6-8 hours before assaying, media was changed to serum-free media (DMEM + 5mg/ml BSA) to stabilise basal pERK signalling. Cells were incubated at 37°C with the appropriate receptor agonist for 5 minutes, then fixed immediately in 4% paraformaldehyde. Treatment with 90% methanol, for 10 minutes at -20°C was used to unmask pERK epitopes. Immunocytochemical detection of pERK was performed as described in Chapter 2, utilising the following antibodies: rabbit anti-phospho-p44/42 MAPK (Thr202/Tyr204), anti-HA (where required), goat anti-rabbit Alexa Fluor 594, goat anti-mouse Alexa Fluor 488). Images were acquired using ImageXpress

Micro XLS automated microscope (Molecular Devices, CA, USA) as described in Chapter 2, and processed using a custom journal in MetaMorph (version 10, Molecular Devices). This custom analysis journal was written by Natasha Grimsey (University of Auckland, New Zealand), and acts to restrict the pERK analysis to only cells which are transfected with the receptor of interest (i.e. labelled with the HA antibody, or expressing Venus) by excluding all areas of each site which do not have HA/Venus expression above a user-defined threshold. Then the pERK antibody labelling is acquired in an analogous method to the "Total Grey Value Per Cell" protocol, described in Chapter 2. This is required to compensate for the variable transfection efficiency of the constructs (i.e. proportion of cells detectably expressing the transfected construct).

Measurement of bioluminescence resonance energy transfer (BRET) measurement

Cells were assayed 48 hours after transfection. Assay buffer contained HBSS with 1mg/ml BSA. Cells were rinsed with HBSS to remove traces of phenol red from the plating media. Cells were then incubated with assay buffer for 30 minutes, and subsequently coelenterazine h (Promega, WI, USA and Nanolight, AZ, USA) was applied to a final concentration of 5μM and allowed to equilibrate for a further 5 minutes before BRET measurement. BRET measurements were taken using a VictorXLight plate reader (Perkin Elmer, MA, USA), with Rluc8 emission collected at 460/25nm and Venus emission collected at 535/25nm.

BRET analysis

Calculations for BRET ratio, transfection and expression ratios are detailed in Table 3.1. Once BRET saturation data were plotted, hyperbolic curves were fitted using Prism (version 6, GraphPad, CA, USA).

Immunocytochemistry

Cells were fixed in 4% paraformaldehyde for 10 minutes at room temperature and immunocytochemistry was performed to detect whole-cell receptor expression levels, as described in Chapter 2. In order to visualise 3HA-hCB1-Rluc8 and 3HA-hD2-Rluc8 localisation, samples were incubated with mouse anti-HA antibody, followed by goat anti-mouse Alexa 594, and nuclei stained with Hoechst. Images were acquired using ImageXpress Micro XLS automated microscope at 10x magnification, using the filters described in Table 2.4.

Image analysis

Microscope images were processed using MetaMorph (version 10, Molecular Devices) using the "Total Grey Value Per Cell" method, which enabled the intensity of fluorescent labelling to be measured, as described in Chapter 2.

Multiwavelength cell scoring and thresholded intensity data were then processed by Excel (Microsoft), followed by graphing and statistical analysis in Prism (version 6, GraphPad). For pERK data, results were analysed using one way ANOVA with Dunnett's post-test, with matching within an experimental replicate. "Rluc8 activity per receptor" calculation results were analysed by paired T-tests, with pairing between replicate experiments. BRET saturation results (Kd and Bmax from hyperbolic curve fits) were analysed with one way ANOVA with Tukey's post-test.

Table 3.1 Calculations used for analysis of BRET experiments.

Parameter	Data source	Calculation
Rluc8 activity per receptor	Rluc8 activity: Plate reader, 460/25nm filter HA labelling: fluorescent antibody labelling, imaged by microscopy	$= \frac{\text{peak Rluc8 activity}}{\text{fluorescent antibody labelling of Rluc8 construct per cell}}$
BRET ratio	Rluc8: Plate reader, 460/25nm filter Venus: Plate reader, 535/25nm (Venus) filter	$= \frac{\text{Venus emission}}{\text{Rluc8 emission}} - \frac{\text{Venus emission when Rluc8 alone}}{\text{Rluc8 emission when Rluc8 alone}}$
Transfection ratio	Transfection calculations	$= \frac{\text{ng of Venus plasmid DNA}}{\text{ng of Rluc8 plasmid DNA}}$
Expression ratio using luciferase activity	Venus: fluorescence imaged by microscopy, background subtracted Rluc8 activity: Plate reader, 460/25nm filter	$= \frac{\text{Venus fluorescence per cell}}{\text{peak Rluc8 activity}}$
Expression ratio using protein expression	Venus: fluorescence imaged by microscopy, background subtracted Rluc8: fluorescent antibody labelling, imaged by microscopy, background subtracted	$= \frac{\text{Venus fluorescence per cell}}{\text{fluorescent antibody labelling of Rluc8 construct per cell}}$

Results

CB1 and D2 BRET constructs signal through pERK

The human CB1 and D2 receptors were C-terminally tagged with Rluc8 or Venus, in order to create all possible combinations of receptor and tag. These constructs were then transiently transfected into HEK FT cells and a pERK assay was performed to determine whether they had maintained their signalling capacity. As shown in Figure 3.1, all the constructs were able to signal through pERK to an equivalent degree as the control receptors.

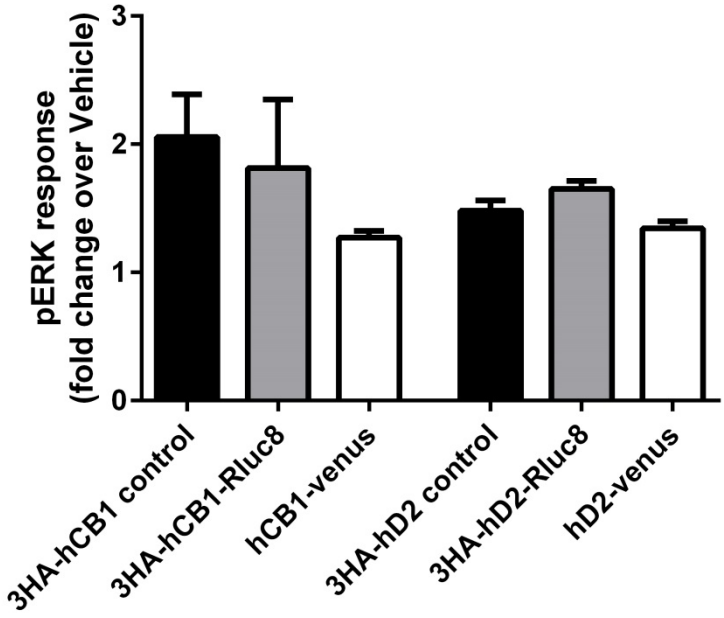

Figure 3.1 pERK signalling of receptor constructs used in BRET interaction studies.

Transfected cells were treated for 5 minutes with 1 μM CP55,940 or quinpirole, for CB1 and D2 receptor constructs respectively. Mean ± SEM for two to five independent experiments. No statistical difference was observed in the extent of receptor mediated activation of pERK compared to control receptors for either CB1 or D2 BRET constructs (one-way ANOVA with Dunnett's post-test).

Transfection and expression efficiency under co-transfection conditions

Next, we began the optimisation of the BRET experiments for both the D2 homodimer (as a positive control (Guo *et al.*, 2003; Guo *et al.*, 2008)) and the CB1-D2 heterodimer. In parallel with the BRET assays detailed below, we also determined the expression levels of each construct in every transfection condition. Samples were therefore processed by immunocytochemistry of the HA tag on Rluc8 constructs and quantified by automated fluorescent microscopy for HA staining and Venus fluorescence to determine expression of the two co-expressed constructs. This allowed the measurement of the receptor expression independent of the BRET interaction.

Although all transfection conditions contained the same quantity of receptor-Rluc8 plasmid, this did not yield equal expression of this construct. When transfection conditions were modified to introduce varying quantities of a second receptor construct (i.e. to enable a "saturation" experiment), a substantial reduction in receptor-Rluc8 expression levels was observed, as shown in Figure 3.2. That is, when co-transfected with a Venus construct, both 3HA-hD2-Rluc8 and 3HA-hCB1-Rluc8 showed a considerable decrease in expression compared to when transfected alone, with receptor levels as low as 10-30% of the cell population transfected with receptor-Rluc8 alone. This was despite all transfection conditions having been transfected with the same total quantity of plasmid DNA, with non-coding empty pcDNA3.1+ vector used to compensate for changes in coding plasmid.

The receptor expression profiles are shown in Figure 3.2, with the percentage of cells expressing the Rluc8-tagged receptor plotted as a function of the quantity of receptor-Venus plasmid in the transfection condition. When only D2 constructs were transfected, 3HA-hD2-Rluc8 expression reduced as the quantity of hD2-Venus plasmid was increased (Figure 3.2(A)). However, when CB1 was transfected with D2 (with either tag pairings) this reduction was dramatic even for transfection conditions containing very low quantities of plasmid encoding the receptor-Venus construct (Figure 3.2(B, C)).

The only difference in the transfection conditions was the quantity of plasmid encoding the Venus-receptor construct. There was no change in cell density/growth, indicating that this effect is not merely related to toxicity of the receptor constructs. As the HA tag used for the immunocytochemical detection of the Rluc8-receptor constructs was on the N-terminus of the receptor, held on the opposite side of the plasma membrane from the C-terminal Rluc8 and Venus tags, it is highly unlikely that changes in HA antibody binding to the Rluc8-tagged receptor construct would be affected merely by the presence of the Venus on the introduced receptor construct. These experiments seem to show that receptor expression resulting from transient transfection cannot be inferred directly from the amount of DNA transfected. Given that the ratio of receptor expression is pertinent to interpretation of BRET saturation assays, these experiments imply that it may be more accurate to measure expression directly.

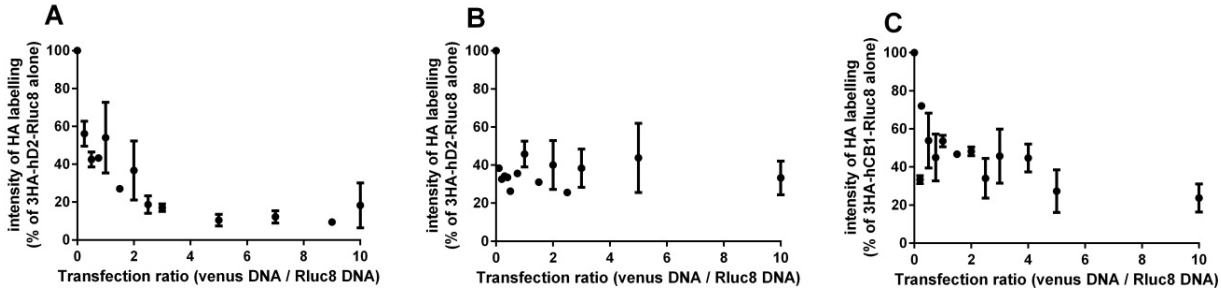

Figure 3.2 Receptor expression of cells transfected for BRET saturation assays.

HA labelling, indicative of Rluc8-tagged receptor expression, in BRET saturation experiments with A.) 3HA-hD2-Rluc8 and hD2-Venus; B.) 3HA-hD2-Rluc8 and hCB1-Venus; or C.) 3HA-hCB1-Rluc8 and hD2-Venus. Cells were transfected with a constant quantity of 3HA- and Rluc8-tagged receptor encoded in plasmid DNA, and increasing quantities of Venus-tagged receptor plasmid. HA labelling was normalised as a percentage of HA-labelling in the transfection condition containing no Venus-tagged receptor. Mean ± SEM of three independent experiments.

Luciferase emission in cells co-transfected with BRET receptor constructs

As demonstrated above, it is important to have a measure of receptor-Rluc8 expression, as this is significantly affected by co-transfection conditions. Previous studies have utilised luciferase signal (as measured in a luminometer plate reader) as a surrogate measure of Rluc8-tagged receptor expression. However as described in the Introduction, in theory this approach might not be accurate. To investigate whether luciferase activity and protein expression were correlated, luciferase activity was compared to

immunocytochemical labelling of the HA epitope both in the presence and absence of a Venus tagged receptor. As represented in Figure 3.3(A), luciferase activity and anti-HA labelling of Rluc8-tagged receptors are poorly correlated. Cells with essentially identical HA labelling demonstrate markedly different luciferase activity, and cells with very similar luciferase counts can have very different quantities of HA-labelling. In general, it appeared that cells transfected with less receptor-Venus construct gave higher luciferase counts, compared to other transfection conditions with similar HA-labelling but co-transfected with more Venus.

In cells not co-transfected with Venus, we noticed a lower-than-expected luminescence emission. As shown in Figure 3.2, cells transfected with Rluc8-tagged receptor alone have much higher protein expression (measured by HA-labelling) than cells which are co-transfected with Venus-tagged receptors. The HA quantification for true receptor-Rluc8 expression can be utilised to adjust the luminescence data for this change in overall expression, thus allowing direct comparison of the luciferase output per receptor expressed by dividing Rluc8 light emission by HA-labelling measured by microscopy and normalising for any variation in cell number. This is shown in Figure 3.3(B), which summarises the luciferase emission per receptor between Rluc8-tagged receptors transfected alone, compared to when they are co-transfected with Venus-receptor construct. The analysis demonstrates that, when expressed with an excess of Venus-tagged receptor, both 3HA-hD2-Rluc8 and 3HA-hCB1-Rluc8 emit more light in the 460/25nm range compared to when they are expressed alone.

Regardless of the mechanism of these observations, these results demonstrate that luciferase emission does not exhibit a linear relationship with receptor expression levels.

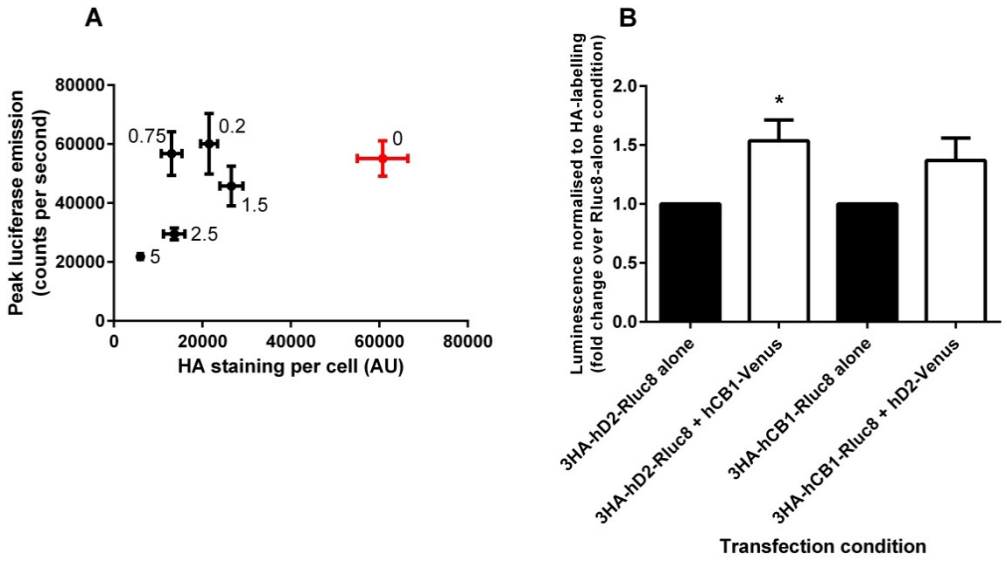

Figure 3.3 Comparison of HA-labelling with Rluc8 activity under various transfection conditions.

*Cells were transfected with the same quantity of HA- and Rluc8-tagged receptor plasmid, and varying quantities of Venus-tagged receptor. A.) 3HA-hCB1-Rluc8 luciferase emission compared to HA labelling detected by immunocytochemistry (arbitrary units). Each data point is labelled with the proportion of hD2-Venus in the transfection compared to 3HA-hCB1-Rluc8. Black data points are for transfection conditions containing 3HA-hCB1-Rluc8 and hD2-Venus, red data point is 3HA-hCB1-Rluc8 transfected alone. Representative results from one of three experiments using 3HA-hCB1-Rluc8, showing mean ± SEM of technical replicates. Similar results were obtained using 3HA-hD2-Rluc8. B.) Rluc8 activity per receptor when expressed alone (transfection ratio 0), and when co-transfected with five times excess of plasmid coding for Venus-tagged receptors. For each experiment, mean peak luminescence of 6 wells was divided by the mean HA-labelling of 12 sites detected by fluorescence microscopy and data were normalised to cell number. Results from three to five independent experiments, mean ± SEM. * $p<0.05$.*

BRET saturation experiments for D2-D2 and CB1-D2 dimers with normalisation of receptor expression by transfection ratio versus expression ratio calculated by two methods

BRET saturation experiments were performed to determine whether the putative D2-D2 and CB1-D2 interactions reported in the literature represented specific dimerisation interactions. Cells were transfected with a constant quantity of receptor-Rluc8 construct, and increasing quantities of receptor-Venus construct. BRET assays were performed to measure constitutive interactions (that is, without the influence of receptor ligands). The results from a saturation experiment can have a rectangular hyperbola fitted by nonlinear regression. This yields a Bmax measured in BRET ratio arbitrary units (i.e. the predicted maximum energy transfer), and a Kd measured in receptor expression ratio (also arbitrary units). Kd is the receptor expression ratio required to reach half-Bmax BRET ratio.

In order to carry out BRET saturation experiments, BRET ratios should be plotted in correlation with the ratio of receptor-Rluc8 to receptor-Venus expression. As demonstrated above, neither the amount of DNA transfected nor luciferase activity correlated well with true receptor expression, yet these measures

are both commonly assumed to represent expression and are widely utilised in the literature to assess BRET saturation curve data. We were therefore interested to assess the results from BRET saturation assays analysed with these measures in comparison with data from the immunocytochemistry analysis noted above, which is seemingly a more accurate measure of expression. Therefore, first, the BRET signal was plotted against the transfection ratio (i.e. copies of receptor-Venus plasmid DNA). Then, results were re-plotted against the luciferase-derived expression ratio, a method which is commonly used in the literature. Finally, the BRET results were plotted against the immunocytochemistry-derived expression ratio. In the immunocytochemistry normalisation, the arbitrary units between 3HA-hCB1-Rluc8 and 3HA-hD2-Rluc8 conditions cannot be compared, as considerably different image exposure times were required to detect sufficient signal arising from the CB1 construct (which is expressed at much lower levels).

As shown in Figure 3.4 below, saturation curves could be fitted for all receptor-receptor interactions as would be predicted if dimer is forming, regardless of the methodology used. In contrast, neither 3HA-hCB1-Rluc8 nor 3HA-hD2-Rluc8 showed any specific interaction with unconjugated Venus (as evidenced by a linear relationship between Venus expression and BRET ratio), confirming that the BRET tags hold no appreciable intrinsic affinity for each other. When looking at the data for 3HA-hD2-Rluc8/hD2-Venus and 3HA-hD2-Rluc8/hCB1-Venus dimer pairs, saturation curves with very similar shapes were generated for all three methods (Figure 3.4(1A-1C; 2A-2C)). However, the 3HA-hCB1-Rluc8/hD2-Venus saturation curve (Figure 3.4(3A-3C) most noticeably “flattened out” when the BRET signal was plotted as a function of the expression of Venus and HA as measured by ICC, as compared to the other expression ratio calculations. This is because data points tended to be shifted right-wards on the X axis. This has occurred because, at a fixed expression level of 3HA-hCB1-Rluc8 receptor, luciferase signal is higher than predicted by HA labelling (if expression were correlated linearly with luciferase activity) in conditions with higher Venus co-expression. In other words, in conditions where there is a higher level of Venus expression, when luciferase activity is used as the expression ratio/fraction denominator it produces a lower expression ratio than when the denominator is the HA labelling.

As shown in Table 3.2, the three analysis methods did not change Bmax in a statistically significant manner ($p>0.05$). This is to be expected, since this parameter is most influenced by the BRET ratio, which is identical between analysis methods. Unfortunately, we cannot compare the Kd of the saturation curves between BRET pairs, due to the different microscope exposure times needed to image CB1 and D2 constructs. However, they can be compared within an experiment, making this a useful measure when investigating dynamic receptor changes (see Chapter 4).The curve fits to the saturation curves are all consistent with a saturation of heterodimerisation sites. Of particular interest are the curves fitted when the expression of Venus and HA as measured by ICC, which may be considered the least likely to show false-positive results. In these curves the CB1-D2 BRET pairs (Figure 3.4(2C, 3C)) do not get as close to Bmax and the D2-D2 heterodimer does (Figure 3.4(1C)).

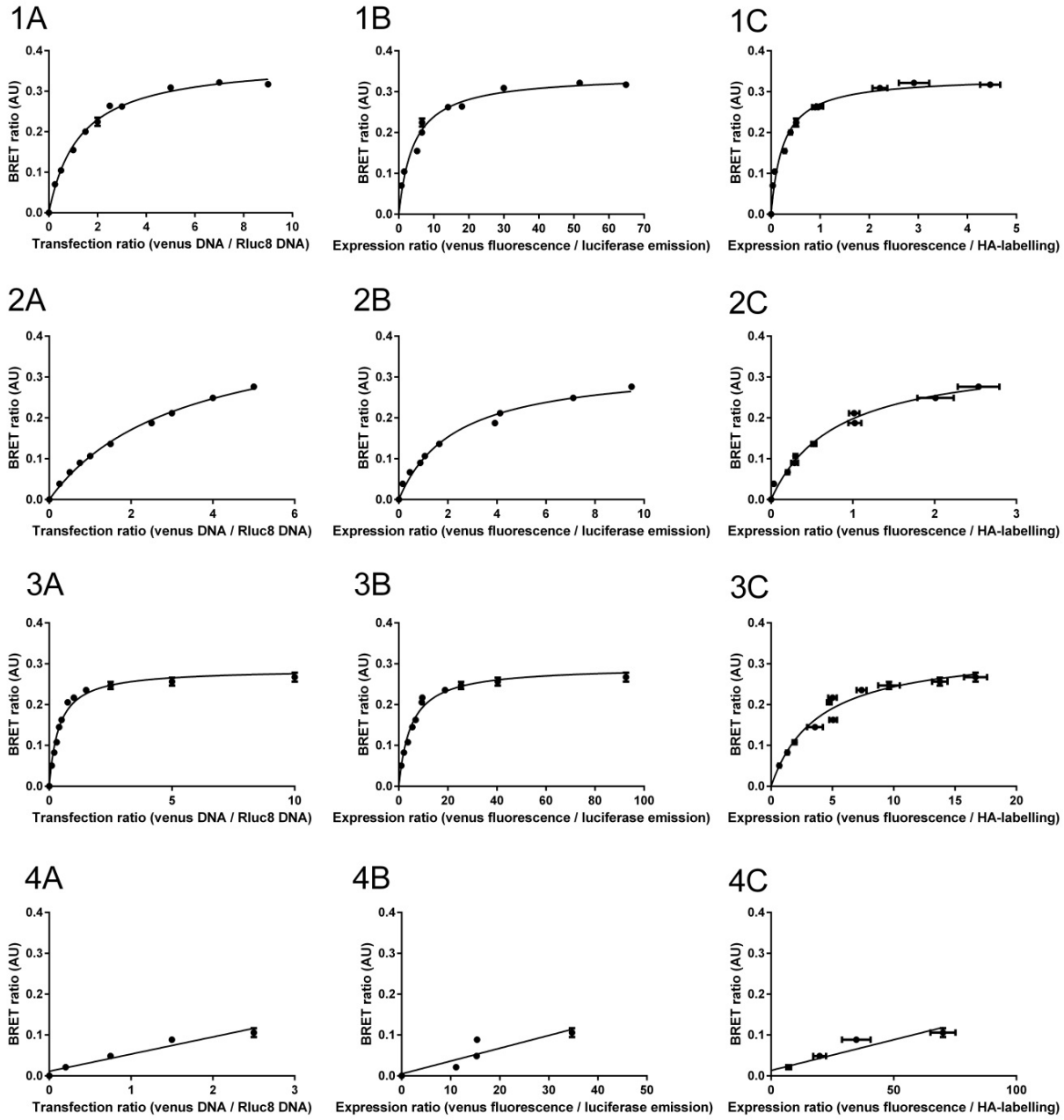

Figure 3.4 Comparison of data from BRET saturation experiments utilising three methods for assessing receptor expression ratios.

Saturation curves were composed of the following pairs of receptors: 1.) 3HA-hD2-Rluc8 and hD2-Venus; 2.) 3HA-hD2-Rluc8 and hCB1-Venus; 3.) 3HA-hCB1-Rluc8 and hD2-Venus; or 4.) 3HA-hCB1-Rluc8 and unconjugated Venus. BRET ratios were plotted A.) against transfection ratio; B.) against Venus/luciferase emission expression ratio; and C.) against Venus/HA ICC expression ratio. Representative data of one of three experiments. Mean ± SEM of four to six technical replicates per experiment, fitted with a hyperbolic curve (1, 2, 3) or linear regression (4).

Table 3.2 Bmax of hyperbolic curve fit of BRET saturation experiments analysed with three methods for assessing receptor expression ratios.

Summary results from three or four independent experiments. All units are expressed as BRET ratio (AU). No statistically significant results within each receptor combination (one-way ANOVA with Tukey's post-test).

Receptor combination	Transfection ratio	Expression ratio: Venus fluorescence / luciferase activity	Expression ratio: Venus fluorescence / HA labelling
3HA-hD2-Rluc8 + hD2-Venus	0.356±0.020	0.333±0.030	0.322±0.026
3HA-hD2-Rluc8 + hCB1-Venus	0.587±0.094	0.426±0.045	0.396±0.007
3HA-hCB1-Rluc8 + hD2-Venus	0.291±0.015	0.298±0.003	0.325±0.027

Discussion

In this study, we have used a rationalised experimental design to measure constitutive CB1-D2 heterodimerisation. In order to analyse receptor dimerisation and expression by bioluminescence and fluorescent microscopy, the GPCRs of interest were tagged with either a fluorescent Venus, or the bioluminescent Rluc8 and a triple-HA tag. After demonstrating that the GPCR-luciferase and GPCR-fluorophore fusion proteins were functional in a generic signalling assay, we assessed their expression efficiency, measured by luminescence, fluorescence and immunocytochemistry.

Standard BRET experiments often use the quantity of DNA transfected as an assumed measure of protein expression. Therefore, we first sought to confirm that this is a fair assumption by determining by immunocytochemistry whether Rluc-tagged receptor expression was affected by co-transfection with a second, Venus-tagged receptor. Controlling protein expression levels is important for BRET assays, which rely heavily on the tight control of transiently-expressed proteins. In a co-transfection paradigm, we showed that the expression of the luciferase-tagged receptor changes as a function of acceptor-tagged receptor co-expression. In these experiments, this effect reduced the expression of the luciferase receptor by up to 90%. This calls into question the relevance of normalising BRET experiments to DNA content in the transfection, as transfection and translation efficiencies may not be equal.

Next, we determined whether measuring luciferase activity in a sample was an accurate measurement of Rluc8-tagged receptor expression. This is a frequently-used way of measuring the expression of the Rluc8-tagged protein. These experiments demonstrated that light emission in the luciferase channel does not correlate well with the immunocytochemical labelling of the luciferase-receptor construct. To demonstrate this, peak luciferase emissions (measured in the 460/25nm channel of a plate reader) were

plotted against image analysis data of immunocytochemical labelling of the receptor. If luciferase activity were proportional to antibody staining we would expect a linear relationship between these variables. Comparing only samples where Venus was co-transfected with the luciferase, we observed that samples could have remarkably similar Rluc8-construct expression (as detected by immunocytochemistry), but have different luminescence emissions. In general, the more Venus was co-transfected with Rluc8, the lower the detected luminescence in the 460/25nm (Rluc8) channel of the plate reader. This is in line with RET theory, as increasing acceptor concentration quenches the luminescence of the energy donor.

However, cells transfected with only the Rluc8-tagged receptor had an unexpectedly low luminescence reading in comparison with cells which were co-transfected with a Venus-tagged receptor. This is the opposite of what was expected based on RET theory, by which we would predict that the absence of the acceptor fluorophore would result in no quenching of the luciferase, thus more light emission. On the other hand, luciferase emission may be more sensitive to environmental factors, such as substrate concentration, that could result in non-linear data output.

As the luminescence generated by Rluc8 is produced by enzymatic oxidation of the substrate coelenterazine (Hart *et al.*, 1979), it would be expected that a lower-than-expected enzymatic rate reflects a limitation of substrate availability. If both coelenterazine and oxygen were available in excess, then the Rluc8 enzyme should be functioning at its maximum rate. However, if one or both of these substrates are available in limited supply, the rate of Rluc8-catalzyed light emission would be reduced. Since luminescence-yield-per-receptor is apparently reduced in conditions with higher Rluc8 expression, we can infer that this may be due to depletion of one or both substrates. A straightforward way to test whether coelenterazine concentration could resolve this would be to add more coelenterazine per sample. Unfortunately, coelenterazine h is particularly insoluble in water and needs to be resuspended in ethanol or methanol (Pfleger *et al.*, 2006b). This limits the quantity of coelenterazine h which can be applied to cells, due to the toxic effects of the solvent. However, the concentration of coelenterazine h used in this assay (5μM) is commonly used in the literature, for example (Frederick *et al.*, 2015; Jonas *et al.*, 2015; Pfleger *et al.*, 2006b; Szalai *et al.*, 2014), suggesting that this may be a limitation in other studies also. An alternative approach would be to decrease the expression of Rluc8, however this has been observed to increase the noise in the assay, as the luminescence dropped below the linear dynamic range of the detectors in the plate reader (Receptor Signalling Laboratory, unpublished data).

These experiments therefore indicate that a more appropriate methodology for the assessment of receptor expression for BRET analysis is to utilise immunocytochemical labelling to measure receptor number, which, while common in receptor trafficking assays has not to our knowledge previously been utilised in saturation BRET assays. (Although it has been used previously for BRET competition assays (Felce *et al.*, 2014).) There is no evidence that this receptor detection system produces non-linear results, as the same monoclonal antibody and the same (or similar) analysis software have been used often in our laboratory to produce data which does not appear skewed (Cawston *et al.*, 2013; Grimsey *et al.*, 2011; Grimsey *et al.*, 2010; Grimsey *et al.*, 2008b).

Finally, we showed that normalising BRET saturation experiments to the receptor expression ratio results in subtly modified saturation curves in comparison with the expression ratio calculated from luminescence readings. This approach is aimed at more accurately reflecting the expression of receptors

in the experimental samples, as we have shown that luciferase emissions do not faithfully represent protein expression. In our hands, when expression ratio is calculated for samples showing unequal donor expression using luminescence readings, it results in expression ratios which are skewed leftward – i.e. showing a more dramatic saturation which yields a lower Kd. Therefore, this makes this method more likely to give false-positive results in a BRET saturation assay. While normalising by luciferase emission versus protein expression had a minimal effect on the D2-D2 homodimer, it had a greater effect on the data from the CB1-D2 heterodimer saturation curves. This is likely because, when CB1-Rluc8 and D2-Rluc8 receptors are co-transfected in heterodimer conditions, even a small quantity of Venus-tagged receptor has a dramatic effect on the Rluc8-tagged receptor expression. In D2 homodimer co-transfection conditions, the expression of the D2-Rluc8 is relatively unaffected by low quantities of D2-Venus.This may indicate that CB1 is sensitive to co-expression conditions, as has been alluded to before in one previous study (Przybyla *et al.*, 2010).

Previous attempts to design qualitative and quantitative BRET assays have almost always assumed that protein expression can be tightly controlled by the experimenter. However this is not a straightforward task, and protein expression should therefore be measured to normalise BRET signal to receptor expression changes. While some authors (e.g. Carriba *et al.*, 2007, Kocan *et al.*, 2011) use luciferase activity as a surrogate marker for protein expression, the data shown here demonstrates that this is an imperfect correlate. Instead, antibody-based detection of the luciferase-tagged receptor gives a more reliable measurement of transgene expression in these samples. In this instance the distortions of data due to other detection methods were not so pronounced as to change the qualitative interpretation of the results of saturation assays. However, because measuring expression ratio by protein expression appears less likely to give a false-positive result compared to other methods, it would be interesting to see whether this analysis sheds light on the presence of more controversial GPCR heterodimers, such as dopamine D1-D2 receptors (Frederick *et al.*, 2015). The results of this study also apply to the "competition" style BRET assay, where it is imperative to ensure that the BRET-tagged receptors maintain constant expression levels when co-transfected with an untagged competing receptor, in order to interpret whether competition is in effect (Felce *et al.*, 2014).

Regardless of the method utilised, the experiments presented in this chapter confirmed constitutive dimerisation of D2-D2 and CB1-D2 dimer pairs. Consistent with the standard interpretation of saturation assays, increasing Venus-tagged receptor proteins occupy specific interaction sites on the Rluc8-tagged receptor. When all of these Rluc8 interaction sites are occupied, no more heterodimerisation can occur and "saturation" is achieved. The interpretation of a specific interaction is confirmed by swapping the BRET tags over, so that the direction of energy transfer is changed. Neither 3HA-hCB1-Rluc8 nor 3HA-hD2-Rluc8 showed any specific interaction with unconjugated Venus, suggesting this response was specific. Both of these dimer pairs would be predicted from the literature, as discussed in Chapter 1, therefore this work has refined the methodology used and confirmed that BRET is a suitable method for further study of CB1-D2 dimer function.

4. CB1-D2 ligand-dependent dimerisation and heterodimer interface

Introduction

In Chapter 3, a constitutive CB1-D2 heterodimer was demonstrated using bioluminescence resonance energy transfer (BRET). The constitutive component of the CB1-D2 heterodimer has been reported before, using both co-immunoprecipitation (Khan *et al.*, 2014) and fluorescence resonance energy transfer (FRET) (Marcellino *et al.*, 2008). However, the CB1-D2 heterodimer may also have a more transient component, which is sensitive to receptor activation state. Short-term (7 minute) receptor co-activation with agonists was found to dramatically increase CB1-D2 co-immunoprecipitation (Kearn *et al.*, 2005). Both a constitutive and ligand-driven heterodimerisation was found after long-term (20 hour) agonist treatment measured by bimolecular fluorescent complementation (BiFC) (Przybyla *et al.*, 2010). However, a key limitation to the BiFC approach is the time scale that these experiments can be measured on. The BiFC interaction requires the folding of two complementary tags, which fluoresce when fully-folded. This process takes hours (Demidov *et al.*, 2006; Reid *et al.*, 1997), and therefore is not suitable for measuring acute and transient changes in receptor interactions. Furthermore, this folding is generally non-reversible, and thereby "traps" interacting proteins together (Kerppola, 2006). For these reasons, BRET is a more suitable method for measuring the dynamic interactions of a transient heterodimer interaction. In this Chapter, we first investigated whether ligand-mediated CB1-D2 heterodimer could be measured using BRET.

Next we investigated the interface of the CB1-D2 heterodimer. Professor Reggio (University of North Carolina, Greensboro) has kindly provided a computational model of the CB1-D2 heterodimer (Tyrrell *et al.*, 2008), and predictions of the interface were based on this. Since neither CB1 nor D2 receptor structures have been crystallised, the heterodimer model was constructed through homology models with other GPCRs which have been crystallised. The CB1 receptor model was based on rhodopsin, and validated through various experimental techniques (Barnett-Norris *et al.*, 2002; Hurst *et al.*, 2006; Kapur *et al.*, 2007; McAllister *et al.*, 2004; McAllister *et al.*, 2003; Picone *et al.*, 2005; Reggio *et al.*, 2002; Song *et al.*, 1996). The D2 receptor model was based on the crystal structure of the β2-adrenergic receptor, which appears to be a more appropriate fit for the structural data available for D2 (Rasmussen *et al.*, 2007; Shi *et al.*, 2001). The CB1-D2 heterodimer model predicted that the transmembrane 1 (TM1) region of both CB1 and D2 interact to form this interface. TM1 has been implicated in the dimerisation of several other GPCR pairs (Guo *et al.*, 2008; Huang *et al.*, 2013; Mancia *et al.*, 2008; Manglik *et al.*, 2012), making this a credible heterodimer interface which warrants investigation.

Methods

Cell culture and transient transfection

HEK FT cells were grown and transfected using the PEI method as described in Chapter 2. BRET constructs were co-transfected at various ratios, using empty pcDNA3.1+ plasmid to maintain equal total DNA content when required. Cells were replated into poly-L-lysine treated white Optiplates (for BRET assays) or clear Nunc plates (ThermoFisher Scientific, MA, USA) for immunocytochemistry and pERK assays), 24 hours after transfection. BRET assays and ICC detection were performed 48 hours after transfection.

Plasmid construction

The BRET-tagged receptor constructs used are described in Chapter 2, namely: 3HA-hCB1-Rluc8, 3HA-hD2-Rluc8, pplss-hCB1-Venus, hD2-Venus. All constructs had linkers separating the C-terminus of the GPCR and the BRET tag which were four amino acids long. Linker extensions were added to the Rluc8-tagged receptors by inserting short synthesised double-stranded DNA oligonucleotides by restriction digestion, ligation and subsequently sequence-verified. This generated constructs with linkers of eight amino acids.

TM1 residues which were predicted to contribute to the heterodimer interface were mutated using inverse PCR. Briefly, a forward primer was designed which contained the 3-4 codon changes for generating the required mutation set. The reverse primer was designed so that it was complementary to the template plasmid, and so that the primers were “back-to-back” on the template plasmid. PCR (utilising KAPA HiFi polymerase (KAPA biosystems, MA, USA)) was performed using these plasmids, to amplify (with the desired mutation) the entire plasmid in one linear extension. The PCR product was then purified, ligated (utilising T4 ligase (Promega, WI, USA)) onto itself, and sequence-verified. Receptor mutations are detailed in Table 4.1, where residue 1 equals the start codon of the wildtype receptor (i.e. excluding any N-terminal epitope tags). Both Rluc8- and Venus-tagged constructs were made of each wildtype and mutant receptor.

Table 4.1 CB1-D2 heterodimer interface mutations.

Receptor	Leucine substitutions	Phenylalanine substitutions
hCB1	A120L V121L T128L	A120F V121F L124F T128F
hD2	N35L T39L T42L A46L	N35F T39F T42F A46F

pERK signalling assay

Signalling of the original receptor constructs (with a 4 amino acid linker) was verified in Chapter 3. In this chapter constructs with longer linkers or mutations were verified using an immunocytochemistry-based pERK assay, as described in Chapter 3.

BRET assays

BRET assays were performed as described in Chapter 2. To summarise, cells were assayed in HBSS with 1 mg/ml BSA. After equilibrating with assay buffer for 30 minutes, coelenterazine h (Nanolight, AZ,

USA) was applied to give a final concentration of 5 μM and allowed to equilibrate for a further 5 minutes. Immediately before BRET measurement, CP55,940 and quinpirole (or vehicle) was applied to the cells. BRET measurements were taken for approximately 20 minutes using a VictorXLight plate reader (Perkin Elmer, MA, USA), with Rluc8 emission collected at 460/25 nm and Venus emission collected at 535/25 nm.

Immunocytochemistry

The expression ratio was calculated based on fluorescent microscopy images of a sample of cells from each transfection condition. Immunocytochemistry plates were stained by the protocol described in Chapter 2, using anti-HA antibody to fluorescently label Rluc8-tagged receptors, and the intrinsic fluorescence of the Venus tag. Images were acquired using ImageXpress Micro XLS automated microscope (Molecular Devices, CA, USA), and processed using a custom journal in MetaMorph (version 10, Molecular Devices), as described in Chapter 2.

Data analysis and statistics

All immunocytochemistry and BRET data was analysed using Prism (version 6, GraphPad, CA, USA). pERK assays were plotted as fold-over-vehicle in order to take into account inter-experimental variations in the background pERK signalling. pERK data were then analysed using paired t-tests (two samples per plate) or paired ANOVA (three or more samples per plate) with Dunnett's multiple comparison to compare each BRET construct to the control receptor.

BRET ratios were calculated by dividing Venus emission by Rluc8 emission, and subtracting the BRET ratio of the Rluc8-alone condition. Expression ratios were calculated by dividing background-corrected Venus fluorescence by the fluorescent antibody labelling of the Rluc8-construct. Once BRET saturation data were plotted, hyperbolic curves were fitted using Prism (version 6, GraphPad). The effect of altering the linker length to BRET Bmax was analysed by unpaired t-tests (as not all conditions were assayed simultaneously), comparing the 4 amino acid linker construct to the 8 amino acid construct. Similarly, the Bmax obtained from each combination of receptor mutants was compared to the corresponding wildtype receptor pairing, and analysed by unpaired one-way ANOVA with Dunnett's multiple comparison test. To analyse the difference between receptor mutants' responsiveness to ligand treatment, repeated measures two-way ANOVA with Sidak's multiple comparison test was performed.

Results

Validation of CB1 and D2 BRET constructs by pERK signalling assays

The new BRET-tagged receptor constructs were validated in a pERK signalling assay (results for the constructs with a four amino acid linker can be found in Chapter 3). For both receptors, the Venus-tagged receptors did not signal as efficiently as the wildtype control receptors, however they still retained some signalling function and the difference failed to reach statistical significance ($p>0.05$; Figure 4.1).

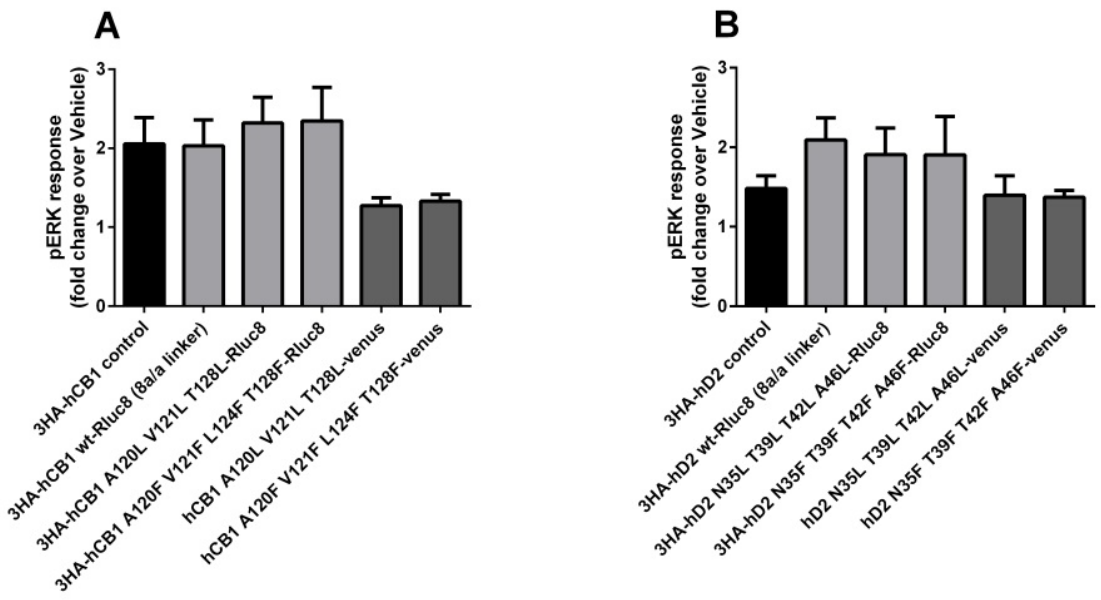

Figure 4.1 pERK signalling of extended linker and mutant receptor constructs used in BRET interaction studies.

pERK response after 5 minute agonist treatment. A.) Cells transfected with CB1 constructs were treated with 1 μM CP55,940. B.) Cells transfected with D2 constructs were treated with 1 μM quinpirole. Mean ± SEM for two to four independent experiments. No statistical difference was observed in the extent of receptor mediated activation of pERK compared to control receptors for either CB1 or D2 BRET constructs (one-way ANOVA with Dunnett's post-test).

Microscopy images were inspected to determine the nature of receptor expression. Qualitatively, the wildtype Rluc8-tagged receptors appeared to be more efficiently expressed when the linker region was extended to eight amino acids. In general, mutant receptors were expressed in a qualitatively and quantitatively similar manner to their wildtype equivalents, with one exception. The hCB1 A120L V121L T128L-Venus construct was expressed at very low levels, and was detectable only in a low proportion of cells. Although this was sufficient for the pERK signalling assay (which excludes untransfected cells in the image analysis), it was difficult to obtain the transfection efficiencies required for subsequent saturation assays.

Effect of receptor co-activation on the CB1-D2 heterodimer and effect of linker extensions on BRET efficiency

Once the constructs were validated, we used the constitutive CB1-D2 heterodimer as a basis for investigating further heterodimerisation in response to agonist treatment. Previous studies have indicated that co-stimulation with CP55,940 and quinpirole (CB1 and D2 agonists, respectively), increases CB1-D2 heterodimerisation. Of particular interest was the acute phase of this interaction, which has been shown previously to peak at 7 minutes after agonist application (Kearn *et al.*, 2005). Figure 4.2(A, B) utilised the same receptor constructs as were utilised in Chapter 3, which have four amino acids separating the GPCR C-terminus and the BRET tag. Ligand-directed changes to heterodimerisation can affect the

maximum BRET signal (Bmax, as fitted by a hyperbolic curve) and/or the affinity for the receptors to form dimer (represented by Kd, the receptor expression ratio required to reach 50% of Bmax) (Ayoub *et al.*, 2010). No agonist detected alteration in signal was observed in this experiment (Table 4.2) for ligands individually or in combination. We therefore extended the linker on the Rluc8-tagged receptors to eight amino acids; because the energy transfer in a BRET interaction is dependent on both distance and dipole orientation, therefore lengthening this linker sequence may offer more flexibility to show ligand-induced structural changes.

Saturation assays were performed with the BRET constructs with extended linkers (Figure 4.2 (C, D), Table 4.2). Altering the linker lengths changed the Bmax of the saturation assays under constitutive dimerisation conditions with the eight amino acid linker 3HA-hCB1-Rluc8/hD2-Venus condition having less efficient energy transfer compared to the four amino acid linker version. The 3HA-hD2-Rluc8/hCB1-Venus eight amino acid linker condition was more efficient than the four amino acid linker version. This indicates that the distance and/or dipole orientation of the tags has altered, but these constructs are still able to detect constitutive heterodimerisation. Cells were then treated with 1 μM CP55,940 and 1 μM quinpirole, in an attempt to observe ligand-mediated changes in heterodimerisation state. The time-courses of these ligand-induced interactions were carefully compared, but no clear peak interaction was identified (Figure 4.3). Therefore, ligand-induced heterodimerisation was measured after 5 minutes of agonist exposure, for a total of 5 minutes (i.e. the 5-10 minutes after agonist addition). As shown in Figure 4.2 and Table 4.2, ligand application did not alter the BRET interaction, as determined by Bmax.

Kd is not strictly comparable between receptor combinations, as different imaging exposures were required for the 3HA-hCB1-Rluc8 and 3HA-hD2-Rluc8 constructs, which affects the scale of the expression ratio units. Expression ratio calculations may also vary due to differences in antibody batch and incubation time, and this would need to be controlled more carefully in order to compare the absolute values of the expression ratio Kd values obtained. However, Kd values can be directly compared easily within an experiment, where antibody conditions and microscopy exposure times are identical. Between conditions, a fold-change value can be calculated to determine whether drug treatment has altered the curve fit. As demonstrated in Table 4.2, no change in Kd was detected due to drug treatment.

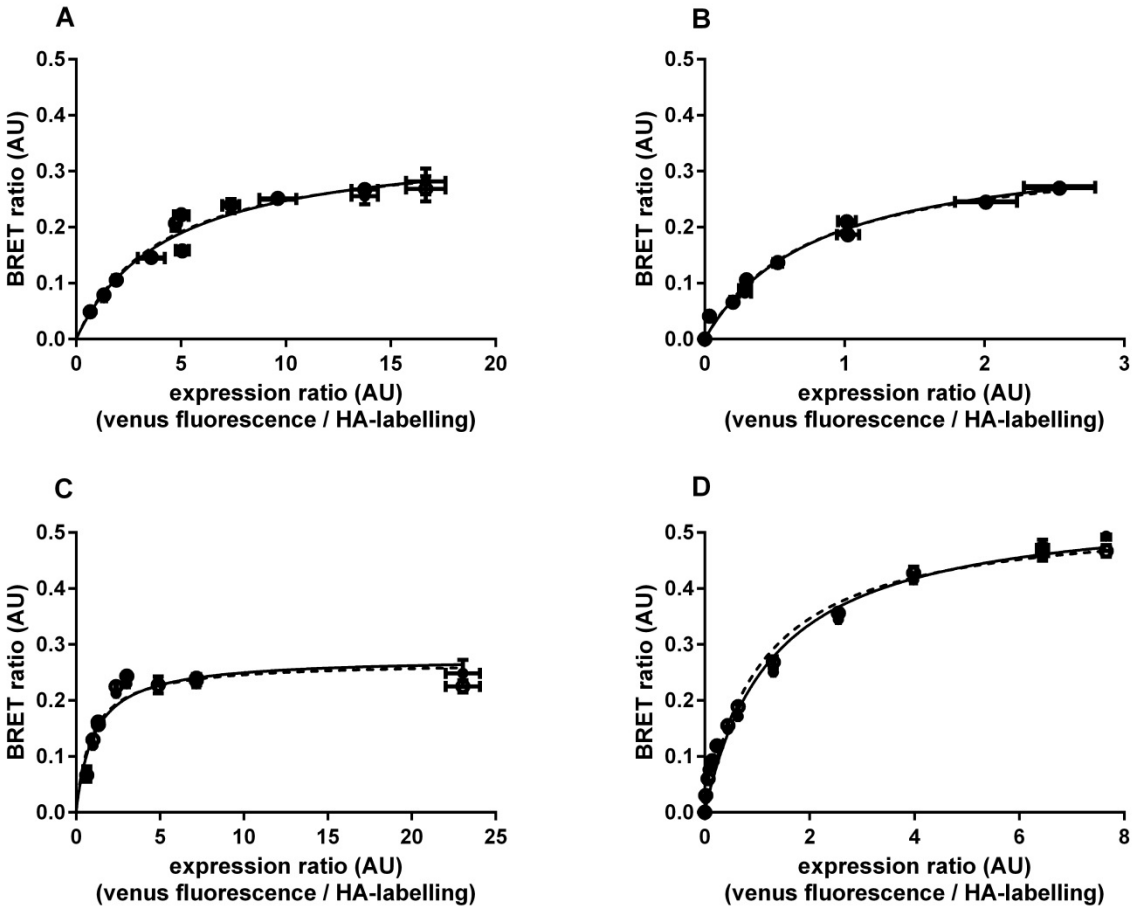

Figure 4.2 CB1-D2 BRET saturation curves utilising receptor constructs with different linker lengths, and the effect of receptor co-stimulation.

CB1-D2 BRET interactions were measured in the presence of 1 μM CP55,940 and 1 μM quinpirole (solid line) or vehicle (dashed line), 5-10 min after drug addition. A.) 3HA-hCB1-Rluc8 (4 amino acid linker) + hD2-Venus; B.) 3HA-hD2-Rluc8 (4 amino acid linker) + hCB1-Venus; C.) 3HA-hCB1-Rluc8 (8 amino acid linker) + hD2-Venus; D.) 3HA-hD2-Rluc8 (8 amino acid linker) + hCB1-Venus. Representative results from one of three or four independent experiments. Error bars represent the mean ± SEM of three technical replicates.

Table 4.2 Bmax and Kd measurements for BRET wildtype receptor constructs containing 4 and 8 amino acid linker sequences.

*Mean ± SEM of three to four independent experiments. * p<0.05 compared to corresponding 4 amino acid linker construct. No statistical significance in Bmax or Kd was found between vehicle- and agonist-treated samples.*

Receptor combination		Bmax (BRET ratio)		Kd, CP55,940 + quinpirole (fold change compared to vehicle-treated)
Rluc8-tagged receptor	Venus-tagged receptor	Vehicle	CP55,940 + quinpirole	
3HA-hCB1 (4 amino acid linker)	hD2	0.333±0.010	0.336±0.012	1.014±0.033
3HA-hD2 (4 amino acid linker)	hCB1	0.433±0.045	0.437±0.048	1.043±0.038
3HA-hCB1 (8 amino acid linker)	hD2	0.256±0.008*	0.256±0.004	1.089±0.093
3HA-hD2 (8 amino acid linker)	hCB1	0.534±0.030*	0.533±0.027	1.086±0.060

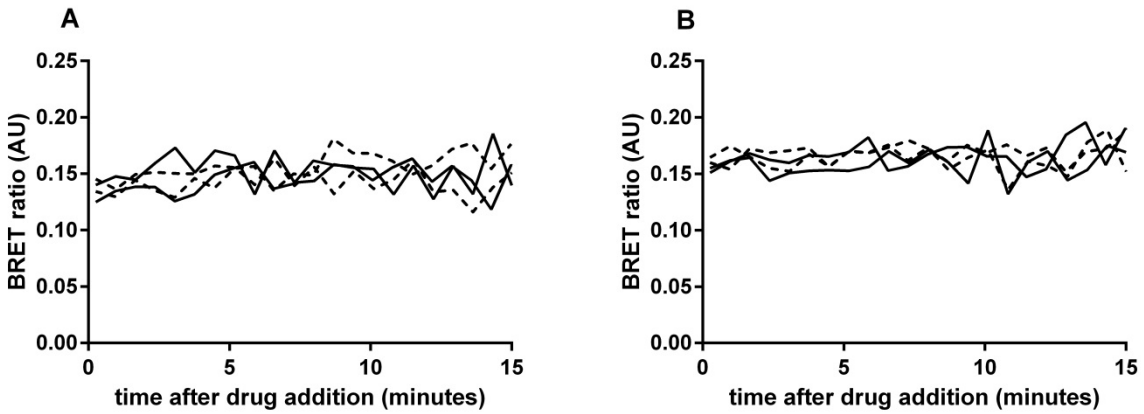

Figure 4.3 Time-course of BRET interaction between CB1 and D2 receptors.

Cells were treated with vehicle (dashed line) or 1 μM CP55,940 and 1 μM quinpirole, and BRET measured approximately every 40 seconds for at least 15 minutes. Two technical replicates are plotted separately for each condition. A.) 3HA-hCB1-Rluc8 (8 amino acid linker) + hD2-Venus, expression ratio of 2.89. B.) 3HA-hD2-Rlu8 (8 amino acid linker) + hCB1-Venus, expression ratio of 0.15. Representative data of three independent experiments, each performed with two or three technical replicates per experiment.

Testing the predicted CB1-D2 heterodimer interface by receptor mutagenesis

As the results presented in Chapter 3 showed strong evidence of CB1-D2 constitutive heterodimerisation, we attempted to alter the predicted receptor interface using amino acid residue mutations. The heterodimerisation interface was predicted by a computational model to be on TM1 of both CB1 and D2. Four key residues were identified in TM1 of each receptor, and mutated to either leucine or phenylalanine variants. The mutational strategy was to substitute large residues into the heterodimerisation interface, thereby preventing a normal interaction from occurring. The substituted residues for each receptor are detailed in Table 4.1.

Cells were transfected with CB1 and D2 BRET pairs, where one or both of the receptors contained the mutated residues. Saturation assays were performed and Bmax and Kd values were determined. As demonstrated in Figure 4.4 and Table 4.3, no significant changes were observed when CB1 or D2 mutants were used, compared to wildtype receptors. There was, however, a small (but not statistically-significant) reduction in saturation assay Bmax which was observed in some receptor pairings, although this may be explained by minor alterations in receptor folding and are unlikely to be from gross changes in the receptor dimerisation state.

As mentioned above, the hCB1 A120L V121L T128L-Venus construct was poorly expressed under these transfection conditions. Although no clear saturation curve could be obtained, it is interesting to note that even when some receptors were expressed (expression ratios of approximately 0.2), no BRET was observed. It may be that this receptor construct is very poorly trafficked to the cell surface. If this set of mutations altered heterodimerisation meaningfully, we would expect to see a significantly reduced BRET signal when this receptor was tagged with Rluc8 (and paired with hD2-Venus), however this was not the case.

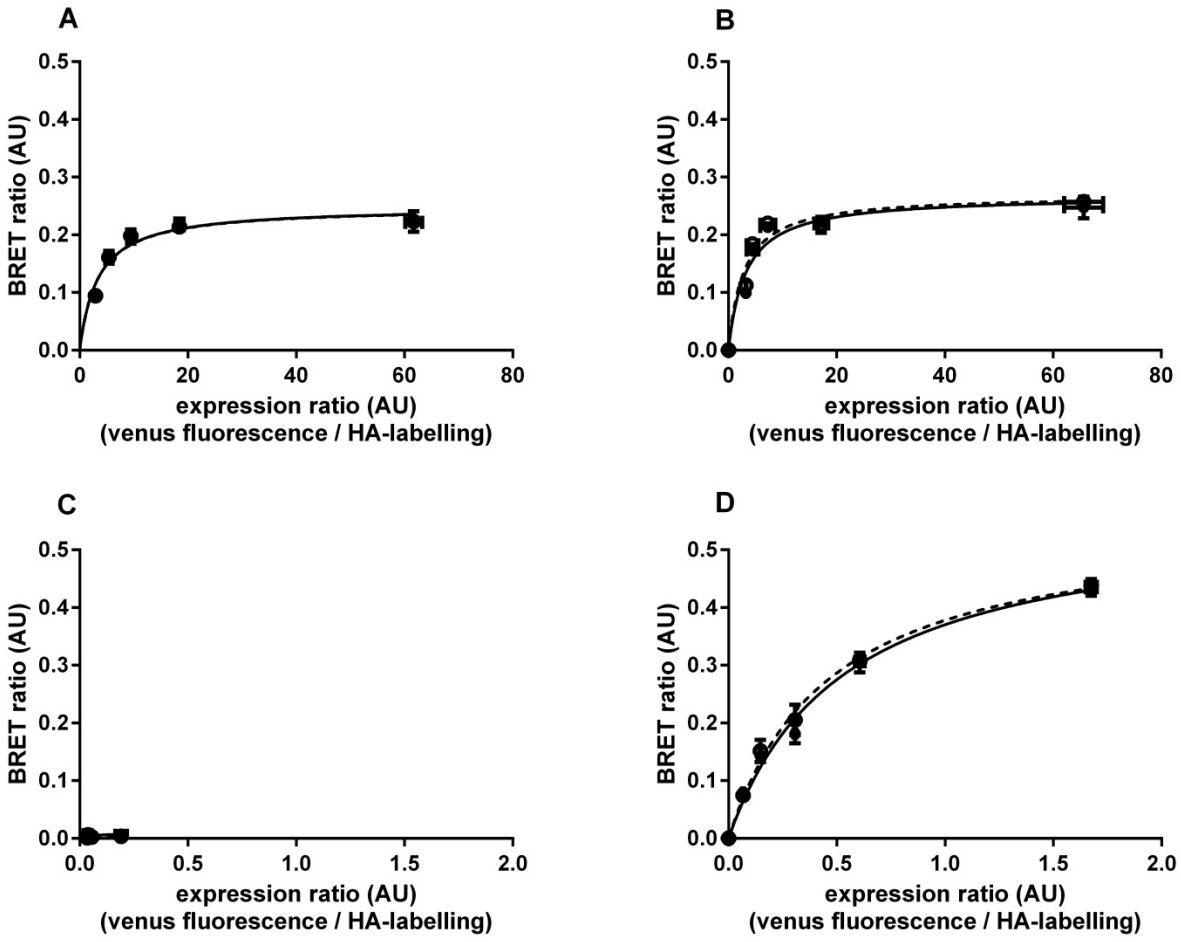

Figure 4.4 BRET saturation curves generated by CB1 and D2 TM1 mutants.

Cells were transfected with BRET pairs of CB1 and D2 containing TM1 mutations. Solid lines represent vehicle-treated samples, and dotted lines represent samples treated with 1 μM CP55,940 + 1 μM quinpirole. A) 3HA-hCB1 A120L V121L T128L-Rluc8 + hD2 N35L T39L T42L A46L-Venus; B.) 3HA-hCB1 A120F V121F L124F T128F-Rluc8 + hD2 N35F T39F T42F A46F-Venus; C.) 3HA-hD2 N35L T39L T42L A46L-Rluc8 + hCB1 A120L V121L T128L-Venus; D.) 3HA-hD2 N35F T39F T42F A46F-Rluc8 + hCB1 A120F V121F L124F T128F-Venus. Representative data from three independent experiments performed in triplicate. Error bars represent the mean ± SEM of three technical replicates.

Table 4.3 BRET Bmax and Kd from CB1-D2 wildtype and TM1 mutant receptor pairings.

*Cells were transfected with BRET pairs of CB1 and D2 containing wildtype or TM1 mutations. Mean ± SEM, of three to four independent experiments. * p<0.05 compared to vehicle. No statistically significant differences in Bmax or Kd were found between wildtype and TM1 mutant receptors.*

Receptor combination		**Bmax (BRET ratio)**		**Kd, CP55,940 + quinpirole (fold change compared to vehicle-treated)**
Rluc8-tagged receptor	**Venus-tagged receptor**	**Vehicle**	**CP55,940 + quinpirole**	
hCB1 wt	hD2 wt	0.256±0.008	0.256±0.004	1.088±0.093
hCB1 wt	hD2 N35L T39L T42L A46L	0.214±0.001	0.210±0.007	1.144±0.002 *
hCB1 wt	hD2 N35F T39F T42F A46F	0.229±0.005	0.225±0.003	0.924±0.025
hCB1 A120L V121L T128L	hD2 wt	0.256±0.023	0.254±0.007	1.003±0.000
hCB1 A120L V121L T128L	hD2 N35L T39L T42L A46L	0.252±0.008	0.252±0.010	1.133±0.105
hCB1 A120F V121F L124F T128F	hD2 wt	0.280±0.031	0.281±0.022	1.029±0.046
hCB1 A120F V121F L124F T128F	hD2 N35F T39F T42F A46F	0.275±0.009	0.272±0.013	1.095±0.025
hD2 wt	hCB1 wt	0.534±0.030	0.533±0.027	1.086±0.060
hD2 wt	hCB1 A120L V121L T128L	n/a	n/a	n/a
hD2 wt	hCB1 A120F V121F L124F T128F	0.523±0.027	0.513±0.030	1.004±0.065
hD2 N35L T39L T42L A46L	hCB1 wt	0.534±0.013	0.526±0.010	1.024±0.092
hD2 N35L T39L T42L A46L	hCB1 A120L V121L T128L	n/a	n/a	n/a
hD2 N35F T39F T42F A46F	hCB1 wt	0.519±0.008	0.508±0.006	1.030±0.018
hD2 N35F T39F T42F A46F	hCB1 A120F V121F L124F T128F	0.574±0.011	0.573±0.005	1.095±0.014

Discussion

Previous studies have shown that CB1 and D2 co-immunoprecipitate upon agonist co-stimulation, implying that this heterodimerisation interaction is somewhat dependent on receptor activation. In order to measure this, we used the BRET assay which was developed to detect constitutive CB1-D2 heterodimerisation in Chapter 3. Saturation curves were created by transfecting a constant quantity of Rluc8-tagged receptor, and increasing quantities of Venus-tagged receptor. Each assay transfection condition had protein expression measured by immunocytochemistry, to ensure that accurate expression ratios were used to calculate the saturation curve.

Co-application of CP55,940 and quinpirole at high concentrations did not alter the BRET interaction of CB1-D2, as determined by saturation curves using the original BRET-tagged receptors. These receptors had relatively short (four amino acid) linkers between the receptor C-terminus and the Rluc8 or Venus tag. Since BRET interactions are determined by the distance and dipole orientation of each of the tags, the linkers were extended for the Rluc8-tagged receptors. This was done with the hope that it may change the orientation of the tags and expose ligand-mediated heterodimer changes.

Saturation curves with BRET constructs that had extended linkers showed saturable BRET signals. The Bmax was changed for both receptor combinations, with the 3HA-hCB1-Rluc8/hD2-Venus pairing having a lower Bmax, and the 3HA-hD2-Rluc8/hCB1-Venus pairing a higher Bmax. This is not necessarily indicative of any change in the receptors' interaction state, only an indication that energy transfer has become less efficient in the case of 3HA-hCB1-Rluc8/hD2-Venus pairing and more efficient in the 3HA-hD2-Rluc8/hCB1-Venus pairing combinations. The new receptor pairings were also tested for responsiveness to agonist co-stimulation, but again the BRET signal was again unaltered (both Bmax and Kd; Table 4.2).).

The observation that the BRET signal did not change upon agonist application does not necessarily indicate that there has been no change in the structure of the CB1-D2 heterodimer. As BRET is a function of both distance and dipole orientation, it is possible for the acceptor and donor tags to change distance and orientation as a result of changes in receptor position, but for the BRET signal to stay the same. The hypothesis that the CB1-D2 heterodimer is a transient interaction came from a study which utilised co-immunoprecipitation (Kearn *et al.*, 2005). This study found that the heterodimer co-immunoprecipitated more efficiently when both receptors were stimulated with agonist simultaneously. The discrepancy between the co-immunoprecipitation study and these BRET results may help elucidate the true nature of the CB1-D2 heterodimerisation interaction, as dimerisation conditions may affect each assay differently.

Co-immunoprecipitation efficiency is affected by the chemical nature of the protein interactions. Depending on the lysis and precipitation conditions, different interactions can be preferentially co-precipitated. However, in a BRET assay we are not privy to the nature of the protein interactions, merely whether the tagged receptors are close enough together for the RET interaction. As the results of this BRET study, and other studies (Kearn *et al.*, 2005; Khan *et al.*, 2014; Marcellino *et al.*, 2008; Navarro *et al.*, 2010) which describe a constitutive heterodimer, it is likely that these receptors are constitutively

present in an oligomeric complex. Perhaps the chemical nature of the heterodimer interface is modified by co-stimulation, but that this does not significantly alter the localisation and orientation of the individual receptors. It is also possible that an interacting protein, not yet identified, is recruited to the CB1-D2 constitutive heterodimer, and that this is the "bridge" which allowed co-immunoprecipitation.

As the constitutive heterodimer proved stable through ligand treatment, we tested residues on each receptor which were predicted to constitute the CB1-D2 interface. A computational model, based on the crystal structures of related GPCRs, was kindly provided by Professor Reggio. In this model, the CB1-D2 heterodimer interface was predicted to contain four amino acid residues on the TM1 of each receptor. These residues were mutated to leucine and phenylalanine residues, in an attempt to prevent heterodimerisation by steric hindrance. However, none of these mutant receptors altered CB1-D2 heterodimerisation significantly. Some differences were seen in the saturation curve Bmax when the CB1-Rluc8 receptor (wildtype and mutants) were measured, although these failed to reach statistical significance. BRET pairings containing the hCB1 A120L V121L T128L-Venus construct did not show any interaction, although qualitative analysis of the accompanying immunocytochemistry images indicates this was due to poor construct expression, and lack of co-transfection, rather than a disruption in the receptor interaction. If this combination of mutated residues was sufficient to inhibit CB1-D2 heterodimerisation, we would expect to see this when the BRET tags were swapped (i.e. the CB1 receptor was tagged with Venus), however this was not observed.

Other studies have identified other sites for the CB1-D2 heterodimer interface. These include intracellular loop (IL) 3 of both CB1 and D2 (Navarro *et al.*, 2010); and the CB1 C-terminus (C417-S431 in rat; which is identical throughout to human C415-S429) with D2 IL3 (Khan *et al.*, 2014). Intracellular loops have been identified as contributing to the interaction of other receptor dimers (e.g. Huang *et al.*, 2013), notably including IL3 in heterodimers containing the D2 receptor (Ciruela *et al.*, 2004; O'Dowd *et al.*, 2012; O'Dowd *et al.*, 2013). However, affinity purification assay screening (in which cell lysates are incubated with peptide fragments, followed by co-precipitation) has demonstrated no direct interaction between the full-length CB1 receptor and the whole D2 receptor IL3 peptide fragment (Khan *et al.*, 2014), indicating the relevance of D2 IL3 is not yet fully resolved. The identification of interacting residues in the C-terminal tail is an interesting finding (Khan *et al.*, 2014), which was published during the course of our investigations. The C-terminal tail of two other receptors, namely the dopamine D5 (O'Dowd *et al.*, 2013) and adenosine A2A (Ciruela *et al.*, 2004; Navarro *et al.*, 2010) receptors, have been demonstrated to interact with the D2 receptor in their respective heterodimerisation partnerships. This perhaps suggests a common way in which D2 can interact with potential heterodimerisation partners.

Neither of the previous two studies of the CB1-D2 heterodimer identified interaction sites using predictions from a computational model. Therefore, this was the first study which used a model to rationally identify target residues. Unfortunately, the quality of computational models is determined by the crystallography data available. At the time this model was developed, the most closely related receptors were rhodopsin for CB1 and β2-adrenergic for D2. However, GPCR crystallisation techniques have developed significantly in recent years, and it is likely this model could be refined upon with this new data. In 2012, the S1P1 receptor was crystallised (Hanson *et al.*, 2012), which the sequence of this receptor is more similar to CB1 than rhodopsin (Hurst *et al.*, 2013). Similarly, the D3 receptor has been

crystallised (Chien *et al.*, 2010), which may offer a better fit for homology modelling of D2 (Katritch *et al.*, 2012). However, the dimer interface predicted by the computational model used here is in line with previous observations of a TM1-TM1 interaction. This dimer interface has been shown for the κ-opioid (Wu *et al.*, 2012), and β1-adrenergic receptor homodimers (Huang *et al.*, 2013). However, the finding that IL3 may contribute to the CB1-D2 heterodimer interface is not unprecedented, as TM5-TM6 interactions have been described for the chemokine CXCR4 (Wu *et al.*, 2010) and μ-opioid receptor homodimers (Manglik *et al.*, 2012), and IL3 is the intracellular region which connects these transmembrane domains. Therefore, further investigation into the role of TM5-IL3-TM6 regions in CB1-D2 heterodimerisation is warranted.

Overall, these results show that a BRET interaction between CB1 and D2 receptors is not significantly altered by receptor activation by agonists. This finding does not necessarily mean that the nature of the heterodimer interaction is not altered by receptor activation, only that any alteration cannot be detected by BRET. We also tested residues on TM1 of each receptor, which had been predicted by receptor modelling to contribute to the CB1-D2 heterodimer interface. While the results of the tested TM1 interface did not confirm this interaction, recent advancements in GPCR crystallography offer the chance to improve this computational model in the future.

5. CB1-D2 trafficking

Introduction

Receptor trafficking is a mechanism for influencing the potential for GPCR signalling by modifying subcellular GPCR distribution. The classical sequence of events is that an activated GPCR is phosphorylated by G protein-coupled receptor kinases (GRKs) and binds β-arrestin proteins (Jean-Alphonse *et al.*, 2011; Marchese *et al.*, 2008; Reiter *et al.*, 2006). Phosphorylated receptors can no longer activate G proteins, and the associated β-arrestins obliterate G protein coupling. β-arrestins then recruit clathrin to bring the GPCR into clathrin-coated pits, from which they are internalised (Marchese *et al.*, 2008). Internalised GPCRs are dephosphorylated in endosomes, and are sorted into either a recycling pathway, or a degradative pathway (Jean-Alphonse *et al.*, 2011; Marchese *et al.*, 2008). There is emerging evidence that some GPCRs are still able to signal via G proteins and β-arrestins from endosomes (Irannejad *et al.*, 2013; Irannejad *et al.*, 2014; Murphy *et al.*, 2009), which likely contributes to the biphasic signalling responses seen for many receptors. In these instances, a second phase of receptor signalling is observed even after the bulk of surface receptors have been internalised.

GPCR oligomerisation has been shown to affect internalisation and post-endocytic trafficking for many receptors. For example, the substance P-μ opioid receptor heterodimer undergoes cross-phosphorylation and co-internalisation when only one component receptor is stimulated (Pfeiffer *et al.*, 2003). Similarly, V1a and V2 vasopressin receptor heterodimerisation alters β-arrestin recruitment (Terrillon *et al.*, 2004). Even for non-heterodimeric GPCR systems, signalling pathways can influence receptor trafficking; for example, PKA activity modulates the recycling pathway of the β-adrenergic receptor (Vistein *et al.*, 2013). Considering that the post-endocytic fate of receptors determines resensitisation profiles, it is of therapeutic interest to determine how receptor recycling and degradation pathways are altered by oligomerisation.

Individually, both CB1 and D2 have already been shown to affect the trafficking of other GPCR heterodimerisation partners. For example, co-expression of CB1 and orexin 1 receptors affects the receptor localisation pattern of the orexin 1 receptor (Ellis *et al.*, 2006; Ward *et al.*, 2011). Similarly, the D2-adenosine A2A heterodimer shows interacting internalisation pathways, whereby treatment with high concentrations of D2 agonist or A2A agonist induces co-aggregation and co-internalisation of both receptors (Genedani *et al.*, 2005; Hillion *et al.*, 2002). Interestingly, the D1-D2 dopamine receptor heterodimer has been shown to have the same properties (So *et al.*, 2005).

Given the evidence that either CB1 or D2 could influence the internalisation and trafficking of a heterodimerisation partner, we investigated whether a similar interaction occurred in the CB1-D2 heterodimer. Since CB1 is observed to give a robust internalisation response (Coutts *et al.*, 2001; Grimsey *et al.*, 2010; Hsieh *et al.*, 1999; Rinaldi-Carmona *et al.*, 1998), but D2 does not (Celver *et al.*,

2010; Octeau *et al.*, 2014; Sharma *et al.*, 2013; Skinbjerg *et al.*, 2009; So *et al.*, 2005), it was hypothesised that co-stimulation with CB1 and D2 agonists may increase the extent of D2 internalisation. However, heterodimerisation was not expected to affect post-endocytic receptor fate, as both CB1 and D2 receptors are generally observed to be degraded (Bartlett *et al.*, 2005; Grimsey *et al.*, 2010; Ji *et al.*, 2009; Marley *et al.*, 2010), although D2 has also been reported as having a mixed phenotype (Namkung *et al.*, 2009; Vickery *et al.*, 1999).

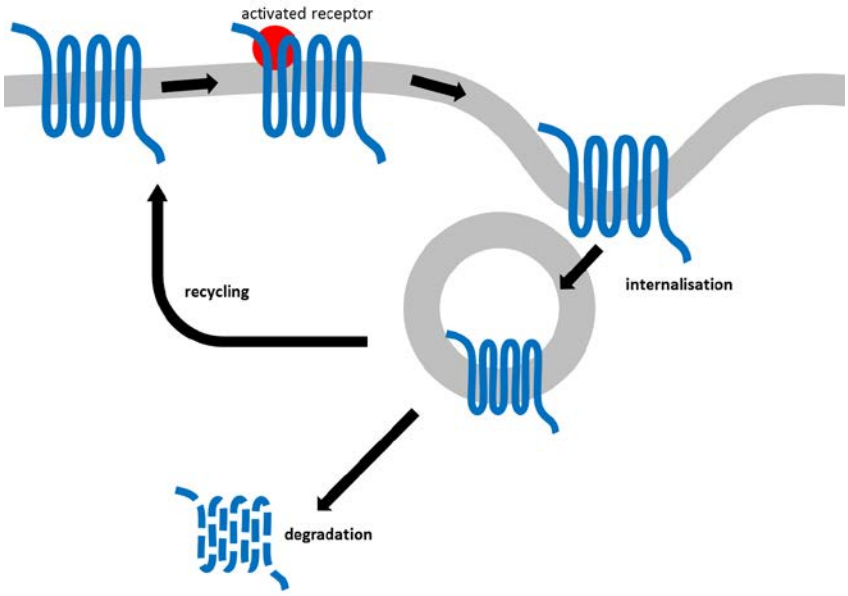

Figure 5.1 Simplified schematic of GPCR agonist-induced trafficking.

When activated by an agonist, the GPCR is internalised and trafficked through either degrading or recycling pathways. Recycled receptors are returned to the cell surface, available to bind agonist again. If a receptor is degraded, de novo synthesis of receptor proteins is required for resensitisation.

Methods

Cell culture

This chapter utilises the stable cell lines HEK 3HA-hCB1/flag-hD2 and HEK 3HA-hCB1, which are described in Chapter 2.

General receptor internalisation assay technique

Receptor internalisation assays were based on protocols previously described by Grimsey *et al.* (2011; 2010; 2008b). Cells were plated on poly-L-lysine treated Nunc 96-well plates (ThermoFisher Scientific, MA, USA) and assayed after 24 hours, at approximately 75% confluency. Immediately before assaying, cells were serum starved in DMEM with 5mg/ml BSA for 30 min at 37°C. For pre-drug antibody staining and drug treatments, cells were incubated at 37°C. For internalisation time-course experiments, plates were transferred to a 37°C waterbath (without CO_2 control) for the final 15 min of drug stimulation, in order to maintain an even temperature between time points. At the end of the stimulation time, plates were placed on ice for approximately 5 min to stop receptor trafficking before incubating with primary

antibody at room temperature. All antibody incubations performed before fixation selectively labelled surface receptors. All live-cell antibody and drug incubations were performed in DMEM + 5mg/ml BSA, and post-fixation antibody incubations were performed in immunobuffer (PBS-T with 1% normal goat serum and 0.4mg/ml thiomersal) and processed as described in Chapter 2. Antibodies used are described in Table 5.1.

Constitutive internalisation assays

A standard assay to measure constitutive receptor internalisation does not require the application of any drugs to the cells. In this experimental design we applied agonists to the non-tracked receptor in cells co-expressing CB1 and D2 (i.e. D2 agonist, when labelling for CB1 trafficking, and *vice versa*). This was done in order to see whether there were any cross-over effects from the activated receptor to the constitutive internalisation of the non-activated receptor. To detect the internalisation of each receptor, primary antibody is applied before vehicle or drug incubation. After an extended incubation time, secondary antibody is applied to the cells at room temperature (to prevent further trafficking). This selectively labels the receptors which had been labelled with primary antibody at the beginning of the incubation period and remained at the cell surface at the end of the incubation.

Recycling assays

In order to investigate repopulation of the cell surface with CB1 and D2 following agonist-induced internalisation, a combination of labelling paradigms was utilised. In the "recycling" assay, receptors were first labelled with primary antibody, then internalised with agonist for 30 minutes. Agonist was washed off and inverse agonist was then applied for a variable amount of time. A high concentration of inverse agonist was used in order to compete with any remaining agonist and ensure minimal internalisation occurred during the "repopulation" phase of the assay and to accumulate any returning receptor on the cell surface. After inverse agonist incubation, secondary antibody was applied to the live cells to label any receptors which had been recycled to the cell surface. The net surface population was measured by applying primary antibody at the end of drug incubation to previously unstained cells.

Table 5.1 Antibodies used in receptor trafficking experiments.

Antibody	Species raised in	Supplier (catalogue number)	Dilution, live-cell incubation	Dilution, fixed-cell incubation
anti-HA monoclonal	Mouse	Covance, NJ, USA (MMS-101P)	1:500	n/a[a]
anti-flag polyclonal	Rabbit	Sigma-Aldrich, MO, USA (F7425)	1:400	n/a
anti-mouse, Alexa 488	Goat	Molecular Probes, Life Technologies, CA, USA (A11029)	1:300	1:400
anti-rabbit, Alexa 594	Goat	Molecular Probes (A11037)	1:300	1:400

[a] n/a, not applicable

Table 5.2 Summary of internalisation and trafficking assay designs utilised.

Assay format	Assay design
Concentration-response internalisation	An agonist for one receptor is applied at varying concentrations. An agonist for the other receptor is co-applied at a constant concentration. Drugs are applied for a set period of time (60 minutes). Receptors are labelled with primary antibody at the end of the drug incubation to measure the net change in cell surface receptor density.
Time-response internalisation	Agonists for one or both receptors are applied at a constant concentration for varying lengths of time. Drug addition was staggered such that all incubations concluded simultaneously. Receptors are labelled with primary antibody at the end of the drug incubation to measure the net change in cell surface receptor density.
Constitutive internalisation	Primary antibody is applied to detect one receptor. Then a constant concentration of agonist is applied to stimulate the non-tracked receptor in cells co-expressing CB1 and D2 (i.e. when CB1 is labelled with antibody, a D2 agonist is applied). After incubating cells in media for varying lengths of time, the primary antibody-labelled receptors remaining on the cell surface are then stained with secondary antibody.
Recycling/repopulation assay	Recycling: Receptors are first labelled with primary antibody, then internalised with agonist for 30 minutes. Agonist is then washed off and inverse agonist applied to compete with any remaining agonist and ensure no further internalisation occurs. After inverse agonist incubation, secondary antibody is applied to the live cells to label any receptors which had been previously labelled with primary antibody, then either been retained on the cell surface or returned to the cell surface. The proportion of recycled receptors is calculated by comparing the proportion of receptors remaining immediately after agonist treatment, to the number of receptors labelled after inverse agonist treatment. Repopulation: Cells are treated with agonist as per the “recycling” protocol, but primary antibody is instead added at the end of the inverse agonist treatment. This allows visualisation of the total number of receptors on the cell surface at the end of agonist treatment, consisting of those receptors that had remained at the cell surface, and/or had been delivered during the incubation time (including both recycled and newly-synthesised receptors).

Microscopy and image analysis

Images were acquired using the Discovery-1 or ImageXpress Micro XLS automated microscopes (both from Molecular Devices, CA, USA). Using automated focussing, four sites per well and 3-4 wells per conditions per replicate experiment were collected at 10x magnification to record AlexaFluor 488, AlexaFluor 594 and Hoechst staining (labelling CB1 receptors, D2 receptors, and nuclei, respectively). Images were processed using MetaMorph software (versions 6.2r6 and 10, Molecular Devices), using the "Total Grey Value Per Cell" method previously described by Grimsey, *et al.* (2008b). This analysis method measures the intensity of fluorescent staining (proportional to the abundance of receptor) above a user-defined background, and averages it across the total number of nuclei counted per image.

Curve fitting and statistical analysis

GraphPad Prism software (version 6) was used for all graph fitting and statistical analysis. All results were normalised to the experimental condition which had not been exposed to any agonists. For concentration-response internalisation assays, sigmoidal concentration response curves were fitted (Hill slope = 1). For time-response internalisation curves, exponential decay curves were fitted with or without a lag time (comparison of two curves, best curve fitted). Parameters derived from these curves were analysed with one-way ANOVA and Tukey's test (detailed further in Chapter 2), with significance defined as $p<0.05$.

Results

Concentration-response internalisation

Receptor density on the surface of cells was measured by antibody labelling after drug treatment. In the concentration-response assay paradigm, various concentrations of receptor agonists were applied to cells for 60 minutes. These experiments showed that the density of cell-surface CB1 was reduced by the CB1 agonist CP55,940 in a concentration-dependent manner (Figure 5.2(A)). Internalisation in response to CP55,940 had a mean EC50 of 4.14 nM. As shown in Table 5.3, co-application of quinpirole at either 0.1 or 10µM did not significantly change the EC50 of CP55,940-induced CB1 internalisation. However, 10 µM quinpirole did significantly decrease the maximum extent of CB1 internalisation when co-applied with CP55,940. When CP55,940 was applied alone, on average 24% of CB1 receptors remained on the cell surface after 60 minutes, whereas when CP55,940 and quinpirole (10 µM) were applied together 41% of CB1 remained. Unlike CB1, D2 did not internalise in this assay in response to quinpirole, either when quinpirole was applied to cells alone or in combination with CP55,940, as shown in Figure 5.2(B) and Table 5.4.

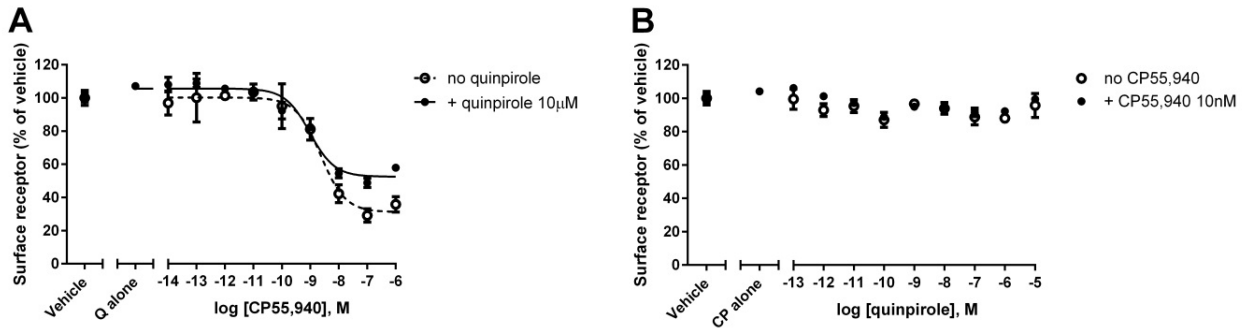

Figure 5.2 Internalisation of CB1 and D2 in response to 60 minute incubation with varying concentrations of their respective agonists, in the presence or absence of agonist to the other receptor.

(A) CB1 internalisation in response to CP55,940 alone, and in the presence of quinpirole. (B) D2 internalisation in response to quinpirole alone and in the presence of CP55,940. Representative results from one of three experiments. Error bars represent the SEM of three technical replicates.

Table 5.3 Summary of CB1 internalisation 60 minute concentration-response to CP55,940 in the presence and absence of the D2 agonist quinpirole.

*Data shown as mean ± SEM of three experiments. * p<0.05.*

	Condition			
Parameter	**No quinpirole**	**Quinpirole 0.1 μM**	**Quinpirole 10 μM**	**Significance**
EC50 of CP55,940	4.1±1.6 nM	5.7±1.6 nM	4.5±2.2 nM	ns
Bottom-of-curve (% of surface labelling remaining)	23.7±6.3%	24.0±8.1%	40.5±8.0%*	* compared to No quinpirole

Table 5.4 Summary of D2 internalisation 60 minute concentration-response to quinpirole in the presence and absence of the CB1 agonist CP55,940.

Data shown as mean ± SEM of three experiments.

	Condition				
Parameter	**No CP55,940**	**CP55,940 0.1 nM**	**CP55,940 1 nM**	**CP55,940 10 nM**	**Significance**
Surface D2 in response to 10 μM quinpirole (% of surface labelling remaining)	98.9±3.5	96.3±7.2	98.8±8.1	97.0±2.4	ns

Time-response internalisation

In order to observe the time-course of receptor internalisation, a fixed concentration of agonist was applied for various lengths of time. In these assays, the CB1 receptor internalised robustly in response to 10 nM CP55,940 (Figure 5.3(A)). Co-application of quinpirole (10µM) affected neither the rate of CB1 internalisation, nor the percent of receptor remaining at 60 minutes (Table 5.5). This is in agreement with the results of identical ligand conditions seen in the 60 minute concentration-response data (shown in Figure 5.2 and Table 5.3). Interestingly, a trend was noted that the lag time between agonist application and initiation of detectable internalisation increased when cells were co-stimulated with quinpirole, however the length of this time varied between replicate experiments and this effect failed to reach statistical significance.

It is notable that the concentration-response and time-response experimental paradigms produced results showing different extents of CB1 internalisation. In the concentration-response paradigm, 60 minute treatment with 10 nM CP55,940 left 44±8% of CB1 receptors remaining on the cell surface, whereas the same drug conditions in the time-response paradigm resulted in 8±2% remaining ($p=0.004$). This effect was also seen in the 10 nM CP55,940 + 10 µM quinpirole conditions: 60±8% in the concentration-response, and 14±2% in the time-response condition ($p=0.001$).

Similarly, in the time-response assay paradigm, the D2 receptor was observed to internalise to a moderate extent, with approximately 70% of D2 remaining on the cell surface at 60 minutes. Co-application of CP55,940 did not affect this internalisation profile, as shown in Figure 5.3(B) and Table 5.6.

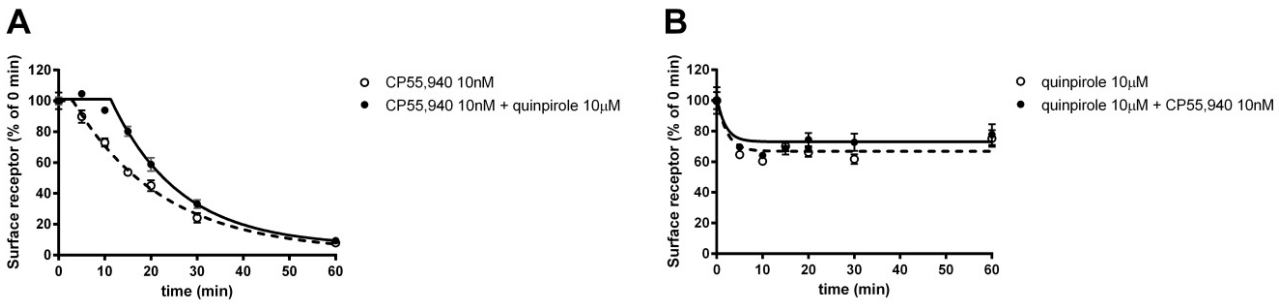

Figure 5.3 Internalisation of CB1 and D2 in response to agonist treatment over time.

(A) CB1 or (B) D2 agonist-induced internalisation responses to their respective agonists in the presence or absence of agonist stimulation of the other receptor. Representative results from one of three to five experiments, error bars represent the SEM of three technical replicates.

Table 5.5 Summary of CB1 internalisation time-course in response to 10 nM CP55,940 in the presence and absence of 10 μM quinpirole.

Data shown as mean ± SEM of four or five experiments.

	Condition			
Parameter	**No quinpirole**	**Quinpirole 0.1 μM**	**Quinpirole 10 μM**	**Significance**
Lag time before initiation of internalisation ("plateau at start", min)	3.3±1.9	5.5±2.3	8.9±2.1	ns
Exponential decay constant (K, min^{-1})	0.05±0.00	0.08±0.02	0.08±0.01	ns
Surface CB1 in response to 60min CP55,940 (% of vehicle)	7.5±1.8%	9.0±0.9%	13.6±2.0%	ns

Table 5.6 Summary of D2 internalisation time-course in response to 10μM quinpirole in the presence and absence of 10 nM CP55,940.

Data shown as mean ± SEM of three or four experiments.

	Condition		
Parameter	**No CP55,940**	**CP55,940 10 nM**	**Significance**
Lag time before initiation of internalisation ("plateau at start", min)	0.0±0.0	0.0±0.0	ns
Exponential decay constant (K, min^{-1})	0.04±0.02	0.15±0.06	ns
Surface D2 in response to 60min CP55,940 (% of vehicle)	70.0±3.3%	67.4±7.0%	ns

Constitutive internalisation

A 10 hour constitutive internalisation time-course assay was performed in order to determine whether exposure to opposite-receptor agonist affected CB1 or D2 constitutive trafficking. During the extended incubation time, agonist targeting the non-tracked receptor was applied in order to determine whether this altered the constitutive trafficking of the receptor of interest.

CB1 constitutive internalisation was clearly detected with 100% of surface receptors internalised within 10 hours (Figure 5.4(A) and Table 5.7), which was unchanged by exposure of D2 to quinpirole (0.1 µM). While D2 was observed to be constitutively internalised, neither a one-, two- or three-phase decay curves fitted this data (Figure 5.4(B)). Over 10 hours, approximately 80% of surface D2 was internalised, both in the presence and absence of CP55,940. While at early time points the data was suggestive of more rapid internalisation of D2 in the presence of 10 nM CP55,940, there was no statistical difference at any time point (p=0.1423).

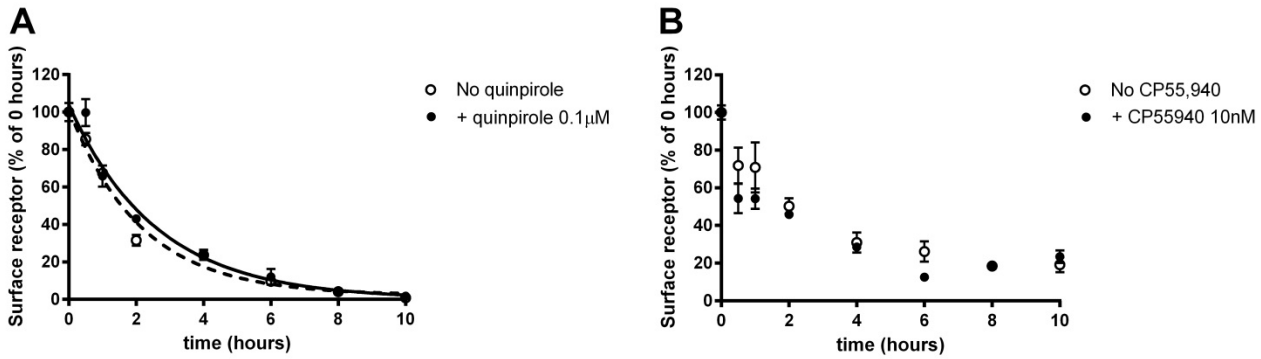

Figure 5.4 Time course of CB1 and D2 constitutive internalisation.

Constitutive internalisation of (A) CB1 and (B) D2 in the presence of vehicle or agonist to the non-labelled receptor. Representative results from one of three experiments, error bars represent the SEM of three or four technical replicates.

Table 5.7 Summary of CB1 constitutive internalisation time-course in cells co-expressing CB1 and D2 and in the presence and absence of 0.1 µM quinpirole.

Data shown as mean ± SEM of three experiments.

Parameter	Condition		Significance
	Vehicle	0.1 µM quinpirole	
Exponential decay constant (K, hours^{-1})	0.3±0.1	0.3±0.0	ns
Maximal CB1 internalisation (% of 0 hours)	0.7±0.7%	3.3±3.2%	ns

Recycling and repopulation

Recycling experiments were performed to determine whether CB1's phenotype was altered by co-expression and co-stimulation. CB1 is known to degrade when expressed in HEK cells (Grimsey *et al.*, 2010), therefore these experiments focussed on whether CB1 changed to a recycling phenotype and whether delivery of receptors to the cell surface (as measured by inverse agonist exposure) was altered (termed repopulation). Due to the low level of quinpirole-driven D2 internalisation detected above (Figure 5.2(B)), the D2 receptor was not included in this experiment, since internalisation is the first step in either the recycling or degradative pathways.

A 30 minute pulse of agonist was utilised to internalise receptors, followed by application of inverse agonist (to compete for any continued agonist activity) and antibody labelling to determine receptor recycling and/or repopulation (Figure 5.5). Treatment with CP55,940 resulted in a similar degree of CB1 internalisation whether or not quinpirole was present. Co-incubation with 0.1 μM quinpirole during the agonist pulse did not result in CB1 gaining a recycling phenotype. Instead, CB1 is rapidly internalised and these receptors do not return to the cell surface for the duration of the assay.

The repopulation assay utilises the same ligand treatments as the recycling assay, but instead detects surface receptors at the end of the ligand treatments, so as to show the net change in receptor localisation. In this labelling paradigm, we see that the initial agonist pulse reduces the total amount of CB1 on the cell surface, but to a lesser degree than seen in the recycling assay paradigm. This is because CB1 is still being delivered to the cell surface during agonist treatment, which can be detected by the repopulation labelling paradigm, but not the recycling paradigm. The cell surface repopulates with CB1 during incubation with inverse agonist, which acts to stabilise surface receptors and prevent further internalisation. The cell surface is repopulated back to basal level in approximately 1.5 hours, and by 4 hours of inverse agonist incubation reaches well above the initial receptor density. The repopulation of the cell surface with CB1 was not changed by the presence of quinpirole in the agonist pulse, and D2 antagonist in the recycling/repopulation phase.

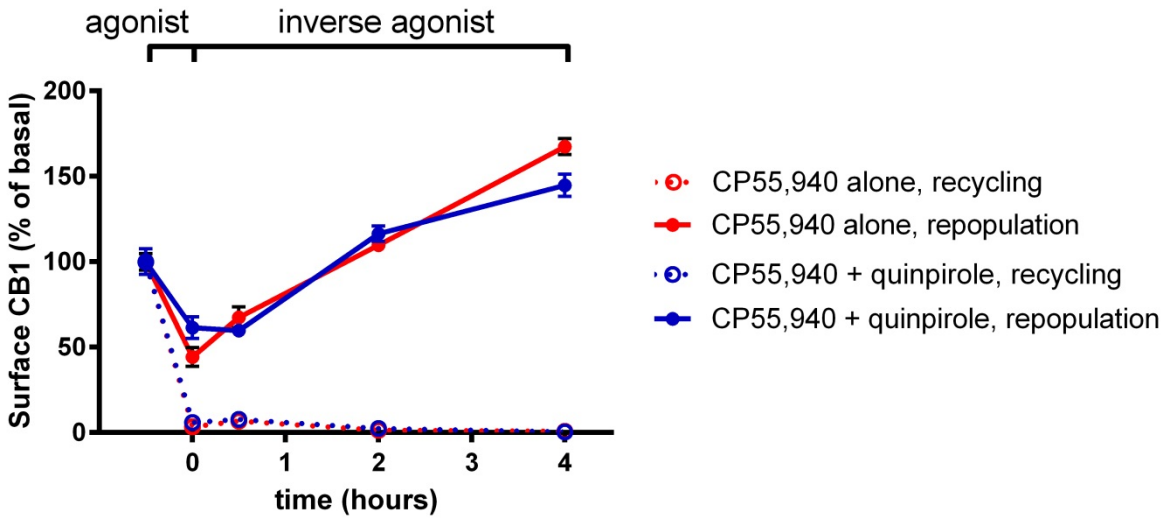

Figure 5.5 CB1 recycling and surface repopulation subsequent to 30 minutes of agonist exposure.

Cells were treated with 10 nM CP55,940, or 10 nM CP55,940 and 0.1 μM quinpirole for 30 minutes, followed by the CB1 inverse agonist SR141716A (1 μM) and D2 antagonist raclopride (10 μM). In the recycling assay, surface receptors were labelled with primary antibody prior to drug treatment, and secondary antibody was used to detect remaining/returning surface receptors at the end of the assay (dashed lines). In the repopulation assay, surface receptors were labelled at the end of the assay, thus demonstrating net change in receptor number (solid lines). Representative results from one of two or three experiments, error bars represent SEM of four technical replicates.

Table 5.8 CB1 recycling and repopulation following internalisation for 30 minutes with CP55,940 in the presence and absence of 0.1 μM quinpirole.

Data shown as mean ± SEM of two or three experiments.

Parameter	Condition		Significance
	10 nM CP55,940	10 nM CP55,940 + 0.1 μM quinpirole	
Recycling at 4 hours (% of original population)	2.9±2.1%	2.9±2.4%	ns
Repopulation at 4 hours (% of original population)	147.6±19.8%	135.6±9.2%	ns

Discussion

Receptor internalisation and trafficking experiments were performed to investigate whether CB1-D2 co-expression affects these receptor functions. Using antibody-based assays, each receptor was traced in trafficking pathways which may be affected by co-stimulation or cross-stimulation of the CB1-D2 heterodimer: agonist-induced and constitutive internalisation, and recycling/repopulation.

Statistically significant differences were seen in the extent of CB1 internalised after 60 minutes of agonist stimulation, with co-application of very high concentrations of both CP55,940 and quinpirole. These agonist conditions somewhat decreased the maximum extent of CB1 internalisation. This may have been caused by a delay in the initiation of CB1 internalisation when D2 was stimulated. As observed in time-course experiments using a lower concentration of CP55,940, this lag lasted 3.3 minutes on average when 10 nM CP55,940 was applied alone, but 8.9 minutes when 10 μM quinpirole was added with CP55,940, although this effect failed to reach statistical significance (Table 5.4). Meanwhile, the initiation of D2 internalisation occurred prior to the first measured time point (5 minutes) regardless of whether CB1 was stimulated.

On balance, these data probably indicates that CB1 and D2 follow separate internalisation pathways; although initial CB1 internalisation may be delayed by D2 stimulation, perhaps due to an acute competition for internalisation machinery, CB1 and D2 ultimately internalise at different rates and to differing extents suggesting physical separation of the receptors following stimulation. Conversely, while not a dramatic change in phenotype, the subtle influence of D2 stimulation on CB1 internalisation should not be discounted, as this may be indicative of altered molecular mechanisms of internalisation; for example, a change in GRK or β-arrestin recruitment profiles. Exemplifying this possibility, the thyrotropin-releasing hormone receptor TRHR2 interacts with β-arrestin2 when it is expressed alone, but when heterodimerised with TRHR1 it can also interact with β-arrestin1 (Hanyaloglu *et al.*, 2002). This was found not to be through TRHR1 recruiting β-arrestin1 on behalf of its heterodimer partner, but through TRHR2 itself acquiring altered recruitment properties (Hanyaloglu *et al.*, 2002).

A difference was seen between the two agonist-induced internalisation assay paradigms; the concentration-response assay appeared to produce a lesser extent of receptor internalisation than the time-response assay. This was seen for both CB1 and D2, with the concentration-response paradigm showing 20-30% less internalisation than the equivalent drug condition in the time-response paradigm. The effect was particularly apparent for D2, which had no detectable internalisation in the concentration-response experiments, but 30% of D2 were removed from the cell surface in the time-response experiment. These observations could only feasibly be due to confounding factors in the experimental design, as the concentration of drugs over the 60 minute incubation time were theoretically identical in these conditions.

The most notable difference in the experimental designs is the CO_2 control (and, by extension, buffer pH). In the time-response experiment, the experimental samples were removed from a CO_2-controlled atmosphere and incubated on the surface of a 37°C waterbath for the final 15 minutes of incubation in an attempt to ensure consistent temperature control during addition of drugs at acute time points (which was

not a concern in the single time point concentration response assays). Indeed, the time course experiments suggest that D2 internalisation response plateaus rapidly at approximately 5 minutes after drug addition (shown Figure 5.3(B)), whereas in the 60 minute concentration response experiment, when the entire incubation was performed in a CO_2-controlled atmosphere, D2 was not observed to internalise at all. This might indicate an interaction effect of drug/media addition and CO_2 environment whereby receptor internalisation is accelerated, resulting in a greater degree of internalisation when not in a CO_2-controlled atmosphere. As all time points for the time-course experiments were on the same multi-well plate this effect would be expected to influence all time points assayed, and thereby could explain the overall greater extent of both CB1 and D2 internalisation observed in the time-courses in comparison with the concentration responses.

Only a combination of a high concentration of CP55,940 (0.1-1 μM) and quinpirole (10 μM) produced any statistically significant changes in CB1 trafficking, decreasing the total magnitude of CB1 internalisation at 60 minutes. Considering quinpirole's low-nanomolar affinity for D2 receptors (Seeman *et al.*, 1994), it would be expected that 0.1 μM would also be sufficient to produce a strong functional effect, however this was not the case. At 10 μM, quinpirole could potentially be interacting with a range of other GPCRs, including other dopamine receptors and 5-HT receptors (Knight *et al.*, 2004; Seeman *et al.*, 1994), several of which have been detected in HEK cells (namely dopamine D2, D4 and 5-HT receptors) (Atwood *et al.*, 2011). Therefore, it is conceivable that the small functional effect of 10 μM quinpirole in these cells was not specifically and exclusively due to D2 co-expression.

Lastly, experiments were performed over longer periods of time (hours), in order to observe constitutive trafficking and recycling in cells which co-express CB1 and D2 receptors. Stimulation with agonist to the dimer partner did not alter constitutive trafficking of the labelled receptor. CB1 constitutive internalisation demonstrated a one-phase exponential decay, as has been shown before (Grimsey *et al.*, 2010). However D2 did not follow this pattern of internalisation and no standard exponential decay curves could model this data. Overall, D2 had slower constitutive trafficking compared to CB1: in 10 hours, only 80% of the original surface receptor population was removed (CB1 achieved this level of internalisation in 4-5 hours). This may be due to a slower basal rate of constitutive internalisation and/or constitutive receptor recycling pathways returning pre-labelled receptors to the cell surface. Constitutive internalisation over a short time-course (one hour) has been shown in HEK cells at a similar rate to that found in this study (Vickery *et al.*, 1999). D2 has also been shown to undergo constitutive recycling in neurons (Li *et al.*, 2012), although the rate of this is not well-defined. Regardless of the balance of constitutive recycling and degradation, the results of this study indicate that it is likely to be unchanged by co-stimulation of CB1.

Both CB1 and D2 receptors are generally reported to degrade following internalisation, rather than recycle to the cell surface (Bartlett *et al.*, 2005; Grimsey *et al.*, 2010). Trafficking pathways have been suggested to be altered in other GPCR dimers (Michael *et al.*, 2008; Terrillon *et al.*, 2004), therefore we tested whether co-activation of D2 receptors resulted in CB1 gaining a recycling phenotype. Only CB1 was monitored in the agonist-induced recycling assay, as D2 did not provide a robust internalisation response, a requirement for the measurement of subsequent receptor recycling. CB1 was tested for a shift to a recycling phenotype by first internalising CB1 with a "pulse" of agonist, and then observing if

any of the original receptor population returns to the cell surface. As expected, a recycling phenotype was not observed with CB1 agonist treatment alone, and this phenotype was unchanged by co-stimulation of D2 by quinpirole. These assays were performed with a concentration of agonist which was capable of achieving a near-maximal internalisation response, so as to facilitate maximal inverse agonist-mediated competition (Grimsey *et al.*, 2010). (This assay design is further discussed by (Grimsey *et al.*, 2010).) It is possible, however, that the very high concentrations identified as efficacious in the internalisation concentration-response are required to produce the most dramatic effects on CB1's internalisation phenotype (and potentially trafficking), however these cannot be feasibly tested using this assay design.

The key limitation to studying D2 post-endocytic trafficking in HEK cells is the low proportion of receptors which are internalised, although this cell line has been used extensively to study both D2 receptor function and GPCR internalisation in general (Alberts *et al.*, 2000; Gazi *et al.*, 2003; McAllister *et al.*, 1995; Salahpour *et al.*, 2011). In the experiments where D2 was observed to internalise, it did so to a maximum of 30% of the starting surface population. This is in line with internalisation patterns reported in the literature, with agonist-induced internalisation only resulting in 20-40% loss of surface D2 receptors in various cell models, including SH-SY5Y (Iizuka *et al.*, 2007), COS-7 (Iwata *et al.*, 1999) and HEK293 (Namkung *et al.*, 2009). The degree of D2 internalisation is reportedly enhanced by GRK2 (Guo *et al.*, 2010; Ito *et al.*, 1999), a regulatory protein which HEK293 cells are reported to have negligible expression of (Atwood *et al.*, 2011). The various GRK subtypes act to phosphorylate the intracellular face of the receptor, uncoupling it from G protein signalling and enhancing recruitment of further internalisation machinery (Reiter *et al.*, 2006). Interestingly, GRK2 is also required for CB1 internalisation in cultured rat neurons (Kouznetsova *et al.*, 2002), however CB1 internalises rapidly in HEK293 cells. HEK293 cells do, however, express GRK3 (Atwood *et al.*, 2011), which has also been implicated in both CB1 and D2 desensitisation (Jin *et al.*, 1999; Namkung *et al.*, 2009).

Previous studies have demonstrated that CB1 internalises rapidly in response to agonist in non-neuronal cell lines, with a time-course similar to that observed in this study (Cawston *et al.*, 2013; Hsieh *et al.*, 1999; Jin *et al.*, 1999; Rinaldi-Carmona *et al.*, 1998). In neuronal cells, however, this down-regulation process has been suggested to occur more slowly, with maximum internalisation generally detected at 16 hours (Blair *et al.*, 2009; Coutts *et al.*, 2001; Leterrier *et al.*, 2006; Tappe-Theodor *et al.*, 2007), although these experiments were performed by labelling receptors after drug incubation, and so the detected loss of surface CB1 may be a balance of internalisation and surface delivery. The difference in internalisation rate may be due to the configuration and/or expression of the various interacting proteins required in order to internalise CB1. These interacting proteins include AP-3 (which controls surface levels of CB1 by facilitating constitutive endocytosis (Rozenfeld *et al.*, 2008)), the aforementioned GRK subtypes, the cellular machinery of clathrin-coated pits (the mechanism by which CB1 is internalised (Hsieh *et al.*, 1999)), and GASP1 (which is involved in targeting CB1 and D2 for degradation (Bartlett *et al.*, 2005; Tappe-Theodor *et al.*, 2007; Thompson *et al.*, 2007)). The only feasible approach to overcome the limitations of the host cell proteosome would be to attempt these trafficking assays on endogenously-expressed CB1 and D2 receptors in primary neuronal cultures, although this would require antibodies targeting the N-terminus of each receptor. If CB1-D2 trafficking pathway interactions were found under these assay conditions, it would be interesting to determine whether the interaction is due to the

heterodimer itself, or mere competition between CB1 and D2 for their common trafficking partners (e.g. GRK2, GASP).

To date, only one study has attempted to relate agonist-driven receptor trafficking to the CB1-D2 heterodimer in a cell line. Przybyla, *et al.* (2010) found that long-term (10-30 hours) drug treatment with CP55,940 and quinpirole increased the proportion of receptors in a CB1-D2 heterodimer . Unfortunately, a key limitation to the interpretation of this study is that heterodimer formation was measured by bimolecular fluorescence complementation (BiFC), a detection technique which locks interacting proteins together with a slowly folding, irreversible protein tag interaction (Przybyla *et al.*, 2010). Using this experimental design, heterodimer formation could not be measured at incubation times shorter than 10 hours (Przybyla *et al.*, 2010). Previous studies have demonstrated that a considerable constitutive heterodimer interaction is present in transfected HEK cells (Chapter 3) (Marcellino *et al.*, 2008; Navarro *et al.*, 2008a; Przybyla *et al.*, 2010), however there may be stronger, temporary CB1-D2 heterodimer interactions which occur at approximately 7 minutes after agonist co-treatment (Kearn *et al.*, 2005). This would correlate with the theory that, if CB1 and D2 do have any trafficking interaction, it is subtle and is restricted to first 10 minutes of agonist application.

On the whole, it appears that the trafficking patterns of CB1 and D2 are not meaningfully affected by receptor co-expression and co-stimulation. While GPCR heterodimerisation is known to affect the trafficking properties of some receptor pairs, this is not a defining quality of heterodimers and so these results do not contradict the presence of CB1-D2 heterodimer. This study provides confidence that studies which investigate the trafficking of either of these receptors individually are likely to also reflect the behaviour of the receptor in cells which do express the CB1-D2 heterodimer.

6. Modulation of D2 expression as a result of co-expression of CB1

Introduction

In Chapter 5, the trafficking of hCB1 in the presence of hD2 was assessed. Interestingly, while dual-expressing HEK 3HA-hCB1/flag-hD2 clonal cell lines were established with relative ease, the long-term maintenance of a single-expressing HEK flag-hD2 cell line proved impossible. While we could transiently express the flag-hD2 construct easily in HEK wildtype cells, expression (as measured by antibody labelling) was very low immediately after antibiotic selection. Even after clonal selection, no populations of cells could be found with sufficiently high flag-hD2 expression on which to perform immunocytochemistry-based trafficking assays.

Based on this observation, we hypothesised that co-expression of the 3HA-hCB1 construct helped to stabilise surface flag-hD2 expression. There is precedent in the literature for such a phenomenon, for example the co-expression of CB1 with the angiotensin AT1 receptor resulted in a large increase in CB1 surface expression (Rozenfeld *et al.*, 2011). Another example is the $GABA_B$ receptor, which is an established example of a GPCR "obligate heterodimer", whereby association of the $GABA_{B(1)}$ and $GABA_{B(2)}$ units (each a seven transmembrane protein in their own right) must occur before release from the endoplasmic reticulum (Margeta-Mitrovic *et al.*, 2000). While $GABA_B$ is a Class C GPCR, a family which is now well-established to form obligatory dimers (Kniazeff *et al.*, 2011), this phenomenon has also been described for some Class A GPCRs. For example, α_{1D} adrenergic receptors, when expressed alone, are only found intracellularly, but co-expression with α_{1B} adrenergic receptors is sufficient to direct α_{1D} to localise to the cell surface in a variety of cell types (Hague *et al.*, 2004). Furthermore, the vasopressin V1a and V2 receptors form constitutive heterodimers in the endoplasmic reticulum and undergo post-translational modifications as heterodimers with the oxytocin receptor (Terrillon *et al.*, 2003). It has been hypothesised that this stabilisation of expression occurs via physical dimerisation; either interaction via the synthetic pathway promotes correct receptor folding and surface delivery, or interaction at the plasma membrane alters the life cycle of the receptor (Minneman, 2007).

In this study, we investigated whether CB1 co-expression altered the nature of flag-hD2 transgene expression during the selection and maintenance of stable cell lines.

Methods

Stable transfection experiments

In order to track the efficiency of stable transfection, HEK wildtype (wt), HEK 3HA-hCB1 or HEK 3HA-hCB2 cell lines were transfected with circular flag-hD2 pcDNA3.1+ plasmid, using Lipofectamine 2000

(Invitrogen, CA, USA) following the manufacturer's instructions. Two days after transfection, cells were transferred to flasks and 550 µg/ml G418 was added to the growth media to select for cells harbouring stably-integrated plasmid. Cell lines were passaged twice-weekly, being allowed to get no more than 90% confluent before passaging, and remaining in 550 µg/ml G418 for the duration of the experiment.

Immunocytochemistry

Immunocytochemistry was used to detect receptor expression on the cell surface, as described in Chapter 2. Permeabilised labelling was also performed to visualise total receptor expression, although neither antibody proved satisfactory for image analysis. The antibodies used are detailed in Table 6.1. Image acquisition was performed utilizing the ImageXpress XLS Micro automated microscope, and analysis was performed utilizing MetaXpress and MetaMorph as described in Chapter 2.

Table 6.1 Antibodies used in flag-hD2 stable transfection immunocytochemistry experiments.

Antibody	Species raised in	Supplier (catalogue number)	Batch/lot number	Dilution, live-cell incubation	Dilution, fixed-cell incubation
anti-HA monoclonal	Mouse	Covance (MMS-101P)	Various	1:500	n/a
anti-flag polyclonal	Rabbit	Sigma (F7425)	001M4789	1:400	n/a
			093M4798	1:400	n/a
anti-flag monoclonal (M2)	Mouse	Sigma (F1804)	Unknown	1:500	n/a
			SLBH1191V	1:2000[a]	n/a
anti-mouse, Alexa 488	Goat	Molecular Probes (A11029)	Various	n/a	1:400
anti-mouse, Alexa 594	Goat	Molecular Probes (A11032)	Various	n/a	1:400
anti-rabbit, Alexa 594	Goat	Molecular Probes (A11037)	Various	n/a	1:400

[a] This lot was supplied at a higher concentration than the previous lot, and was therefore optimised in parallel with the previous lot in order to maintain qualitatively and quantitatively equivalent labelling.

cAMP assay

Cytoplasmic cAMP signalling was measured using the V8-CAMYEL biosensor, as described in Chapter 2. Cells were treated with 5 µM forskolin to activate adenylate cyclase, and 1 µM quinpirole as a D2 agonist.

Protein alignments

The Emboss Needle protein alignment tool (http://www.ebi.ac.uk/Tools/psa/emboss_needle/) was used to determine the homology between specific sequences of 3HA-hCB1 and 3HA-hCB2. Sequences of

interest were chosen from interaction residues identified in the literature as important in the CB1-D2 dimer interface (as described in Chapters 1 and 3)).

Chronic drug treatments

A clonal HEK 3HA-hCB1/flag-hD2 cell population was treated for 3 days with 1 μM CP55,940 (CB1 agonist), SR141716A (CB1 inverse agonist), quinpirole (D2 agonist), or raclopride (D2 antagonist) in standard growth media (DMEM + 10% FBS). Receptor expression was analysed by immunocytochemistry, as described in Chapter 2.

Data analysis and statistics

Data were analysed using Prism (version 6, GraphPad, CA, USA), with additional statistical analysis performed by SPSS Statistics (version 21, IBM, NY, USA). In experiments comparing antibody labelling and cell line effects, two-way ANOVA was used with repeated measures matching and Sidak's multiple comparisons test. In other experiments, comparing receptor binding and function, repeated measures one-way ANOVA was performed with Tukey's post-test. The results of chronic drug treatments were compared to the vehicle-treated condition using one-way ANOVA and Dunnett's post-test.

Results

Antibody detection of flag-hD2 throughout the generation of stable cell lines

In order to substantiate our previous observations regarding the flag-hD2 construct, cells stably expressing the receptors of interest were generated as per standard laboratory procedure. Three HEK cell lines were transfected with the flag-hD2 pcDNA3.1+ plasmid, stable cell lines were generated using antibiotic selection, and antibody labelling was measured every second passage for 56 days. The parental cell lines were HEK wildtype (wt), or HEK stably transfected with either 3HA-hCB1 or 3HA-hCB2. Two different antibodies were used to label the flag epitope. These were the polyclonal rabbit anti-flag antibody (from the same manufacturer as was used in Chapter 5, except from different batches) and the monoclonal mouse anti-flag antibody. Although the original intention was to compare surface and total flag-hD2 labelling, both antibodies produced extensive nonspecific labelling and images were not quantifiable. An existing clonal cell line, HEK 3HA-hCB1/flag-hD2, was used as a control. This cell line had previously been observed to maintain a stable phenotype in continuous culture, and was therefore used to normalise antibody labelling across time points.

In the transient transfection phase (2 days post-transfection), striking differences between the anti-flag antibodies was observed (Figures 6.1, 6.2(A)). While two antibodies were originally utilized in order to validate the labelling profiles, they showed markedly different results. The rabbit anti-flag antibody showed approximately equivalent staining between the HEK wt, HEK 3HA-hCB1 and HEK 3HA-hCB2 cell backgrounds, while the mouse anti-flag antibody labelling was considerably different. In all the experimental samples, the mouse anti-flag antibody labelled fewer cells than the rabbit anti-flag, an effect which was especially pronounced in the HEK wt cell background (see Figure 6.2(A), 6.3, Table 6.2).

Antibiotic selection took approximately 14-18 days, as determined by the death of all cells in a flask of untransfected cells for each cell background. Immediately after antibiotic selection (day 21, 6 passages post-transfection), the difference between rabbit and mouse anti-flag staining was even more pronounced. The mouse anti-flag staining indicated near-complete loss of flag-D2 expression when transfected alone, whereas expression was apparently maintained in co-transfection with CB1 or CB2 (Figure 6.1(B, D); Table 6.2). This is qualitatively similar to that seen previously, which used a different batch of polyclonal rabbit anti-flag. Conversely, the current batches of rabbit anti-flag antibody suggested that flag-D2 expression was maintained whether or not CB1 or CB2 were present, although overall more cells were labelled with rabbit anti-flag antibody when the cell background contained 3HA-hCB1 or 3HA-hCB2, compared to HEK wt cells. (Figure 6.1(A, C); Figure 6.2(B); Table 6.2). It is important to note that under the incubation conditions utilised in these experiments neither antibody labelled any of the untransfected parental cell lines (i.e. no nonspecific binding). After long-term culture (day 56, 16 passages post-transfection), the proportion of cells labelled with rabbit anti-flag stayed approximately the same for all parental cell lines (HEK wt, HEK 3HA-hCB1, and HEK 3HA-hCB2; $p>0.05$)

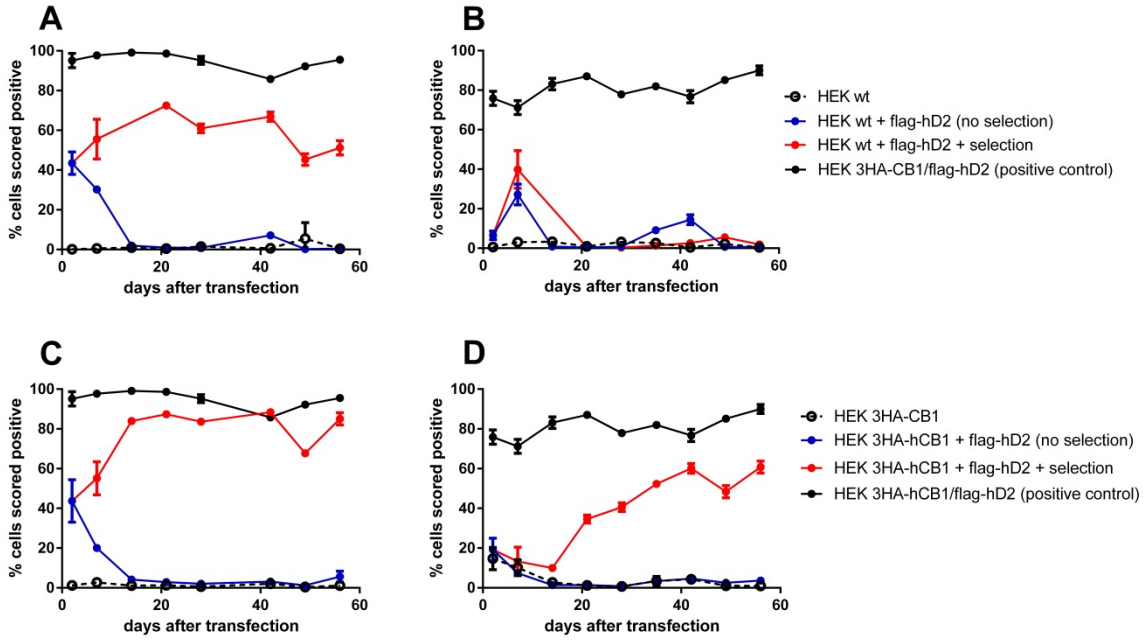

Figure 6.1 Expression of flag-hD2 in different HEK cell backgrounds, as detected by two anti-flag antibodies.

Flag-hD2 was transfected into HEK wt (A, B) or HEK 3HA-hCB1 (C, D) cell backgrounds. Staining of the experimental samples (red) was compared to that of the parental cell line (dashed lines), cells transfected but not under antibiotic selection pressure (blue lines), and a stably-transfected clonal cell line (black). Surface receptors were stained with either rabbit anti-flag polyclonal (A, C), or mouse anti-flag M2 monoclonal (B, D) antibodies. Example data representing three independent experiments. Similar results were obtained from the HEK 3HA-hCB2 cell background.

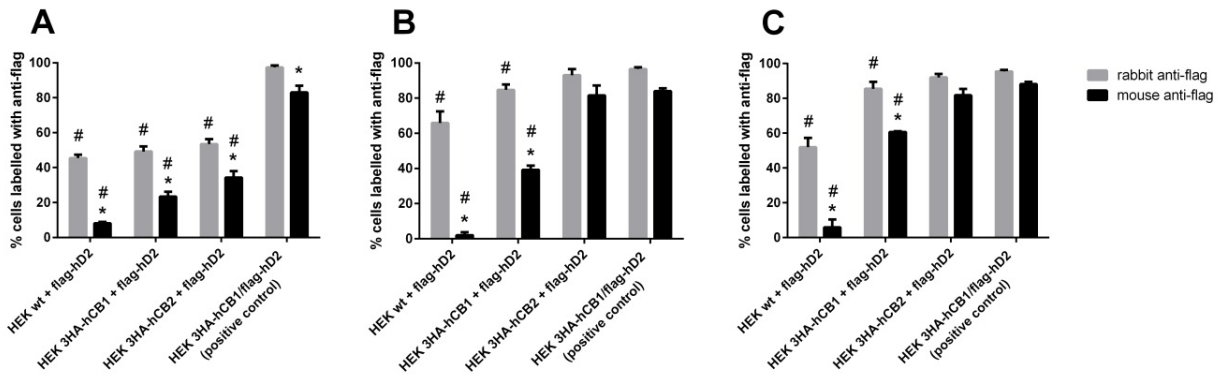

Figure 6.2 Percent of positively-labelled cells as determined by anti-flag antibody labelling in different HEK cell backgrounds.

*Cell lines were analysed 2 days (transient expression phase; A), 21 days (immediately after stable selection; B), and 56 days (after continuous selection and maintenance; C) after transfection. Mean ± SEM from three independent experiments. p<0.05, * significant within cell line, rabbit anti-flag vs mouse anti-flag; # significant compared to HEK 3HA-hCB1/flag-hD2 control cell line with same antibody.*

Table 6.2 Percent of positively-labelled cells as determined by anti-flag antibody labelling in different HEK cell backgrounds.

Mean ± SEM of three independent experiments.

	Antibody								
	Rabbit anti-flag polyclonal			**Mouse anti-flag M2 monoclonal**			**Anti-HA**		
Transfection condition	**Day 2**	**Day 21**	**Day 56**	**Day 2**	**Day 21**	**Day 56**	**Day 2**	**Day 21**	**Day 56**
HEK wt + flag-hD2	45.4 ±1.9	65.9 ±6.5	51.9 ±5.4	8.0 ±0.9	2.1 ±1.6	5.8 ±4.7	4.5 ±3.5	0.6 ±0.2	5.7 ±4.2
HEK 3HA-hCB1 + flag-hD2	49.2 ±2.9	84.7 ±3.1	85.5 ±4.0	23.3 ±2.8	39.2 ±2.4	60.7 ±0.4	92.3 ±2.6	98.7 ±0.4	97.5 ±0.4
HEK 3HA-hCB2 + flag-hD2	53.4 ±2.9	93.0 ±3.5	92.0 ±2.1	34.3 ±3.7	81.5 ±5.7	81.8 ±3.7	99.8 ±0.2	99.7 ±0.2	98.5 ±1.0
HEK 3HA-hCB1/ flag-hD2 (positive control)	97.4 ±1.2	96.5 ±1.1	95.5 ±0.9	83.0 ±3.9	84.0 ±1.6	88.2 ±1.3	97.6 ±1.1	96.8 ±1.1	96.3 ±0.6

The intensity of antibody labelling was also compared across the transfection conditions. Using the same microscopy images as were used for cell scoring, the total intensity of antibody labelling above background was averaged across all cells in the image. In every time point after day 2, all transfected cells are under antibiotic selection and should be transfected. Therefore averaging labelling in this way should overcome the limitation that very low-expressing cells may be below the threshold for the cell scoring analysis. Since each anti-flag antibody provides a different absolute level of staining, labelling was normalised so that untransfected HEK wt cells were set to 0%, and the HEK 3HA-hCB1/flag-hD2 control line was set to 100% labelling for each anti-flag antibody.

The average labelling intensity demonstrated differences in the degree of anti-flag labelling between the parental cell lines, but overall is in agreement with the data analysed by cell scoring. On day 2, in the transient transfection phase, there was low average flag-D2 labelling. This reflects that a low proportion of the cells are transfected. By day 21, the HEK wt cell background had completely lost mouse anti-flag labelling. Transfected HEK wt and HEK 3HA-hCB1 cells retained a lower level of rabbit anti-flag labelling per cell, indicative of a mixed population comprised of many lower-expressing cells compared to the clonal HEK 3HA-hCB1/flag-hD2 control line. Flag-hD2 labelling by both antibodies was significantly higher in the HEK 3HA-hCB2 cell background than in the HEK 3HA-hCB1 background. At day 56, flag-hD2 labelling in the HEK 3HA-hCB2 cell background had reduced to approximately equal to the control cell line, while labelling in the HEK wt and HEK 3HA-hCB1 cell backgrounds remained similar to that seen at day 21.

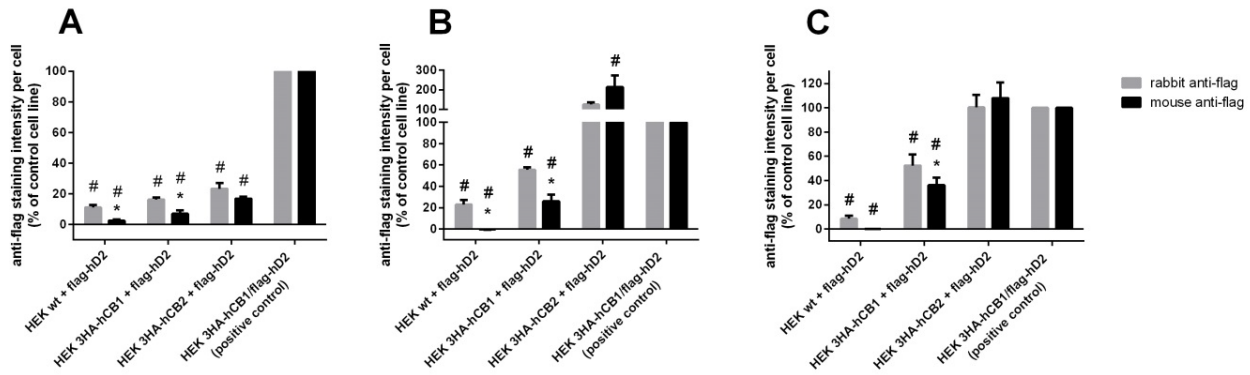

Figure 6.3 Labelling intensity of anti-flag antibodies when flag-hD2 is expressed in different HEK cell backgrounds.

*Cell lines were analysed 2 days (transient expression phase; A), 21 days (immediately after stable selection; B), and 56 days (after continuous selection and maintenance; C) after transfection. Data is normalised to the labelling of the antibody on the HEK 3HA-hCB1/flag-hD2 control cell line. Mean ± SEM from three independent experiments. $p<0.05$; * significant compared to antibody labelling within cell line, rabbit anti-flag vs mouse anti-flag; # significant compared to HEK 3HA-hCB1/flag-hD2 control cell line with same antibody.*

Table 6.3 Receptor staining intensity of flag-hD2 in different HEK cell backgrounds.

All staining was normalised to the intensity of the negative control (untransfected HEK wt; 0%) and positive control (HEK 3HA-hCB1/flag-hD2 clonal population; 100%). Mean ± SEM of three independent experiments.

	Antibody								
	Rabbit anti-flag polyclonal			Mouse anti-flag M2 monoclonal			Anti-HA		
Transfection condition	Day 2	Day 21	Day 56	Day 2	Day 21	Day 56	Day 2	Day 21	Day 56
HEK wt, untransfected	0	0	0	0	0	0	0	0	0
HEK wt + flag-hD2	11.0 ±1.8	22.9 ±4.4	8.5 ±2.4	2.5 ±0.7	-0.2 ±0.4	0.1 ±0.2	0.0 ±0.0	0.0 ±0.1	-0.1 ±0.2
HEK 3HA-hCB1, untransfected	0.0 ±0.0	-0.1 ±0.0	0.5 ±0.4	0.1 ±0.0	-0.3 ±0.4	0.3 ±0.3	40.3 ±8.6	50.5 ±10.1	48.1 ±11.4
HEK 3HA-hCB1 + flag-hD2	16.2 ±1.3	55.3 ±2.4	52.5 ±9.1	7.0 ±2.3	25.9 ±6.3	36.2 ±6.2	19.4 ±9.0	42.6 ±8.8	49.1 ±9.8
HEK 3HA-hCB2, untransfected	0.2 ±0.2	0.0 ±0.1	0.1 ±0.1	0.0 ±0.1	-0.2 ±0.5	-0.1 ±0.2	860.3 ±66.7	1323.1 ±290.1	935.7± 43.2
HEK 3HA-hCB2 + flag-hD2	23.4 ±3.8	124.8 ±11.4	100.3 ±10.4	16.9 ±1.3	213.0 ±60.6	108.1 ±12.9	814.1 ±33.4	939.3 ±223.9	679.1 ±17.7
HEK 3HA-hCB1/flag-hD2 (positive control)	100	100	100	100	100	100	100	100	100

Differences in antibody specificity

The experiments above showed that the rabbit anti-flag and mouse anti-flag antibodies gave markedly different labelling profiles. Therefore, the anti-flag antibodies were tested to verify their sensitivity to the flag epitope. The two different batches of rabbit anti-flag polyclonal were tested alongside a mouse anti-flag monoclonal antibody (M2). Anecdotally, the rabbit anti-flag polyclonal had been identified as being subject to batch-to-batch variability, and this is a widely-noted limitation of polyclonal antibodies (Bradbury *et al.*, 2015; Grimsey *et al.*, 2008a), while the mouse anti-flag monoclonal should not be affected by changes in epitope recognition between batches (assuming consistent handling by the manufacturer).

None of the three anti-flag antibodies tested showed non-specific staining, with negligible binding to HEK wt cells and HEK 3HA-hCB1 cells (Figure 6.4). There were very minor differences between the two batches of rabbit anti-flag polyclonal, although this did not reach statistical significance. This was not, however, the same batch of rabbit anti-flag antibody which was used previously to observe the flag-hD2

expression patterns originally; this early batch of polyclonal antibody was no longer commercially available, and thus its specificity could not be tested further.

As described above, there was a marked difference in the recognition patterns of the rabbit polyclonal compared to the mouse monoclonal antibodies, with the mouse anti-flag antibody seemingly unable to recognise the flag epitope of flag-hD2 when it was expressed alone. The rabbit and mouse antibody staining was statistically equivalent in the HEK 3HA-hCB1/flag-hD2 clonal cell line: the rabbit anti-flag antibody labelled 94% of cells, while the mouse anti-flag antibody labelled 85%, although this difference was only statistically significant between one batch of the polyclonal anti-flag and mouse anti-flag.

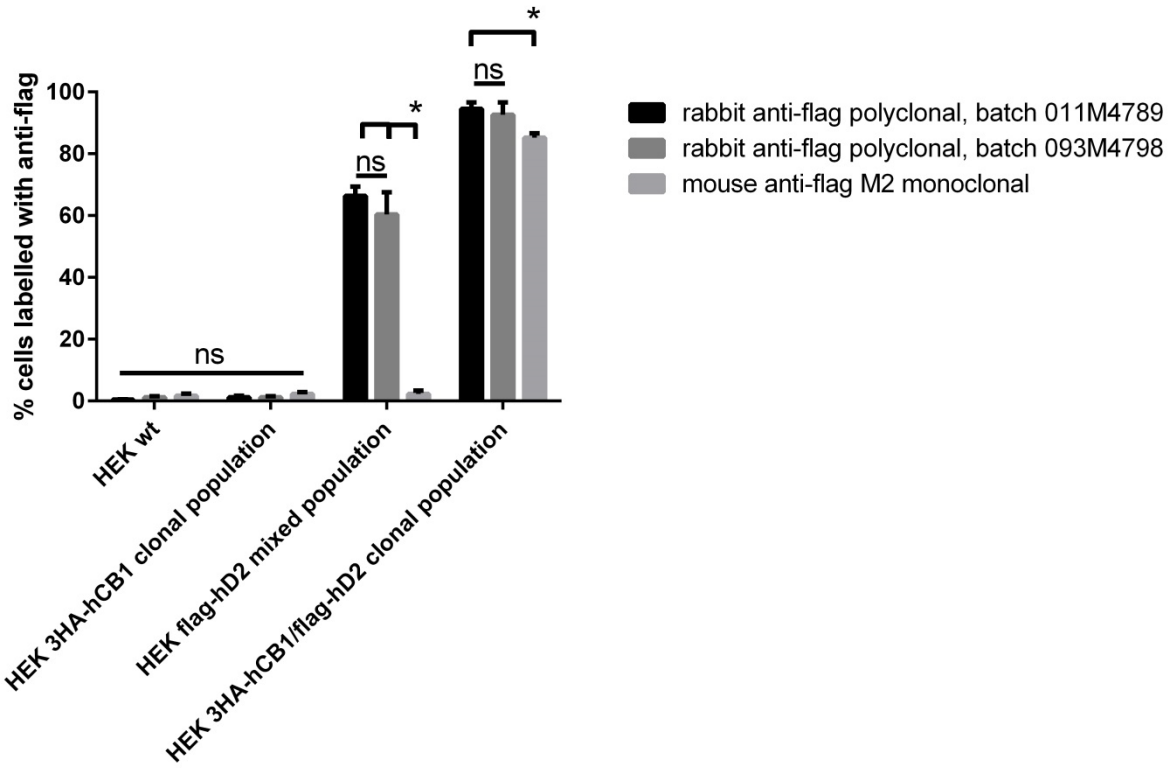

Figure 6.4 Comparison of anti-flag antibodies used for detection of flag-hD2.

*Stable cell lines were labelled under non-permeabilising conditions with anti-flag antibodies and analysed for the percent of cells with detectible antibody labelling. Data shown as mean ± SEM of three or four independent experiments. * p<0.05*

Due to the markedly different labelling observed with the rabbit anti-flag and mouse anti-flag antibodies, binding and functional studies were carried out as alternative means to determine flag-hD2 receptor expression in the cell lines generated.

Radioligand binding

To determine receptor number, whole cell radioligand binding assays were performed 56-57 days/16 passages post-transfection with [^{3}H]-raclopride, a D2-selective antagonist. All cells transfected and

selected for flag-hD2 expression contained approximately equal receptor levels, of 98-131 fmol D2 receptors per mg of total cell protein (differences not statistically significant; Table 5.4). This receptor binding was clearly above the specific binding measured in the parental cell lines, indicating that it was the flag-hD2 transgene which was conferring [^{3}H]-raclopride binding in these samples.

Table 6.4 [3H]-raclopride whole-cell binding in HEK cell lines transfected with flag-hD2.

*Cells were stably transfected with flag-hD2 and assayed day 56-57/16 passages post-transfection. Mean ± SEM of three independent experiments. * p<0.05 significant compared to untransfected parental cell line.*

Cell line	D2 receptors (fmol/mg total protein)	Significance compared to other conditions
HEK wt, untransfected	-1.7±1.7	-
HEK wt + flag-hD2	98.4±14.5*	HEK 3HA-hCB1 + flag-hD2 = ns HEK 3HA-hCB2 + flag-hD2 = ns HEK CB1/D2 control = ns
HEK 3HA-hCB1, untransfected	1.8±0.9	-
HEK 3HA-hCB1 + flag-hD2	130.7±1.8*	HEK 3HA-hCB2 + flag-hD2 = ns HEK CB1/D2 control = ns
HEK 3HA-hCB2, untransfected	0.1±1.5	-
HEK 3HA-hCB2 + flag-hD2	108.9±10.2*	HEK CB1/D2 control = ns
HEK 3HA-hCB1/flag-hD2 control	109.8±35.0	-

cAMP assay

To determine receptor functionality, cAMP assays were performed 57 days/16 passages post-transfection with quinpirole, a D2-selective agonist, and CP55,940, a non-selective CB1/CB2 agonist. As shown in Figure 6.5, all transfected cells were responsive to quinpirole (100 nM) as indicated by a reduction in cAMP relative to forskolin alone (100%). Flag-hD2-transfected cell lines which had originally contained 3HA-hCB1 or 3HA-hCB2 retained their responsiveness to CP55,940. Although all three experimental cell lines trended towards less responsiveness to quinpirole as compared to the HEK 3HA-hCB1/flag-hD2 positive control cell line, this difference was not statistically significant.

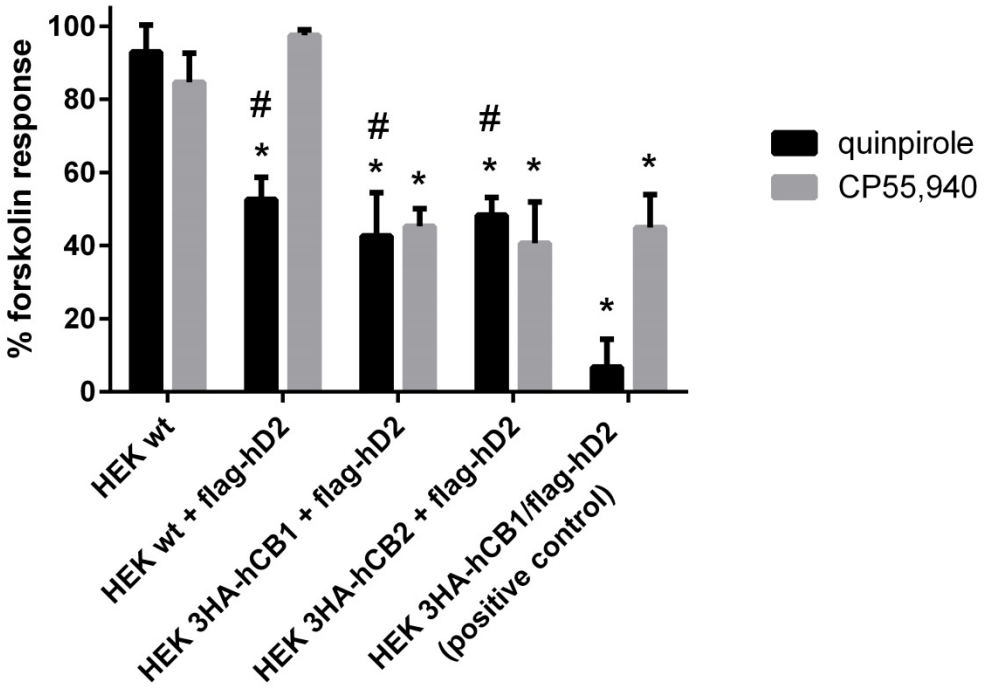

Figure 6.5 cAMP signalling in HEK cell lines stably transfected with flag-D2.

*Ability to inhibit forskolin mediated cAMP was measured at 15 minutes in cell lines 57 days/16 passages post-transfection with flag-hD2. Cells were incubated with 5 μM forskolin and 100 nM quinpirole or 100 nM CP55,940, and responses were normalised to 5 μM forskolin (100%) and vehicle (0%). Mean ± SEM of three independent experiments. p<0.05; * significant compared to forskolin alone; # significant compared to HEK 3HA-hCB1/flag-hD2 control cell line.*

Protein sequence homology between 3HA-hCB1 and 3HA-hCB2

The results above appear to show that both CB1 and CB2 expression alter the ability of the mouse anti-flag antibody to detect the D2 receptor. It is possible that dimer formation with the cannabinoid receptor results in a conformation of the receptor that unmasks the flag epitope, however CB2-D2 dimers have not been previously described. Therefore we considered if the proposed dimer interfaces of CB1-D2 receptors were conserved in CB2. (Here we describe the residues based on their positions in the untagged receptors, i.e. wildtype hCB1 and hCB2.) The TM1 dimer interface, tested in Chapter 4, was predicted to involve hCB1 residues A120, V121, L124, and T128. hCB2 has two of these residues – A37 and V38 (matching CB1's A120 & V121). However, as demonstrated in Chapter 4, there is little experimental support for this interface. Other potential CB1-D2 interaction sites include intracellular loop 3 (T321 and S322) (Navarro *et al.*, 2010), of which there are no homologous residues in hCB2; and the C terminus (C417-S431 in rat, which is identical throughout to human C415-S429) (Khan *et al.*, 2014) with low (26.7%) homology in hCB2.

Chronic drug treatments

As it appeared that CB1 expression markedly altered antibody recognition of flag-hD2 receptors by the mouse anti-flag antibody, we investigated whether the antibody staining profiles seen in the stable

transfection experiments could be recreated by pharmacologically altering CB1 expression in an already established CB1-D2 cell line. To do this, we attempted to reduce CB1 expression in the HEK 3HA-hCB1/flag-hD2 control cell line (as was used in the transfection experiments above), by driving degradation of the 3HA-hCB1 receptor using chronic agonist treatment. Conversely, we also used chronic inverse agonist to reduce constitutive turnover of 3HA-hCB1, which should result in a net gain of CB1 on the cell surface (Bouaboula *et al.*, 1997; Grimsey *et al.*, 2010).

Although chronic (3 days) CB1 agonist treatment did significantly reduce surface CB1 expression by approximately 90%, this did not produce a statistically significant alteration in detectable D2 levels. No other statistically significant effects were found, with either agonist or antagonist treatment. Therefore we can conclude that if any ligand-driven changes were occurring, they were not dramatic enough to detect in this assay.

Table 6.5 Changes in CB1 and D2 surface receptor antibody labelling following chronic drug treatment of the HEK 3HA-hCB1/flag-hD2 cell line.

*Cells were treated with 1 μM of CP55,940 (CB1 agonist), SR141716A (CB1 inverse agonist), quinpirole (D2 agonist) or raclopride (D2 antagonist) for 3 days. Receptor labelling was normalised to the antibody labelling of cells treated with vehicle (100%). Mean ± SEM of two or three independent experiments. *p<0.05 compared to vehicle-treated cells.*

	Staining intensity (% of vehicle treated cells)		
Drug treatment	**CB1, measured by anti-HA**	**D2, measured by rabbit anti-flag**	**D2, measured by mouse anti-flag**
Vehicle, 3 days	100.0±0.0	100.0±0.0	100.0±0.0
CP55,940, 3 days	8.4±0.8*	143.2±15.5 (ns)	145.6±16.0 (ns)
SR141716A, 3 days	127.6±8.8 (ns)	78.2±5.2 (ns)	89.6±12.4 (ns)
Quinpirole, 3 days	102.6±1.3 (ns)	85.3±21.3 (ns)	98.5±20.5 (ns)
Raclopride, 3 days	82.3±5.5 (ns)	84.1±17.8 (ns)	93.5±20.8 (ns)

Discussion

These studies were designed around the hypothesis that CB1 expression assisted expression of the flag-hD2 construct. This hypothesis was based on our observation that stably-transfected flag-hD2 expression appeared to decline in the absence of 3HA-hCB1, but was maintained at a stable level in cells that expressed the 3HA-hCB1 transgene. It is established that some GPCR heterodimers may interact during receptor synthesis pathways (Bulenger *et al.*, 2005), although it was already known that both CB1 and D2 do not need to be expressed together in order to function (Kearn *et al.*, 2005). Interactions during protein synthesis may modify the receptors' tertiary and quaternary structure, or post-translational modifications.

In this Chapter, and throughout this thesis, we used epitope-tagged GPCRs. Epitope tags are generally used for experiments requiring immunocytochemical detection of exogenous GPCRs, primarily because antibodies are difficult to raise to endogenous GPCR epitopes (Michel *et al.*, 2009). Furthermore, the commercially-available antibodies to epitope tags such as haemagglutinin ("HA") and DYKXXD ("flag") are well established in the literature, making the use of epitope tags an attractive approach to these experiments. The hD2 construct we have studied is N-terminally flag-tagged, and indeed "flag" is specifically recommended for internalisation assays (Koenig, 2004; Salahpour *et al.*, 2011).

Using antibody labelling, radioligand binding and a receptor signalling assay, the experiments in this Chapter showed that the flag-hD2 transgene was able to be expressed to similar levels either alone, or in combination with 3HA-hCB1 or 3HA-hCB2 in HEK cells. Therefore, the original hypothesis – that low anti-flag antibody binding reflected very low protein expression levels in HEK flag-hD2 cells – has proven not to be supported by this data. However, the presence of either cannabinoid receptor altered the degree to which the flag epitope could be detected by one of the anti-flag antibodies utilised. This may explain why previous attempts in the Receptor Signalling Laboratory could not establish a HEK flag-hD2 cell line: these cell lines were tested using anti-flag antibody to determine receptor number, and not by radioligand binding or a signalling assay. Although the batches of rabbit anti-flag antibody used to originally observe flag-hD2 expression (evidence which guided our original hypothesis) are no longer available for testing, it is likely they displayed a similar epitope-recognition profile to the mouse anti-flag tested here.

Following the observation that cell background altered the labelling patterns of anti-flag antibodies, we validated the binding profiles of the two commercially-available anti-flag antibodies used in this experiment: rabbit anti-flag polyclonal (Sigma, cat. F7425) and mouse anti-flag M2 monoclonal (Sigma, cat. F1804). Two antibodies were initially chosen to ensure redundancy in the experimental design; an approach which proved warranted when these antibodies showed differing sensitivities to the flag epitope. While there was negligible non-specific binding, an important difference was seen between the ability of the antibodies to detect the flag epitope. Although neither antibody accurately reflected the radioligand binding obtained from the HEK wt cell line transfected with flag-hD2, the mouse anti-flag essentially failed to recognise the flag epitope at all, unless the transgene was expressed with either 3HA-hCB1 or 3HA-hCB2. Since D2 ligand binding is reportedly unaffected by CB1 co-expression (Kearn *et al.*, 2005), it is most likely that the binding data is an accurate reflection of flag-hD2 receptor number in these cell lines and it is the antibodies which are less dependable. Assuming that it is a structural difference which affects the antibodies' affinity for the flag epitope, it is possible that the polyclonal rabbit anti-flag also contains a proportion of antibody idiotypes which are also unable to recognise this epitope. However, because this is a polyclonal antibody, there is sufficient variation in the antibody mixture to still label a significant portion of the flag epitopes regardless.

The anti-flag antibodies evidently show variation in their ability to recognise the flag epitope. Some antibodies are known to be sensitive to epitope post-translational modifications. The only post-translational modification which has been reported to affect recognition of the flag epitope is sulfonation (Choe *et al.*, 2009; Schmidt *et al.*, 2012), although presumably other modifications would have the potential to produce a similar disruptive effect. This sulfonation reaction is reportedly due to the flag

epitope's high acidity and the propensity of the internal tyrosine to be sulfonated (Choe *et al.*, 2009). Sulfonation of the flag epitope has been shown to prevent the mouse anti-flag M2 antibody from binding and reduces the binding of other anti-flag antibodies (Schmidt *et al.*, 2012; Tan *et al.*, 2013). Indeed, sulfonation of the N-terminus of GPCRs has been observed for several GPCRs, including the sphingosine 1-phosphate S1P1 receptor (Fieger *et al.*, 2005), chemokine CCR2 receptor (Tan *et al.*, 2013), and complement component 5a C5aR1 receptor (Liu *et al.*, 2011). Regardless of the specific source of the disruption of M2 binding affinity, it appears that the mouse anti-flag is highly sensitive to this modification, and the rabbit anti-flag polyclonal antibody is somewhat sensitive to this.

When we look specifically at the dopamine D2 receptor, the addition of the flag epitope on the D2 N-terminus is a relatively common way of monitoring D2 receptor expression and trafficking, e.g. (Ji *et al.*, 2009; Kearn *et al.*, 2005; Namkung *et al.*, 2004; Octeau *et al.*, 2014; Sharma *et al.*, 2013), usually without a second antibody to compare labelling profiles. Additionally, the mouse M2 anti-flag antibody specifically has been used for detection of N-terminally-tagged flag-hD2 (Kabbani *et al.*, 2002; Namkung *et al.*, 2004; Octeau *et al.*, 2014; Sharma *et al.*, 2013), which this study has shown has a high sensitivity to modification of flag-hD2. In light of the results of this study, previous studies which utilise this expression system should be reviewed with caution and future work designed to account for this phenomenon.

The result of the stable transfection experiments showed that HEK cells pre-transfected with 3HA-hCB1 and 3HA-hCB2 modify the detectability of the flag-hD2 transgene compared to when HEK wt cells are used as the parental line. When designing these experiments, CB2 was chosen as a control cell line because there is no evidence that a CB2-D2 heterodimer exists. Therefore, it was a surprise to find that 3HA-hCB2 expression also altered flag-hD2 expression in a way that was similar to 3HA-hCB1. There are several regions of CB1 which have been hypothesised and/or experimentally validated as contributing to the CB1-D2 heterodimer interface. Based on the protein sequence alignment of 3HA-hCB1 and 3HA-hCB2, it is unlikely that hCB2 carries enough homology to interact with hD2 by the same mechanisms as hCB1. Although there are no reported studies describing CB2-D2 interactions, there is a slim possibility that these receptors could be co-expressed and form physically-relevant heterodimers or signalling interactions. Reference data available from the Human Protein Atlas (Uhlen *et al.*, 2010) contains mRNA and antibody staining for both hCB2 and hD2. Keeping in mind the aforementioned limitations in GPCR antibodies, there is an indication that there are several tissues which stain positively for both hCB2 and hD2; in particular the appendix and tonsil. However, this data is not supported by mRNA expression patterns, which indicate that there is no overlap in peripheral hCB2 and hD2 expression (Uhlen *et al.*, 2010).

Potentially, the similarity between the effects 3HA-hCB1 and 3HA-hCB2 have on flag-hD2 expression are due to altered cell signalling, rather than a direct heterodimerisation interaction. Both CB1 and CB2 receptors signal through Gαi-pathways, and have similar functional effects in cAMP and pERK signalling (Bouaboula *et al.*, 1996; Galve-Roperh *et al.*, 2002; Pertwee *et al.*, 2010). It could be reasoned that the results of the chronic drug treatment experiments stand against this hypothesis. In this experimental paradigm, a pre-established HEK 3HA-hCB1/flag-hD2 clonal cell population was treated with chronic (3 day) agonist or inverse agonist in an effort to alter both receptor number (by driving receptor degradation, or preventing constitutive degradation respectively) and change constitutive signalling in the cell

population. It was found that although chronic agonist did considerably reduce CB1 levels, this was insufficient to cause a significant change in D2 detection levels. Since all the transgenes used in these studies are controlled by constitutive promoters, and therefore are not subject to changes at the level of protein synthesis, these drug conditions are intervening after receptor protein synthesis. Considering no significant changes were seen in flag-hD2 expression, these results would argue that the process which affects the flag epitope's detectability in the flag-hD2 transgene occurs during protein biosynthesis and are not a product of 3HA-hCB1 and 3HA-hCB2 constitutive signalling affecting this process.

In these experiments, we have demonstrated that in the HEK cell line, the expression pattern of D2 is altered when co-expressed with cannabinoid receptors. One previous study has reported that D2 receptor function is different when it is overexpressed in two different cell lines. These subtle differences in a D2 transgene's function have been reported in HEK, which do not endogenously express D2 (Atwood *et al.*, 2011), when compared to SH-SY5Y, which does endogenously express D2 (Alberts *et al.*, 2000). Given the ubiquity of the HEK cell background for receptor trafficking and signalling studies, it is important to recognise its limitations and to replicate phenomenon found using transgenes in endogenously-expressing cell types whenever possible. However, because relatively little is known about the complexities of protein synthesis and modification pathways, it is impossible to know in advance which cell line is the most physiologically-relevant for receptor characterisation. It would be interesting to determine whether the alteration to the flag epitope seen in this study reflected changes to the D2 receptor protein itself, for example by changes in posttranslational modifications. Furthermore, it would be interesting to test whether similar interactions occur in cells which endogenously express D2.

7. Cell phenotype and cAMP signalling of CB1

Introduction

The primary functional effect attributed to the CB1-D2 heterodimer is its cAMP signalling profile. Expressed alone, both CB1 and D2 are well-defined as Gαi/o-linked receptors, which thereby reduce cAMP production through Gαi/o-mediated inhibition of adenylate cyclases (Beaulieu *et al.*, 2011; Glass *et al.*, 1999). However, when these receptors are co-expressed and treated with agonists concurrently, cellular cAMP accumulates instead. This was first observed in rat striatal neurons (Glass *et al.*, 1997), and then in transfected cell lines (Kearn *et al.*, 2005). One study has also observed that merely co-expressing CB1 in a D2-expressing cell line was sufficient to induce CB1-mediated cAMP accumulation (Jarrahian *et al.*, 2004).

Glass et al (Glass *et al.*, 1997) first observed the CB1-D2 signalling interaction, and hypothesised that the apparent switch in signalling was due to signalling D2 receptors sequestering Gαi away from CB1. This leaves CB1 available to activate the less-favoured Gαs proteins. Supporting this, CB1 is recognised as having a Gαs-like signalling component; treating CB1 expressing cells with pertussis toxin reveals Gαs-like cAMP accumulation (Bonhaus *et al.*, 1998; Felder *et al.*, 1998; Scotter *et al.*, 2010). Unpublished studies from the Receptor Signalling Laboratory have found that expression of CB1 with a preprolactin signal sequence (PPLSS; Belin *et al.*, 1996) results in a dominant Gαs-like phenotype. The key consequence of adding an N-terminal PPLSS to CB1 is that it results in very high receptor expression levels. Thus, we hypothesised that an equivalent “signalling switch”, analogous to that which was observed with D2 receptors, might occur with CB1 receptors alone. In either scenario, high receptor expression essentially exhausts Gαi activation, allowing the lower affinity interaction with Gαs to become dominant. If this were the case, then we would expect that the observed signalling would be correlated to receptor expression; low receptor expression favouring a high affinity Gαi interaction, and higher expression levels favouring the lower affinity Gαs interaction.

It is, however, possible that the addition of PPLSS to CB1 results in other changes in the receptor biology than just expression level. Therefore, the ideal experimental design would be to investigate cAMP signalling in a single cell line with variable expression levels. One way to achieve this is to transiently transfect a clonal cell line (generating a population of cells varying only in their CB1 expression level), sort them by expression level, and then determine the cannabinoid-mediated alterations in cAMP. This became feasible following the development of the V8-CAMYEL biosensor (Chapter 2 and Appendix) which enables detection of changes in cAMP in a smaller number of cells than previous plate-reader-based biosensors. A stably-transfected clonal population of cells expressing V8-CAMYEL provided a homogeneous cell population into which the PPLSS-CB1 receptor could be transiently transfected. Fluorescence-activated cell sorting (FACS) was used to separate cells based on CB1 expression levels.

The high bioluminescence output of V8-CAMYEL permitted us to then perform live-cell cAMP assays on the small cell numbers recovered by FACS. Such an approach ensures that the cellular background is essentially identical between the cell lines being studied.

Methods

cAMP measurement

In order to study cAMP signalling, an Epac-based cAMP biosensor, V8-CAMYEL, was used. V8-CAMYEL indicates cytoplasmic cAMP concentration through changes in bioluminescence resonance energy transfer (BRET) signal, which can be measured in real time in live cells.

Creation and sorting of a 3HA-hCB1 mixed population

HEK-V8-CAMYEL cells (described in Chapter 2) expressing a mixed population of CB1 were generated by transient transfection of the PPLSS-3HA-hCB1 pef4a plasmid (described in Chapter 2) using Lipofectamine 2000 (Invitrogen, CA, USA), following the manufacturer's protocol. Stably transfected and clonally isolated HEK 3HA-hCB1 (as used in Chapters 5 and 6) and stable HEK PPLSS-3HA-hCB1 were used as reference cell lines, to control for antibody staining efficiency. Forty eight hours after transfection, transiently-transfected cells and the stably-transfected reference cell lines were lifted from the culture vessels using Versene (Life Technologies, CA, USA) so as not to cleave surface proteins. Cells were then stained in suspension with mouse anti-HA antibody (Covance, NJ,USA) and goat anti-mouse Alexa Fluor 647 (Molecular Probes, CA, USA). Negative staining controls (unlabelled, or with only secondary antibody) were included to determine the background staining, using the same cell lines.

Cell staining in the 647nm channel was measured in a BD FacsAria flow cytometer (BD Biosciences, NJ, USA), for both the reference cell lines and a sample of the transiently-transfected mixed population. Six collection bands were then defined, relative to the 647nm peaks in the reference populations, such that essentially all cells from the mixed population were collected, provided their receptor expression level was detected as being above background fluorescence (as defined by the negative staining controls).

The HEK-V8-CAMYEL PPLSS-3HA-hCB1 mixed cell population was sorted in assay buffer (HBSS + 1 mg/ml BSA) and collected at room temperature. Cells were then distributed into 96-well plates, at 10,000-20,000 cells/well and then assayed as per the cAMP assay protocol described in Chapter 2.

Data analysis

Data was processed and graphed using Prism (version 6; GraphPad, CA, USA). Statistical significance was determined by one-way repeated measures ANOVA with Tukey's post-test.

Results

CB1 Gαs signalling

We investigated CB1 cAMP signalling in relation to receptor expression levels. The following experiments were based on the observation demonstrated below, in graph 7.1, provided by David Finlay (Receptor Signalling Laboratory, University of Auckland). Here, we see the cAMP signalling response of two cell lines stably expressing 3HA-tagged hCB1. HEK 3HA-hCB1 cells demonstrated concentration-dependent inhibition of cAMP production in response to the CB1 agonist CP55,940, while HEK PPLSS-3HA-hCB1 cells generated a predominant Gαs-like phenotype. The most notable difference between these two cells is that they have markedly different surface density of CB1 as a result of the addition of the pre-prolactin signal sequence (PPLSS), which aides trafficking to the plasma membrane but is cleaved from the protein before reaching the cell surface (Rapoport *et al.*, 1996). Therefore we hypothesised that the Gαs phenotype might be related to high expression levels of CB1.

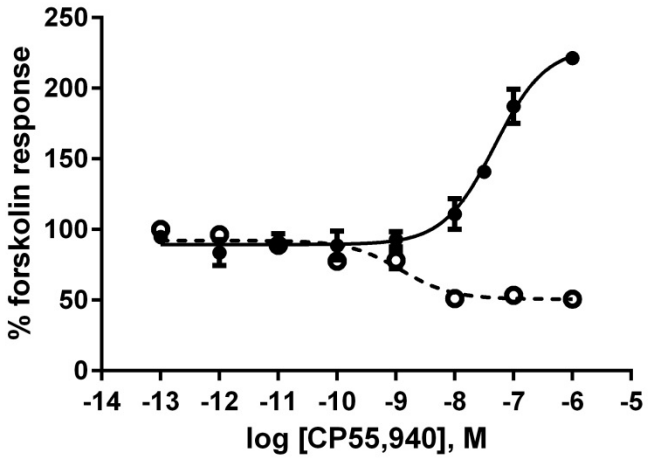

Figure 7.1 cAMP signalling in HEK PPLSS-3HA-hCB1 and HEK 3HA-hCB1 stable cell lines.

cAMP signalling profile of two 3HA-hCB1 stable cell lines, with PPLSS (solid line) or without (dashed line). Cells were treated with forskolin 2.5μM and the CB1 agonist CP55,940. Data supplied by David Finlay.

Cell sorting

The two cell lines described in Figure 7.1 were used as reference cell lines for the following experiments. As shown in Figure 7.2, the two reference populations differed in their surface expression of the 3HA-hCB1 transgene. To test the hypothesis that surface 3HA-hCB1 density determined signalling phenotype, we aimed to create a population of HEK cells which expressed a wide range of surface 3HA-hCB1 densities. In order to achieve this, a HEK-V8-CAMYEL stable cell line was created and clonally

isolated, to ensure that all cells in the mixed population differed only in their 3HA-hCB1 expression and not in biosensor loading.

Transient transfection was used to create a highly mixed population of HEK-V8-CAMYEL PPLSS-3HA-hCB1 cells. The levels of surface 3HA-hCB1 were measured immunocytochemically by flow cytometry and compared quantitatively to the two reference cell lines (Figure 7.2). Flow cytometry cell sorting was then used to divide this population into six subpopulations, as shown in Figure 7.2. These subpopulations were labelled A-F for subsequent analysis.

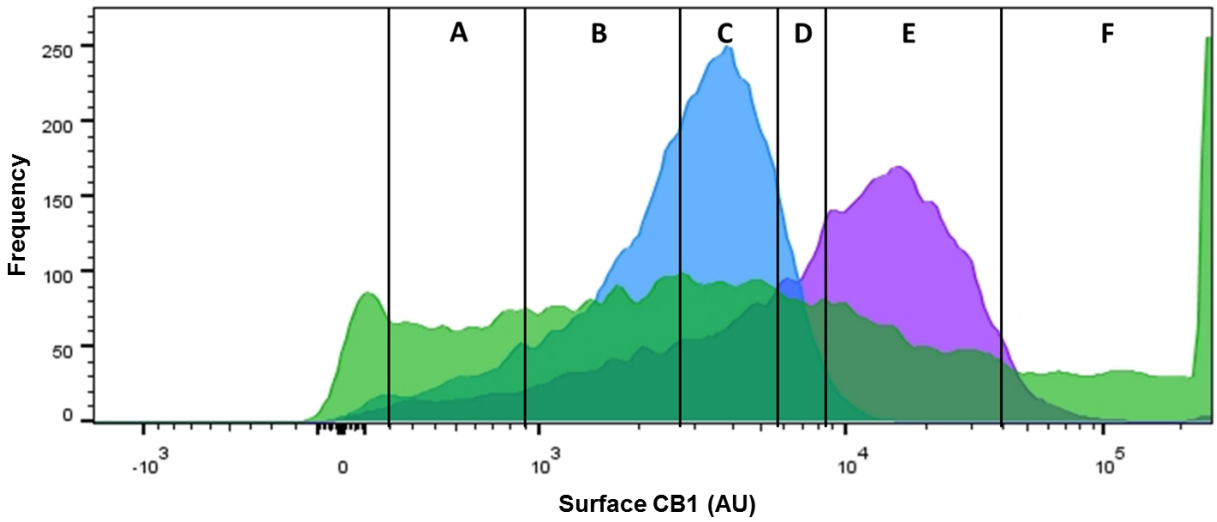

Figure 7.2 Frequency distribution of surface CB1 expression in HEK-V8-CAMYEL cells transiently transfected with PPLSS-3HA-hCB1.

Frequency distribution of surface CB1 expression in HEK cell lines (Gαi-coupling HEK 3HA-hCB1 in blue, Gαs-like HEK PPLSS-3HA-hCB1 in purple) and the transiently-transfected HEK-V8-CAMYEL PPLSS-3HA-hCB1 population (green). Vertical markers represent the sorting parameters for subpopulations A-F. Representative data from one of three independent experiments.

cAMP signalling in 3HA-hCB1 subpopulations

Once cells were sorted into subpopulations, real-time measurement of cAMP signalling was performed to compare cellular responses to CB1 agonists. As shown in Figure 7.3 and Table 7.1, the concentration-response to CP55,940 varied notably between the sorted subpopulations A-F. As expected, the subpopulation with expression matched to the Gαi-signalling reference population (subpopulation C) gave a robust inhibitory response. Subpopulations with lower expression, A and B, gave a weaker inhibitory response. The subpopulation with the highest 3HA-hCB1 surface expression (F), however, gave a stimulatory response, with cAMP formation well above that achieved by forskolin alone. The subpopulations with intermediate expression levels (subpopulation D and E) gave transitional cAMP signalling phenotypes, neither strongly inhibitory nor strongly excitatory.

Sigmoidal curves (Hill slope = 1) were fitted to the results of each experiment, and the summary results are shown in Table 7.1. Overall, the pEC50 of CP55,940 trended towards being higher in subpopulations with higher surface CB1, as compared to those with lower CB1 expression. The maximum signalling plateau (either above or below forskolin) was statistically significantly different. The time-course of cAMP signalling was not qualitatively different between subpopulations, with the inhibitory or stimulatory phenotypes remaining consistent over 20 minutes (Figure 7.4). Responses to both forskolin and CP55,940 with forskolin rise steadily from baseline (vehicle) over 5-7 minutes, followed by an approximate plateau maintained for at least the duration of assay measurement (15 minutes). In subpopulation C (Figure 7.4(A)), the inhibitory phenotype is apparent immediately, with CP55,940 reducing forskolin-stimulated cAMP changes at all time points. Similarly, in subpopulation F (Figure 7.4(B)), cytoplasmic cAMP levels are consistently above those produced by forskolin alone.

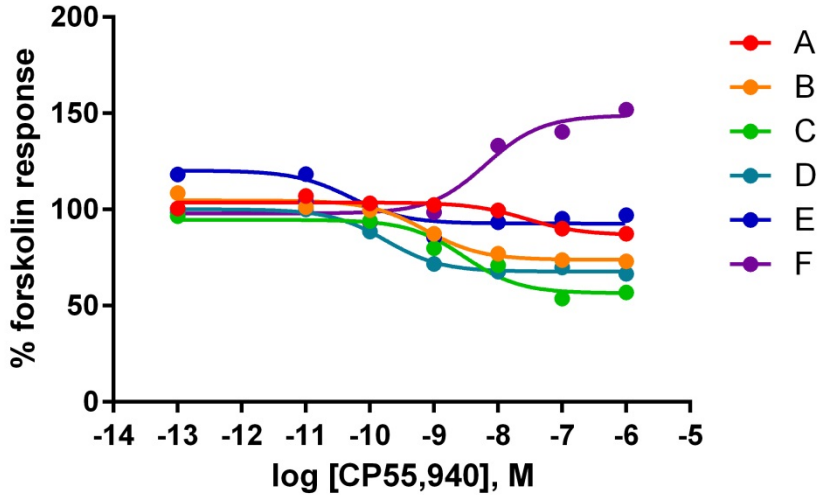

Figure 7.3 cAMP signalling profile of the transiently-transfected HEK-V8-CAMYEL cells sorted by PPLSS-3HA-hCB1 surface expression in response to CP55,940.

Cells were treated with 5 μM forskolin and the various concentrations of the CB1 agonist CP55,940. 20 minute area-under-the-curve for each response was normalised to vehicle (0%) and forskolin (100%). Sigmoidal curves were fitted with Hill slope constrained to 1. Representative data from one of three independent experiments.

Table 7.1 Summary results from CP55,940 concentration-responses generated by transiently-transfected HEK-V8-CAMYEL sorted by PPLSS-3HA-hCB1 surface expression.

Cells were treated with 5 μM forskolin and the various concentrations of the CB1 agonist CP55,940. 20 minute area-under-the-curve for each response was normalised to vehicle (0%) and forskolin (100%). Sigmoidal curves were fitted with Hill slope constrained to 1. Mean ± SEM from three independent experiments.

Subpopulation	Surface receptor density (anti-HA labelling, arbitrary units)	pEC50	Emax, % forskolin response
A	526±24	8.34±0.79[a]	87.6±0.9
B	1519±74	9.34±0.21	79.7±5.9
C	3382±410	9.31±0.40	67.2±5.5
D	8338±1803	10.01±0.13	81.5±10.7
E	22790±5657	8.66±0.82[a]	108.4±9.8
F	108830±10511	8.37±0.12	151.9±5.2
Statistical significance (one-way ANOVA)	p<0.0001	ns	p=0.000

[a] Curves fitted to this data may not be accurate as the total range of inhibition/stimulation did not deviate appreciably from forskolin alone. Exclusion of these conditions did not affect statistical significance.

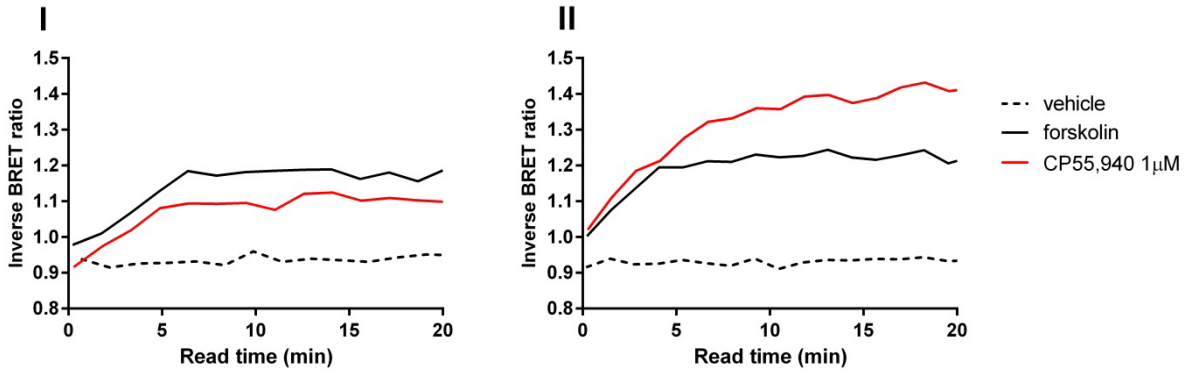

Figure 7.4 Time course of cAMP signalling response in sorted subpopulations of transiently-transfected HEK-V8-CAMYEL PPLSS-3HA-hCB1 cells.

Sorted subpopulations C (I) and F (II) were treated with forskolin (5 μM) with and without CP55,940 (1 μM), and the activity of the V8-CAMYEL biosensor was monitored for 20 minutes. Representative data from one of three independent experiments.

Discussion

To further understand the mechanism of the switch of CB1 from a Gαi- to Gαs-like signalling phenotype, we designed an experiment to test the hypothesis first put forward by Glass *et al.* (1997), regarding G protein competition. In cells which endogenously express CB1 and D2 receptors, co-stimulation with agonists results in an increase in cAMP production, consistent with Gαs coupling, whereas each of these receptors couple to Gαi when stimulated individually. This could be consistent with depletion of cellular Gαi proteins, unmasking a lower-affinity CB1-Gαs interaction. If this were the case, increasing the cellular expression of CB1 alone would produce a similar phenotype.

While it is widely reported that CB1 can increase cAMP concentration in a "Gαs-like" manner, the majority of this data has arisen from experiments which involved removing the Gαi signalling capacity of a cell, usually through pertussis toxin treatment (Bonhaus *et al.*, 1998; Felder *et al.*, 1998; Glass *et al.*, 1997; Gonzalez *et al.*, 2009). To date, very few other experimental designs have demonstrated CB1-mediated cAMP accumulation in untreated cells. For example, WIN55,212-2 gave a Gαs response when applied to rat globus pallidus cells (Maneuf *et al.*, 1997), as did desacetyllevonantradol when applied to a neuroblastoma cell line (Bash *et al.*, 2003). The primary advantage of using untreated cells is that it allows the observation of signalling under more typical cellular conditions. Unpublished observations from the Receptor Signalling Laboratory had found that a Gαs-like phenotype occurred in cells transfected with a CB1 construct tagged with a preprolactin signal sequence. This signal sequence increases the proportion of receptors which are trafficked to the plasma membrane. Therefore, we hypothesised that high surface CB1 expression might create a situation similar to dimer formation, where Gαi becomes limited and a lower affinity (but potentially higher efficacy) Gαs signalling capability of CB1 is "unmasked". To investigate this further we generated a mixed population of cells, differing only in their expression of CB1, and then sorted them based on receptor expression. A key factor in this experimental design was the ability to measure cAMP from small numbers of cells. A clonal HEK cell line expressing the V8-CAMYEL biosensor was developed to ensure stable and homogeneous biosensor expression. This cell line was transiently transfected with PPLSS-3HA-hCB1 to generate a population with a wide range of CB1 expression. Stable expression of the V8-CAMYEL biosensor enabled measurements to be taken from much smaller numbers of cells in a conventional plate reader, with identical biosensor load in all cells.

Using transiently-transfected cells, we sorted six subpopulations based solely on surface 3HA-hCB1 expression. cAMP signalling assays showed that these subpopulations differed markedly in their responses to cannabinoid agonists. When surface 3HA-hCB1 density was very low, cells had a low Gαi-like response to the cannabinoid agonist CP55,940, with the agonist reducing forskolin induced cAMP in a concentration-dependent manner. Then, with moderate expression of 3HA-hCB1, cells demonstrated a more pronounced inhibition of cAMP in response to cannabinoid stimulation. When surface 3HA-hCB1 density was high, cells responded in a Gαs-like manner to CP55,940, with a concentration-dependent increase in cAMP. The time course of cAMP production (Figure 7.4) indicated that both signalling phenotypes, inhibitory or stimulatory, became apparent immediately after drug addition, rather than a two-phase response, as has been reported previously for a CB1 allosteric modulator (Cawston *et al.*,

2013). This is consistent with a change in the qualitative nature of CB1 signalling through adenylate cyclase, rather than a rapid desensitisation of an inhibitory pathway resulting in an overcompensation of cytoplasmic cAMP.

A difference was noted between the results obtained from one of the reference cell lines and the "matched" sorted subpopulation. In the high-expressing stable cell line, used as a staining reference in the sorting experiments, a strong Gαs-like cAMP response was observed (Figure 7.1). However, in cells which had been transiently transfected and sorted to a similar level of surface CB1 expression, we observed only a weak accumulation of cAMP (Table 7.1, subpopulation E). This may be due to the different cell backgrounds used to create these cell lines. While the stable cell line had been generated from a parental HEK wildtype cells, the transiently-transfected population had been produced in HEK-V8-CAMYEL cells, for which the parental line was the HEK FlpIn wildtype cell line. Furthermore, the high-expressing stable cell line may have adaptive changes in the expression of components of the G protein signalling pathways, due to chronic overexpression of high levels of CB1, which is known to be constitutively active (Bouaboula *et al.*, 1997; Nie *et al.*, 2001; Pan *et al.*, 1998). GPCR-mediated down-regulation of G protein subunit expression has been reported previously, albeit in the context of agonist stimulation (Adie *et al.*, 1994; Kai *et al.*, 1996; Milligan *et al.*, 1991; Moravcová *et al.*, 2004; Mullaney *et al.*, 1993). Presumably, this regulation would also apply in the case of constitutively active receptors. Even in this high-expressing stable cell line, we assume that CB1 would preferentially couple through Gαi during constitutive activity, only switching to the predominant Gαs phenotype during ligand-mediated activity, as cellular Gαi is exhausted. This would result in a strong Gαs-like phenotype under agonist-stimulated conditions, as the cells contain less Gαi under basal conditions.

The mechanism of this cAMP signalling switch is unknown, and could be a consequence of several factors. As CB1 is a known promiscuous G protein coupler, but is primarily considered Gαi-linked (Hudson *et al.*, 2010a; Turu *et al.*, 2010), it would be conventional to use pertussis toxin to confirm the cAMP signalling phenotypes seen in the results of this study are due to changes in Gαi-coupling. Further studies would aim to investigate if CB1 Gαi-coupling does still occur in high-expressing cells in addition to the dominant Gαs-like coupling observed here.

However, G protein coupling is only part of the story of cAMP signalling and other interacting factors may also be of interest in future studies. Although CB1 has been shown, in general, to cause a net decrease in cellular cAMP concentration, its acute effects on adenylate cyclases are not always inhibitory. Adenylate cyclase isoforms II, IV, and VII are stimulated by CB1 activation, while others (I, III, V, VI, VIII, and IX) are inhibited (Rhee *et al.*, 1998). Of these "stimulated" isoforms, HEK cells have been reported to only express isoform VII (as well as the inhibited isoforms I, III, V, VI and IX) (Atwood *et al.*, 2011). The nine G protein mediated adenylate cyclase isoforms have been shown to vary in their sensitivity to Gαi subtypes, and also to Gβγ, while all are activated by Gαs (Hanoune *et al.*, 2001; Kamenetsky *et al.*, 2006). Of particular relevance to CB1, adenylate cyclase VII is activated by Gβγ subunits (Hanoune *et al.*, 2001), suggesting that CB1-mediated cAMP accumulation could be a combination of G protein mediated factors. Furthermore, adenylate cyclase isoforms I and VIII are stimulated by calcium. WIN55,212-2 promotes Gαq coupling and release of intracellular Ca2+ stores (Lauckner *et al.*, 2005; McIntosh *et al.*, 2007). This could be a contributing factor to cAMP accumulation and may help to explain

why WIN55,212-2 produced the most robust cAMP accumulation in a screen of CB1 ligands on pertussis toxin-treated cells (Bonhaus *et al.*, 1998).

Other GPCRs have been shown to change their cAMP signalling phenotype under various circumstances. For example, myometrial oxytocin receptors couple to both Gαi and Gαq/11, but during pregnancy this signalling develops a more Gαi-like cellular phenotype, due to downregulation of Gαq and phospholipase C, thus preventing Gαq-mediated Ca^{2+} release and smooth muscle contraction (Zhou *et al.*, 2007). Similarly, vasopressin V1a receptors have also been reported to couple to different G proteins based on cell cycle, being Gαq-linked in proliferating cells, and Gαq- and Gαi- linked in quiescent cells (Abel *et al.*, 2000). Finally, phosphorylation of the β2-adrenergic receptor by protein kinase A, which prevents continued coupling to Gαs, enables this receptor to change to a Gαi signalling phenotype (Daaka *et al.*, 1997).

These studies showed that the surface density of CB1 correlated to this receptor's cAMP signalling phenotype. The vasopressin V1b receptor is another GPCR which has been described as changing signalling phenotype when expressed at various densities. This receptor was reported to exhibit a biphasic concentration-response curve to its endogenous agonist (AVP) when expressed at high receptor densities, but not low or medium densities (Thibonnier *et al.*, 1997), and described as a possible switch between Gαq and Gαs coupling. This finding has since been contradicted in a study which found that the signalling switch was not due to changes in receptor expression levels, although no alternative mechanism was proposed (Orcel *et al.*, 2009). CB1 expression levels has also been shown to influence receptor coupling to Akt in astrocytoma cells, with low receptor expression leading to apoptosis through ERK1/2, and high expression initiating Akt pathways which prevent cell death (Cudaback *et al.*, 2010). It is not clear whether this observation is related to a "switch" in cAMP signalling, as Akt pathways can be both stimulated or inhibited by cAMP, depending on cell type (Insel *et al.*, 2012).

Potentially, receptor expression levels may influence the localisation of GPCRs in membrane microdomains, which modulate receptor signalling phenotypes by being locally enriched for certain signalling proteins (Maurice *et al.*, 2012). The β2-adrenergic receptor is normally located in lipid rafts along with other components of GPCR signalling pathways (Pike, 2003), however when cells are depleted of cholesterol and these lipid rafts are disrupted, β2-adrenergic signalling through Gαs is increased due to decreased desensitisation (Pontier *et al.*, 2008). Considering this, a contributing factor to CB1's density-dependent signalling switch may be that high receptor expression levels cause the receptor to "spill out" from its normal localisation and separate the receptor from its supply of Gαi proteins.

CB1 has been demonstrated to be upregulated in a wide variety of disease states. For example, upregulation has been demonstrated in the frontal cortex in animal models of chronic stress (Zoppi *et al.*, 2011); schizophrenia (Ceccarini *et al.*, 2013; Urigüen *et al.*, 2009); depression-suicide patients (Hungund *et al.*, 2004); in the spine in neuropathic pain models (Lim *et al.*, 2003; Siegling *et al.*, 2001; Wang *et al.*, 2007); in the striatum and hypothalamus of type I diabetes patients (Díaz-Asensio *et al.*, 2008); and in blood vessels and nerves in patients with Achilles tendinosis (Björklund *et al.*, 2011). CB1 upregulation has also been shown in several cancers, including alveolar rhabdomyosarcoma (Marshall *et al.*, 2011); ovarian cancer (Messalli *et al.*, 2014); colorectal cancer (Gustafsson *et al.*, 2011; Jung *et al.*, 2013); and

prostate cancer (Chung *et al.*, 2009; Cipriano *et al.*, 2013; Sarfaraz *et al.*, 2005). While upregulation is generally associated with poorer cancer prognosis, CB1 overexpression in hepatocellular carcinoma provides an improved outcome (Xu *et al.*, 2006). Therefore, signalling responses mediated by CB1 may be modified in these disease states.

This study has documented the phenomenon of CB1 signalling based on surface receptor density. There are many possible factors which could contribute to this cAMP signalling phenotype, and there is considerable evidence that this may be physiologically relevant in a variety of disease states. Of primary interest in this thesis is whether the mechanism which causes CB1's signalling "switch" is the same when CB1 is expressed alone, compared to when D2 is co-expressed. If the theory of G protein competition is true, then it would hold that D2 expression would also be sufficient to exhaust the Gαi capacity of the cell, allowing CB1 to signal through Gαs. Further work could investigate whether CB1's cAMP signalling phenotype is either a cause or an effect of changes in the GPCR signalsome.

8. General discussion

The initial findings of GPCR heterodimerisation has led to the identification of many receptor pairings. Heterodimerisation has been touted as a revolution in drug development, theoretically allowing pharmacological manipulation of specific subpopulations of receptors by heterodimer-targeted drugs. The ability to restrict receptor-mediated drug responses to such a subpopulation would hypothetically reduce off-target effects. The CB1 cannabinoid receptor is an ideal candidate for this style of drug design, due to its widespread tissue distribution.

As the signalling cascades of GPCRs can overlap considerably, the criteria for the presence of a heterodimer requires the demonstration of a functional and physical interaction in native tissues (Pin *et al.*, 2007). The CB1-D2 heterodimer is expressed in the same cells of the nucleus accumbens and prefrontal cortex (Chiu *et al.*, 2010; Pickel *et al.*, 2006), and isolated striatal neurons show a similar cAMP signalling phenotype to transfected cell lines (Glass *et al.*, 1997; Kearn *et al.*, 2005). This phenotype is a "switch" from single-receptor Gαi-coupling to Gαs-like stimulation of adenylate cyclase upon receptor co-activation (Glass *et al.*, 1997; Kearn *et al.*, 2005). Additionally, CB1-D2 heterodimer has been shown using co-immunoprecipitation (Kearn *et al.*, 2005; Khan *et al.*, 2014), FRET (Carriba *et al.*, 2008; Marcellino *et al.*, 2008) and BiFC (Przybyla *et al.*, 2010).

The overarching aim of this thesis was to further characterise the structure and signalling interactions of the CB1-D2 heterodimer.

Measurement of CB1-D2 heterodimerisation

The first aim of this thesis was to optimise a bioluminescence resonance energy transfer (BRET)-based method to identify and characterise the CB1-D2 heterodimer. BRET has been used extensively to measure GPCR dimerisation, but is often suggested to give false-positive results due to inattentive experimental design (James *et al.*, 2006; Pfleger *et al.*, 2006a; Pfleger *et al.*, 2006b; Szalai *et al.*, 2014). The ideal situation for using BRET as a measure of protein interactions is when those interactions can be modulated, for example ligand-mediated heterodimerisation, as described previously for CB1-D2 (Kearn *et al.*, 2005).

We used the BRET "saturation" assay paradigm as the basis for determining CB1-D2 heterodimerisation, as this is the most widely-used experimental design in the literature, likely due to its intuitive interpretation. While validating the expression of the BRET-tagged receptors, we observed that protein expression was related to co-transfection conditions. When cells were co-transfected with both BRET-tagged receptors, they expressed less of the donor-tagged receptor than when this construct was transfected alone. As the saturation assay relies on careful control of the expression of the receptors, we tested two methods of quantifying receptor expression.

First, we tested the predominant method in the literature, which assumes that luminescence emission is correlated directly to the expression of the luciferase-tagged receptor. However, in our hands, we found

little relationship between measured luminescence and the quantity of receptor protein detected by immunocytochemistry. We hypothesise that this is due to two competing processes. Firstly, when Venus is co-expressed with the luciferase, it is capable of quenching the luminescence of Rluc8 through the transfer of energy from the luciferase donor to the fluorescent acceptor (the theory which underpins the BRET technique). This would account for the lower-than expected luciferase emissions when high levels of Venus are co-expressed with luciferase. Secondly, when highly expressed, luciferase emissions are not as high as would be expected based on immunocytochemical detection. We suggest this may be due to the luciferase not reaching its maximum catalytic rate, due to limitations in cytosolic coelenterazine and/or oxygen. Although neither of these made a dramatic difference to the final conclusion of this study, we concluded the most conservative way of normalising BRET data is by protein expression, as measured by immunocytochemistry.

Once the constitutive heterodimer was established, the logical progression was to test for the ligand-mediated nature of the heterodimer interaction. Disappointingly, agonist co-stimulation of CB1 and D2 did not yield any measureable change in BRET efficiency. This is not to say that the nature of the heterodimer interface has not changed, but suggests that either the co-stimulation conditions do not result in movement of the BRET tags, or that they are moving in such a way as to maintain the same transfer efficiency. One possible reason a ligand-mediated dimer may have been co-immunoprecipitated previously (Kearn *et al.*, 2005) is that the stringency conditions of the assay favoured extraction of the activated heterodimer conformer, more so than the inactive conformation (Hall, 2005). Also, the presence of BRET does not rule out other protein components of the signalosome acting as a bridge which allowed co-immunoprecipitation.

As we had good evidence for a constitutive CB1-D2 heterodimer, we then tested a predicted dimer interface. The transmembrane (TM) TM1-TM1 dimer interface was predicted by homology modelling of CB1 and D2 receptors, and four key residues identified in each receptor were modified in order to test this interaction. None of these made a statistically significant difference to the CB1-D2 heterodimer, as determined by qualitative and quantitative analysis of the BRET saturation curve. This is a good indication that the predicted residues did not contribute significantly to the heterodimer interface.

During the course of this investigation, two studies have suggested sites for the CB1-D2 heterodimer interface. These are the intracellular loop (IL) 3 of both CB1 and D2 (Navarro *et al.*, 2010), and the CB1 C-terminus with D2 IL3 (Khan *et al.*, 2014). These are both feasible interaction sites, and warrant further characterisation in terms of heterodimer signalling. So far, the majority of GPCR heterodimer interfaces have been found in the transmembrane domains (Tena-Campos *et al.*, 2014), although the muscarinic M3 homodimer has an IL3-IL3 interaction (Borroto-Escuela *et al.*, 2010a) and the μ-opioid-dopamine D1 heterodimer interaction involves the D1 C-terminal tail (Juhasz *et al.*, 2008). D2, in particular, has a well-characterised interface with the adenosine A2A receptor, which includes the C-terminus of A2A and region of the cytoplasmic end of TM5/IL3 of D2 (Borroto-Escuela *et al.*, 2010b; Ciruela *et al.*, 2004; Navarro *et al.*, 2010) (note that these regions are adjacent and it appears these are similar residues described differently by different authors). However, it is known that oligomerisation between A2A-D2 and CB1-D2 is not mutually exclusive and that these three receptors are likely to form an oligomer *in vivo* (Carriba *et al.*, 2008; Navarro *et al.*, 2008b; Navarro *et al.*, 2010). Thus it is unlikely that CB1 is

competing with A2A for interaction sites on D2. New techniques for GPCR crystallisation have aided in elucidating the dimer interfaces of several receptors (Audet *et al.*, 2012; Venkatakrishnan *et al.*, 2013). Although neither CB1 nor D2 has been successfully crystallised to date, in the future these structures may shed light on the structure of the CB1-D2 heterodimer.

Receptor trafficking and expression phenotype

As a constitutive heterodimer, it may be expected that CB1-D2 interact by constitutive and ligand-mediated receptor trafficking. Many other GPCR heterodimers exhibit trafficking interactions, including heterodimers containing CB1 (Ellis *et al.*, 2006; Ji *et al.*, 2009) or D2 (Agnati *et al.*, 2006; Genedani *et al.*, 2005; Hillion *et al.*, 2002; Octeau *et al.*, 2014). However, this is the first study to investigate this for CB1-D2 directly. Cells co-expressing CB1 and D2 receptors were assayed using a variety of immunocytochemistry-based receptor trafficking assays. In these assays, there was no evidence for gross changes to the ligand-induced trafficking phenotypes. Overall, CB1 gave a robust agonist-induced internalisation response, whereas D2 did not, indicating that these receptors almost certainly do not have significantly different trafficking phenotypes when co-stimulated. Relatively subtle changes were seen in the extent of agonist-induced CB1 internalisation at 60 minutes, when D2 was co-stimulated with very high (10 μM) quinpirole. We can speculate that this may be indicative of differential GRK or β-arrestin recruitment, although further studies would need to investigate this.

There is an inconsistency between the time course of the BRET interaction and the trafficking assays. In the BRET assays, CB1-D2 BRET was stable over at least 15 minutes, although in the trafficking assay it was shown that CB1 would have internalised significantly during that time frame, and D2 had not. Thus we would have predicted to see disruption of the dimer due to CB1 internalisation. This may be due to the differences in the experimental designs for these studies. In the BRET assays, the HEK-FT cell line was used, which provides high protein expression in transient transfections. This overexpression may limit trafficking processes by overwhelming internalisation processes. Furthermore, it has been our observation that in the buffers required for BRET detection, internalisation of stably-expressed GPCRs is slowed (unpublished observations, Receptor Signalling Laboratory). This may be related to buffer composition, with internalisation being carried out in DMEM, while our BRET assay utilised HBSS, however changes to the assay buffer composition (e.g. addition of glucose) prevent BRET detection with our reagents (unpublished observation, Receptor Signalling Laboratory). Finally, it is highly likely that the addition of large C-terminal tags could interfere with the interaction of regulatory proteins required for normal internalisation processes. This is the key limitation of RET techniques – the necessary alterations to physiological conditions may prevent the normal spectrum of receptor regulation processes.

An interesting observation noted during the trafficking assays was that a HEK flag-hD2 cell line could not be established unless CB1 was co-expressed. Although CB1 and D2 have been reported to control the transcription of each other in endogenously-expressing cells (Blume *et al.*, 2013), this was not possible in our transgenic cell line, which utilised constitutive promoters. It was therefore hypothesised that CB1 and D2 interact during protein synthesis to increase D2 expression. To quantify this, HEK cell lines, either wildtype or stably transfected with the CB1 receptor, were transfected with a flag-tagged D2 receptor ("flag-hD2"). While attempting to measure the receptor expression patterns in these cells, we used two anti-flag antibodies which transpired to give remarkably different flag-hD2 labelling results. One of these

antibodies, a mouse monoclonal, gave very low staining for flag-hD2 receptors when they were expressed alone, but not when the cell line also expressed CB1. In contrast, the second antibody, a polyclonal, readily detected flag-hD2 receptors regardless of co-expression of CB1. Receptor binding and signalling assays confirmed that flag-hD2 expression was similar across all conditions; the only difference was in the staining of this one particular anti-flag antibody. This antibody has been described as being sensitive to flag-tag sulfonation, although perhaps other modifications also affect its binding and the exact mechanism by which this occurs remains to be established. Regardless of the mechanism, this data indicates that expression of CB1 can interfere with the structure of the flag-hD2 protein, perhaps by exposing D2 to different posttranslational modifications. Further studies are warranted, to determine the exact nature of this effect and whether it affects the D2 receptor itself, or just the flag epitope tag.

CB1 signalling through Gαs is dependent on the receptor density

Finally, I investigated the phenomenon of CB1-D2 heterodimer-mediated "switch" to Gαs-coupling. This signalling event has been reported many times in the literature (Glass *et al.*, 1997; Jarrahian *et al.*, 2004; Kearn *et al.*, 2005; Khan *et al.*, 2014), but as of yet there has been no testing of the hypothesis first put forth in Glass et al (Glass *et al.*, 1997). Their hypothesis was that in cells which co-express CB1 and D2, there are not sufficient Gαi proteins to allow both receptors to couple to their favoured signalling pathways. This enables more CB1 receptors to couple to the less-favoured Gαs pathway. The findings described in Chapter 7 appear to support this hypothesis, demonstrating a strong correlation between expression levels and signalling. Certainly, CB1 is well known for its ability to recruit Gαs proteins under circumstances where Gαi is scarce, as has been shown by removing Gαi by pertussis toxin (Bonhaus *et al.*, 1998; Calandra *et al.*, 1999; Felder *et al.*, 1998; Glass *et al.*, 1997; Gonzalez *et al.*, 2009). In terms of CB1-D2 co-expression, cAMP accumulation has been shown to be reverted back to inhibition when excess Gαi is added by transfection (Jarrahian *et al.*, 2004) providing further support for this hypothesis.

Apart from CB1, there are other GPCRs which are known to couple simultaneously to multiple G protein subtypes, including the muscarinic M2 (Michal *et al.*, 2001) and M4 receptors (Dittman *et al.*, 1994), serotonin 5-HT4b receptor (Pindon *et al.*, 2002) and the luteinizing hormone receptor (Herrlich *et al.*, 1996). Remarkably similar findings to CB1 have been found with both the muscarinic M2 and M4 receptors, which both show a receptor expression-dependent change from inhibitory action on adenylate cyclases at low receptor expression levels, to stimulatory action (Dittman *et al.*, 1994; Michal *et al.*, 2001). This was reasoned to be due to co-activation of Gαi and Gαs; in the case of the M4 receptor, Gαi activation was found to be approximately 100-fold more efficient than Gαs activation (Dittman *et al.*, 1994; Michal *et al.*, 2001; Okamoto *et al.*, 1992; Tucek *et al.*, 2001). For the M2 receptor, G protein restriction has been hypothesised to be the mechanism for this (Michal *et al.*, 2001).

Furthermore, G protein restriction has been suggested to control the cell-type specific G protein coupling reported for the adenosine A2A receptors. Typically, this receptor couples to Gαs (Olah, 1997; Wu *et al.*, 2013), but has been reported as signalling through $G\alpha_{olf}$ in the striatum, where Gαs is less abundant (Corvol *et al.*, 2001; Drinnan *et al.*, 1991; Herve *et al.*, 1993; Kull *et al.*, 2000; Zalduegui *et al.*, 2011). However, in this example, both of these G protein subtypes have similar effects on stimulating adenylate cyclase activity (Corvol *et al.*, 2001; Zalduegui *et al.*, 2011).

Interestingly, the G protein depletion theory was put forth with no evidence of a CB1-D2 heterodimeric interaction. Assuming the result in Chapter 7 hold for CB1-D2 co-expressing cells, this argues that heterodimerisation is not a requirement for a functional interaction between these receptors. Presumably, co-localisation maintained through heterodimer formation ensures these receptors compete most effectively for G proteins, however it may not be a requirement for the observed signalling interactions.

A key finding for the development of CB1 therapeutics is the description of the CB1 Gαi to Gαs signalling, through the hypothesised G protein competition mechanism. In pathologies where the G protein signalling phenotype is important, perhaps the most efficient therapeutic strategies will revolve around increasing or reducing the ability of CB1 to couple to specific G proteins. For example, CB1 Gαs signalling has been shown to be detrimental to cell health in a cell line model of Huntington's disease, while Gαi is neuroprotective (Scotter *et al.*, 2010). In this example, it would be therapeutically advantageous to increase the available Gαi proteins for CB1, or to develop a biased CB1 agonist which renders the activated receptor unable to couple to Gαs.

Conclusions and future directions

The results of these studies indicates that although CB1 and D2 seem to form a constitutive heterodimer, that this does not affect ligand-mediated receptor trafficking. CB1 expression does, however, change the synthesis and processing of the D2 receptor in a manner that has yet to be determined, even when D2 transcription is controlled by a constitutive promoter. As BRET requires transient overexpression of both receptors, which affects receptor trafficking and signalling, it would be advantageous to develop a method to investigate heterodimer regulation of endogenously-expressed receptors. Currently there is limited technical scope for this, although ligand-FRET, nanobody-FRET, and dimer-specific antibodies are possible approaches (Albizu *et al.*, 2010; Gomes *et al.*, 2014; Rothbauer *et al.*, 2006). While the BRET assay developed in this thesis was ultimately unable to detect ligand-mediated heterodimer regulation, a technique which is capable of detecting this would be useful for ligand screening for drugs capable of specifically targeting CB1-D2 heterodimer, similar to current approaches used for other GPCR dimers (Berque-Bestel *et al.*, 2008; Jörg *et al.*, 2014a; Le Naour *et al.*, 2013).

Although CB1 and D2 appear to be located in a formation consistent with heterodimerisation, evidence from our experiments with CB1 alone indicate that their primary signalling interaction may be due to Gαi competition, rather than an unambiguous dimer mediated "switch" in G protein coupling. If this is the case, then the CB1-D2 interaction may function simply to increase the local competition for G proteins, rather than an allosteric interaction between the receptors. Future studies would be needed to characterise the nature of the proposed G protein competition more thoroughly, for example by determining whether this occurs with other Gαi-linked receptors, and in which tissues is this physiologically relevant.

Appendix: Validation of the V8-CAMYEL biosensor

In order to perform the cAMP signalling assays on small cell populations, such as those used in Chapters 6 and 7, the 'cAMP sensor using YFP-Epac-Rluc' ("CAMYEL") biosensor (Jiang *et al.*, 2007) was modified to increase its bioluminescent output. The luciferase was changed to the luciferase mutant "Rluc8" (Loening *et al.*, 2006) and the fluorescent acceptor was changed to Venus (Nagai *et al.*, 2002), the pairing of which was predicted to increase the quantum yield of the biosensor. This modification was predicted to allow the measurement of biosensor activity from much smaller samples of cells in a conventional plate reader. The new biosensor was called "V8-CAMYEL".

In order to validate V8-CAMYEL, it was tested alongside the original CAMYEL biosensor. These assays were designed to verify that modifications to the bioluminescence resonance energy transfer (BRET) pair did not alter the responsiveness of the biosensor to changes in cytoplasmic cAMP in mammalian cells. Firstly, the biosensors were compared in their responsiveness to an adenylate cyclase agonist, which directly modifies the production of cAMP. Then the biosensors were assayed for responsiveness to Gαi-mediated and Gαs-mediated GPCR signalling. The experimental protocols and calculations are described in Chapter 2.

As predicted, V8-CAMYEL had much higher light emissions in both the 460/25nm and 535/25nm channels, on average a 2.5-fold increase when transiently transfected (Figure A.1(A, B), Table A.1). Concentration-response curves were generated for forskolin (FSK; direct activator of adenylate cyclase; Figure A.1(B)), CP55,940 (agonist at the Gαi-linked 3HA-hCB1 transgene; Figure A.1(C)), and pituitary adenylate cyclase-activating polypeptide (PACAP) (agonist at the endogenously-expressed, Gαs-linked PAC1 receptor; Figure A.1(D)). V8-CAMYEL showed equivalent sensitivity to these agonist-induced cAMP changes compared to the original CAMYEL biosensor. The overall range of inverse BRET ratios measured is reduced in V8-CAMYEL compared to the parental construct, as shown in Figure A.1(E, F). This indicates that, ratiometrically, Venus emissions in V8-CAMYEL are higher relative to luciferase than in the original construct, thus making the inverse BRET ratio lower. This is not entirely surprising, as the increased quantum yield of Rluc8 (Loening *et al.*, 2006) may increase the energy transfer to Venus. There is also likely to be a higher proportion of functional Venus fluorophore in V8-CAMYEL, as this acceptor protein matures faster than other YFP derivatives (Nagai *et al.*, 2002). However, when drug responses are normalised to an internal control (e.g. 5 μM FSK), V8-CAMYEL shows an improved signal-to-noise ratio, approximately 1.78±0.03-fold higher than the original CAMYEL biosensor across the dynamic range.

Overall, V8-CAMYEL was found to perform equivalently to the original CAMYEL biosensor, but with the considerable advantage of increased total luminescence. This was exploited in Chapters 6 and 7, where fewer cells per sample were required to obtain a useable signal in a standard luminescence plate reader.

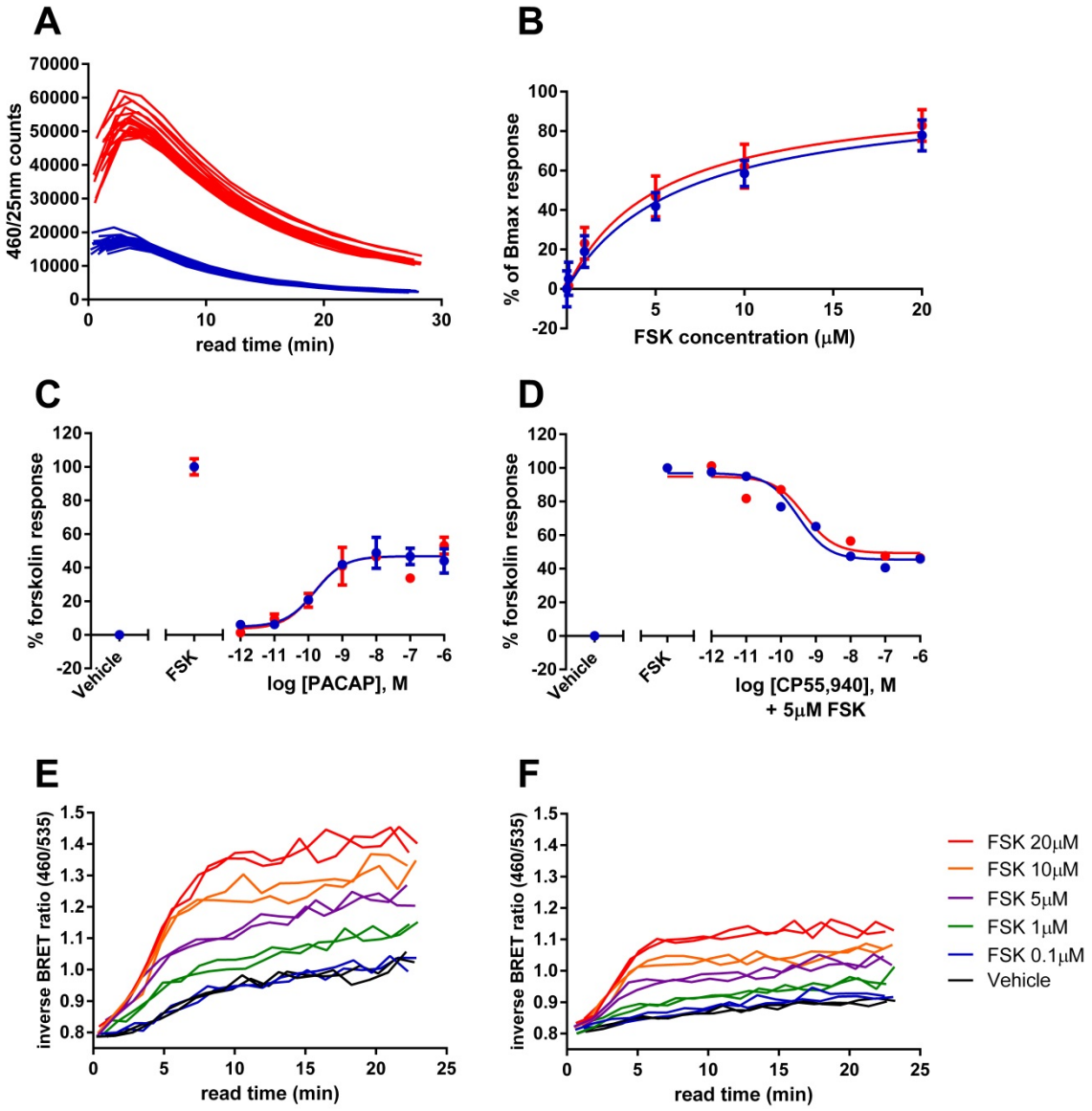

Figure A.1 Comparison of CAMYEL and V8-CAMYEL.

HEK 3HA-hCB1 cells were transiently transfected with either CAMYEL or V8-CAMYEL. (A) Raw luciferase measurements from CAMYEL (blue) and V8-CAMYEL (red). (B, C, D) 15-20 minute cumulative responses from HEK 3HA-hCB1 cells stimulated with FSK (B), PACAP (C) or CP55,940 plus FSK (5μM) (D), showing CAMYEL (blue) and V8-CAMYEL (red). (E) CAMYEL and (F) V8-CAMYEL responses to FSK, duplicate time-courses. All graphs show representative results from one of three experiments.

Table A.1 Summary data comparing CAMYEL and V8-CAMYEL.

Mean ± SEM of three independent experiments.

Parameter		**CAMYEL**	**V8-CAMYEL**	**Statistical significance**
Maximum luciferase counts (AU)		15001±3539	36894±5280	p=0.031
FSK (20 minute AUC, hyperbola)	Kd (μM)	7.802±1.056	7.899±1.751	ns
CP55,940 (0-20 minute AUC)	pEC50	9.43±0.23	9.13±0.10	ns
	Bottom of curve (% forskolin response)	46.50±1.74	50.90±0.82	ns
PACAP (5-20 minute AUC)	pEC50	10.07±0.14	9.884±0.04	ns
	Top of curve (% forskolin response)	38.57±4.12	55.67±5.44	ns

References

Abel A, Wittau N, Wieland T, Schultz G, Kalkbrenner F (2000). Cell Cycle-dependent Coupling of the Vasopressin V1a Receptor to Different G Proteins. *Journal of Biological Chemistry* **275**(42)**:** 32543-32551.

Achour L, Scott MGH, Shirvani H, Thuret A, Bismuth G, Labbé-Jullié C*, et al.* (2009). *CD4-CCR5 interaction in intracellular compartments contributes to receptor expression at the cell surface*. edn, vol. 113.

Adie EJ, Milligan G (1994). Agonist regulation of cellular Gs alpha-subunit levels in neuroblastoma x glioma hybrid NG108-15 cells transfected to express different levels of the human beta 2 adrenoceptor. *Biochem. J* **300:** 709-715.

Agnati LF, Ferre S, Genedani S, Giuseppina L, Guidolin D, Filaferro M*, et al.* (2006). Allosteric modulation of dopamine D2 receptors by homocysteine. *Journal of Proteome Research* **5**(3077-3083).

Agnati LF, Guidolin D, Albertin G, Trivello E, Ciruela F, Genedani S*, et al.* (2010a). An integrated view on the role of receptor mosaics at perisynaptic level: focus on adenosine A2A, dopamine D2, cannabinoid CB1, and metabotropic glutamate mGlu5 receptors. *Journal of Receptors and Signal Transduction* **30**(5)**:** 355-369.

Agnati LF, Guidolin D, Vilardaga JP, Ciruela F, Fuxe K (2010b). On the expanding terminology in the GPCR field: The meaning of receptor mosaics and receptor heteromers. *Journal of Receptors and Signal Transduction* **30**(5)**:** 287-303.

Ahn KH, Mahmoud MM, Shim J-Y, Kendall DA (2013). Distinct Roles of β-Arrestin 1 and β-Arrestin 2 in ORG27569-induced Biased Signaling and Internalization of the Cannabinoid Receptor 1 (CB1). *Journal of Biological Chemistry* **288**(14)**:** 9790-9800.

Albert PR, Neve KA, Bunzow JR, Civelli O (1990). Coupling of a cloned rat dopamine-D2 receptor to inhibition of adenylyl cyclase and prolactin secretion. *Journal of Biological Chemistry* **265**(4)**:** 2098-2104.

Alberts GL, Pregenzer JF, Im WB (2000). Advantages of heterologous expression of human D2long dopamine receptors in human neuroblastoma SH-SY5Y over human embryonic kidney 293 cells. *British Journal of Pharmacology* **131**(3)**:** 514-520.

Albizu L, Cottet M, Kralikova M, Stoev S, Seyer R, Brabet I*, et al.* (2010). Time-resolved FRET between GPCR ligands reveals oligomers in native tissues. *Nat Chem Biol* **6**(8)**:** 587-594.

Alen F, Moreno-Sanz G, Isabel de Tena A, Brooks RD, López-Jimenez A, Navarro M*, et al.* (2008). Pharmacological activation of CB1 and D2 receptors in rats: predominant role of CB1 in the increase of alcohol relapse. *European Journal of Neuroscience* **27**(12)**:** 3292-3298.

Altier C (2012). GPCR and Voltage-Gated Calcium Channels (VGCC) Signaling Complexes. In: Dupré DJ, Hébert TE, Jockers R (ed)^(eds). *GPCR Signalling Complexes – Synthesis, Assembly, Trafficking and Specificity*, edn, Vol. 63: Springer Netherlands. p^pp 241-262.

Antoni FA (2012). New paradigms in cAMP signalling. *Molecular and Cellular Endocrinology* **353**(1–2)**:** 3-9.

Arai R, Nakagawa H, Tsumoto K, Mahoney W, Kumagai I, Ueda H*, et al.* (2001). Demonstration of a Homogeneous Noncompetitive Immunoassay Based on Bioluminescence Resonance Energy Transfer. *Analytical Biochemistry* **289**(1)**:** 77-81.

Arcemisbéhère L, Sen T, Boudier L, Balestre M-N, Gaibelet G, Detouillon E*, et al.* (2010). Leukotriene BLT2 Receptor Monomers Activate the Gi2 GTP-binding Protein More Efficiently than Dimers. *Journal of Biological Chemistry* **285**(9)**:** 6337-6347.

Asimaki O, Mangoura D (2011). Cannabinoid receptor 1 induces a biphasic ERK activation via multiprotein signaling complex formation of proximal kinases PKCε, Src, and Fyn in primary neurons. *Neurochemistry International* **58**(2)**:** 135-144.

Atwood BK, Lopez J, Wager-Miller J, Mackie K, Straiker A (2011). Expression of G protein-coupled receptors and related proteins in HEK293, AtT20, BV2, and N18 cell lines as revealed by microarray analysis. *BMC genomics* **12**(1)**:** 14.

Audet M, Bouvier M (2012). Restructuring G-Protein- Coupled Receptor Activation. *Cell* **151**(1)**:** 14-23.

Ayoub MA, Couturier C, Lucas-Meunier E, Angers S, Fossier P, Bouvier M*, et al.* (2002). Monitoring of Ligand-independent Dimerization and Ligand-induced Conformational Changes of Melatonin Receptors in Living Cells by Bioluminescence Resonance Energy Transfer. *Journal of Biological Chemistry* **277**(24)**:** 21522-21528.

Ayoub MA, Pfleger KDG (2010). Recent advances in bioluminescence resonance energy transfer technologies to study GPCR heteromerization. *Current Opinion in Pharmacology* **10**(1)**:** 44-52.

Azdad K, Gall D, Woods AS, Ledent C, Ferre S, Schiffmann SN (2008). Dopamine D2 and Adenosine A2A Receptors Regulate NMDA-Mediated Excitation in Accumbens Neurons Through A2A-D2 Receptor Heteromerization. *Neuropsychopharmacology* **34**(4)**:** 972-986.

Bagher AM, Laprairie RB, Kelly MEM, Denovan-Wright EM (2013). Co-expression of the human cannabinoid receptor coding region splice variants (hCB1) affects the function of hCB1 receptor complexes. *European Journal of Pharmacology* **721**(1–3)**:** 341-354.

Baker D, Pryce G, Croxford JL, Brown P, Pertwee RG, Huffman JW*, et al.* (2000). Cannabinoids control spasticity and tremor in a multiple sclerosis model. *Nature* **404**(6773)**:** 84-87.

Banères J-L, Parello J (2003). Structure-based Analysis of GPCR Function: Evidence for a Novel Pentameric Assembly between the Dimeric Leukotriene B4 Receptor BLT1 and the G-protein. *Journal of Molecular Biology* **329**(4)**:** 815-829.

Barnes MP (2006). Sativex®: clinical efficacy and tolerability in the treatment of symptoms of multiple sclerosis and neuropathic pain. *Expert Opinion on Pharmacotherapy* **7**(5)**:** 607-615.

Barnett-Norris J, Hurst DP, Buehner K, Ballesteros JA, Guarnieri F, Reggio PH (2002). Agonist alkyl tail interaction with cannabinoid CB1 receptor V6. 43/I6. 46 groove induces a helix 6 active conformation. *International journal of quantum chemistry* **88**(1)**:** 76-86.

Bartlett SE, Enquist J, Hopf FW, Lee JH, Gladher F, Kharazia V*, et al.* (2005). Dopamine responsiveness is regulated by targeted sorting of D2 receptors. *Proceedings of the National Academy of Sciences of the United States of America* **102**(32)**:** 11521-11526.

Bash R, Rubovitch V, Gafni M, Sarne Y (2003). The stimulatory effect of cannabinoids on calcium uptake is mediated by Gs GTP-binding proteins and cAMP formation. *Neuro-Signals* **12**(1)**:** 39-44.

Beaulieu J-M, Gainetdinov RR (2011). The Physiology, Signaling, and Pharmacology of Dopamine Receptors. *Pharmacological Reviews* **63**(1)**:** 182-217.

Beggiato S, Antonelli T, C. Tomasini M, C. Borelli A, F. Agnati L, Tanganelli S*, et al.* (2014). Adenosine A2A-D2 Receptor-Receptor Interactions in Putative Heteromers in the Regulation of the Striato-Pallidal GABA Pathway: Possible Relevance for Parkinson's Disease and its Treatment. *Current Protein and Peptide Science* **15**(7)**:** 673-680.

Belin D, Bost S, Vassalli JD, Strub K (1996). A two-step recognition of signal sequences determines the translocation efficiency of proteins. *The EMBO Journal* **15**(3)**:** 468-478.

Beltramo M, de Fonseca FRg, Navarro M, Calignano A, Gorriti MA, Grammatikopoulos G*, et al.* (2000). Reversal of Dopamine D2 Receptor Responses by an Anandamide Transport Inhibitor. *The Journal of Neuroscience* **20**(9)**:** 3401-3407.

Bensaid M, Gary-Bobo M, Esclangon A, Maffrand JP, Le Fur G, Oury-Donat F*, et al.* (2003). The Cannabinoid CB1 Receptor Antagonist SR141716 Increases Acrp30 mRNA Expression in Adipose Tissue of Obese fa/fa Rats and in Cultured Adipocyte Cells. *Molecular Pharmacology* **63**(4)**:** 908-914.

Berque-Bestel I, Lezoualc'h F, Jockers R (2008). Bivalent ligands as specific pharmacological tools for G protein-coupled receptor dimers. *Curr Drug Discov Technol* **5:** 312-318.

Bhushan RG, Sharma SK, Xie Z, Daniels DJ, Portoghese PS (2004). A bivalent ligand (KDN-21) reveals spinal d and k opioid receptors are organised as heterodimers that give rise to d1 and k2 phenotypes: selective targeting of d-k heterodimers. *J Med Chem* **47**(12)**:** 2969-2972.

Björklund E, Forsgren S, Alfredson H, Fowler CJ (2011). Increased expression of cannabinoid CB1 receptors in Achilles tendinosis. *PLoS ONE* **6**(9).

Blair RE, Deshpande LS, Sombati S, Elphick MR, Martin BR, DeLorenzo RJ (2009). Prolonged exposure to WIN55,212-2 causes downregulation of the CB1 receptor and the development of tolerance to its anticonvulsant effects in the hippocampal neuronal culture model of acquired epilepsy. *Neuropharmacology* **57**(3)**:** 208-218.

Blake DR, Robson P, Ho M, Jubb RW, McCabe CS (2006). Preliminary assessment of the efficacy, tolerability and safety of a cannabis-based medicine (Sativex) in the treatment of pain caused by rheumatoid arthritis. *Rheumatology* **45**(1)**:** 50-52.

Blume LC, Bass CE, Childers SR, Dalton GD, Roberts DCS, Richardson JM*, et al.* (2013). Striatal CB1 and D2 receptors regulate expression of each other, CRIP1A and delta opioid systems. *Journal of Neurochemistry* **124**(6)**:** 808-820.

Bonhaus DW, Chang LK, Kwan J, Martin GR (1998). Dual Activation and Inhibition of Adenylyl Cyclase by Cannabinoid Receptor Agonists: Evidence for Agonist-Specific Trafficking of Intracellular Responses. *Journal of Pharmacology and Experimental Therapeutics* **287**(3)**:** 884-888.

Borroto-Escuela DO, García-Negredo G, Garriga P, Fuxe K, Ciruela F (2010a). The M5 muscarinic acetylcholine receptor third intracellular loop regulates receptor function and oligomerization. *Biochimica et Biophysica Acta (BBA) - Molecular Cell Research* **1803**(7)**:** 813-825.

Borroto-Escuela DO, Marcellino D, Narvaez M, Flajolet M, Heintz N, Agnati L*, et al.* (2010b). A serine point mutation in the adenosine A2AR C-terminal tail reduces receptor heteromerization and allosteric modulation of the dopamine D2R. *Biochemical and Biophysical Research Communications* **394**(1)**:** 222-227.

Bossong MS, van-Berckel BNM, Boellaard R, Zuurman L, Schuit RC, Windhorst AD*, et al.* (2009). Δ9-tetrahydrocannabinol Induces dopamine release in the human striatum. *Neuropsychopharmacol* **34:** 759-766.

Bouaboula M, Perrachon S, Milligan L, Canat X, Rinaldi-Carmona M, Portier M*, et al.* (1997). A selective inverse agonist for central cannabinoid receptor inhibits mitogen-activated protein kinase activation stimulated by insulin or insulin-like growth factor 1. Evidence for a new model of receptor/ligand interactions. *J Biol Chem* **272**(35)**:** 22330-22339.

Bouaboula M, Poinot-Chazel C, Bourrie B, Canat X, Calandra B, Rinaldi-Carmona M*, et al.* (1995). Activation of mitogen-activated protein kinases by stimulation of the central cannabinoid receptor CB1. *The Biochemical journal* **312 (Pt 2):** 637-641.

Bouaboula M, Poinot-Chazel C, Marchand J, Canat X, Bourrié B, Rinaldi-Carmona M*, et al.* (1996). Signaling Pathway Associated with Stimulation of CB2 Peripheral Cannabinoid Receptor. *European Journal of Biochemistry* **237**(3)**:** 704-711.

Boute N, Jockers R, Issad T (2002). The use of resonance energy transfer in high-throughput screening: BRET versus FRET. *Trends in pharmacological sciences* **23**(8)**:** 351-354.

Bradbury A, Plückthun A (2015). Reproducibility: Standardize antibodies used in research. *Nature News* **518**(7537)**:** 27.

Brandt DR, Ross EM (1985). GTPase activity of the stimulatory GTP-binding regulatory protein of adenylate cyclase, Gs. Accumulation and turnover of enzyme-nucleotide intermediates. *J Biol Chem* **260**(1)**:** 266-272.

Breivogel CS, Lambert JM, Gerfin S, Huffman JW, Razdan RK (2008). Sensitivity to delta9-tetrahydrocannabinol is selectively enhanced in beta-arrestin2 -/- mice. *Behav Pharmacol* **19**(4)**:** 298-307.

Bulenger S, Marullo S, Bouvier M (2005). Emerging role of homo- and heterodimerization in G-protein-coupled receptor biosynthesis and maturation. *Trends in Pharmacological Sciences* **26**(3)**:** 131-137.

Cahill K, Ussher MH (2012). Can cannabinoid type 1 receptor antagonists help smokers to quit, and could they also reduce the amount of weight gained during the quitting process?

Calandra B, Portier M, Kernéis A, Delpech M, Carillon C, Le Fur G*, et al.* (1999). Dual intracellular signaling pathways mediated by the human cannabinoid CB1 receptor. *European Journal of Pharmacology* **374**(3)**:** 445-455.

Campbell FA, Tramèr MR, Carroll D, Reynolds DJM, Moore RA, McQuay HJ (2001). *Are cannabinoids an effective and safe treatment option in the management of pain? A qualitative systematic review*. edn, vol. 323.

Carriba P, Navarro G, Ciruela F, Ferré S, Casadó V, Agnati L*, et al.* (2008). Detection of heteromerization of more than two proteins by sequential BRET-FRET. *Nature Methods* **5:** 727-733.

Carriba P, Ortiz O, Patkar K, Justinova Z, Stroik J, Themann A*, et al.* (2007). Striatal Adenosine A2A and Cannabinoid CB1 Receptors Form Functional Heteromeric Complexes that Mediate the Motor Effects of Cannabinoids. *Neuropsychopharmacology* **32**(11)**:** 2249-2259.

Carroll CB, Bain PG, Teare L, Liu X, Joint C, Wroath C*, et al.* (2004). Cannabis for dyskinesia in Parkinson disease: a randomized double-blind crossover study. *Neurology* **63**(7)**:** 1245-1250.

Carroll CB, Zeissler ML, Hanemann CO, Zajicek JP (2012). Δ9-tetrahydrocannabinol (Δ9-THC) exerts a direct neuroprotective effect in a human cell culture model of Parkinson's disease. *Neuropathology and Applied Neurobiology* **38**(6)**:** 535-547.

Caspari D (1999). Cannabis and schizophrenia: results of a follow-up study. *European archives of psychiatry and clinical neuroscience* **249**(1)**:** 45-49.

Castillo PE, Younts TJ, Chavez AE, Hashimotodani Y (2012). Endocannabinoid signaling and synaptic function. *Neuron* **76**(1)**:** 70-81.

Castro SW, Strange PG (1993). Differences in the Ligand Binding Properties of the Short and Long Versions of the D2 Dopamine Receptor. *Journal of Neurochemistry* **60**(1)**:** 372-375.

Cawston EE, Redmond WJ, Breen CM, Grimsey NL, Connor M, Glass M (2013). Real-time characterization of cannabinoid receptor 1 (CB1) allosteric modulators reveals novel mechanism of action. *British Journal of Pharmacology* **170**(4)**:** 893-907.

Ceccarini J, De Hert M, Van Winkel R, Peuskens J, Bormans G, Kranaster L*, et al.* (2013). Increased ventral striatal CB1 receptor binding is related to negative symptoms in drug-free patients with schizophrenia. *NeuroImage* **79**(0)**:** 304-312.

Celver J, Sharma M, Kovoor A (2010). RGS9-2 mediates specific inhibition of agonist-induced internalization of D2-dopamine receptors. *Journal of Neurochemistry* **114**(3)**:** 739-749.

Chagas MHN, Zuardi AW, Tumas V, Pena-Pereira MA, Sobreira ET, Bergamaschi MM*, et al.* (2014). Effects of cannabidiol in the treatment of patients with Parkinson's disease: An exploratory double-blind trial. *Journal of Psychopharmacology* **28**(11)**:** 1088-1098.

Chakrabarti S, Liu N-J, Gintzler AR (2010). Formation of μ-/κ-opioid receptor heterodimer is sex-dependent and mediates female-specific opioid analgesia. *Proceedings of the National Academy of Sciences* **107**(46)**:** 20115-20119.

Chandrasekera PC, Wan TC, Gizewski ET, Auchampach JA, Lasley RD (2013). Adenosine A1 receptors heterodimerize with β1- and β2-adrenergic receptors creating novel receptor complexes with altered G protein coupling and signaling. *Cellular signalling* **25**(4)**:** 736-742.

Chang L, Karin M (2001). Mammalian MAP kinase signalling cascades. *Nature* **410**(6824)**:** 37-40.

Chavkin C, Schattauer S, Levin J (2014). Arrestin-Mediated Activation of p38 MAPK: Molecular Mechanisms and Behavioral Consequences. In: Gurevich VV (ed)^(eds). *Arrestins - Pharmacology and Therapeutic Potential*, edn, Vol. 219: Springer Berlin Heidelberg. p^pp 281-292.

Chemin J, Monteil A, Perez-Reyes E, Nargeot J, Lory P (2001). Direct inhibition of T-type calcium channels by the endogenous cannabinoid anandamide. *EMBO J* **20**(24)**:** 7033-7040.

Cheng Z-J, Miller LJ (2001). Agonist-dependent Dissociation of Oligomeric Complexes of G Protein-coupled Cholecystokinin Receptors Demonstrated in Living Cells Using Bioluminescence Resonance Energy Transfer. *Journal of Biological Chemistry* **276**(51)**:** 48040-48047.

Chien EY, Liu W, Zhao Q, Katritch V, Han GW, Hanson MA*, et al.* (2010). Structure of the human dopamine D3 receptor in complex with a D2/D3 selective antagonist. *Science* **330**(6007)**:** 1091-1095.

Chiodi V, Uchigashima M, Beggiato S, Ferrante A, Armida M, Martire A*, et al.* (2012). Unbalance of CB1 receptors expressed in GABAergic and glutamatergic neurons in a transgenic mouse model of Huntington's disease. *Neurobiology of disease* **45**(3)**:** 983-991.

Chiu CQ, Puente N, Grandes P, Castillo PE (2010). Dopaminergic Modulation of Endocannabinoid-Mediated Plasticity at GABAergic Synapses in the Prefrontal Cortex. *The Journal of Neuroscience* **30**(21)**:** 7236-7248.

Choe H, Farzan M (2009). Chapter 7 Tyrosine Sulfation of HIV-1 Coreceptors and Other Chemokine Receptors. In: Tracy MH, Damon JH (ed)^(eds). *Methods in Enzymology*, edn, Vol. Volume 461: Academic Press. p^pp 147-170.

Christensen R, Kristensen PK, Bartels EM, Bliddal H, Astrup A (2007). Efficacy and safety of the weight-loss drug rimonabant: a meta-analysis of randomised trials. *Lancet* **370**(9600)**:** 1706-1713.

Chung SC, Hammarsten P, Josefsson A, Stattin P, Granfors T, Egevad L*, et al.* (2009). A high cannabinoid CB1 receptor immunoreactivity is associated with disease severity and outcome in prostate cancer. *European Journal of Cancer* **45**(1)**:** 174-182.

Cipriano M, Häggström J, Hammarsten P, Fowler CJ (2013). Association between Cannabinoid CB1 Receptor Expression and Akt Signalling in Prostate Cancer. *PLoS ONE* **8**(6).

Ciruela F, Burgueño J, Casadó V, Canals M, Marcellino D, Goldberg SR*, et al.* (2004). Combining Mass Spectrometry and Pull-Down Techniques for the Study of Receptor Heteromerization. Direct Epitope−Epitope Electrostatic Interactions between Adenosine A2A and Dopamine D2 Receptors. *Analytical Chemistry* **76**(18)**:** 5354-5363.

Ciruela F, Casadó V, Rodrigues RJ, Luján R, Burgueño J, Canals M*, et al.* (2006). Presynaptic Control of Striatal Glutamatergic Neurotransmission by Adenosine A1–A2A Receptor Heteromers. *The Journal of Neuroscience* **26**(7)**:** 2080-2087.

Clifford DB (1983). Tetrahydrocannabinol for tremor in multiple sclerosis. *Annals of Neurology* **13**(6)**:** 669-671.

Collin C, Ehler E, Waberzinek G, Alsindi Z, Davies P, Powell K*, et al.* (2010). A double-blind, randomized, placebo-controlled, parallel-group study of Sativex, in subjects with symptoms of spasticity due to multiple sclerosis. *Neurological research* **32**(5)**:** 451-459.

Consroe P, Laguna J, Allender J, Snider S, Stern L, Sandyk R*, et al.* (1991). Controlled clinical trial of cannabidiol in Huntington's disease. *Pharmacology, biochemistry, and behavior* **40**(3)**:** 701-708.

Corvol JC, Studler JM, Schonn JS, Girault JA, Hervé D (2001). Gαolf is necessary for coupling D1 and A2a receptors to adenylyl cyclase in the striatum. *Journal of Neurochemistry* **76**(5)**:** 1585-1588.

Coulon V, Audet M, Homburger V, Bockaert J, Fagni L, Bouvier M*, et al.* (2008). Subcellular Imaging of Dynamic Protein Interactions by Bioluminescence Resonance Energy Transfer. *Biophysical Journal* **94**(3)**:** 1001-1009.

Coutts AA, Anavi-Goffer S, Ross RA, MacEwan DJ, Mackie K, Pertwee RG*, et al.* (2001). Agonist-Induced Internalization and Trafficking of Cannabinoid CB1 Receptors in Hippocampal Neurons. *The Journal of Neuroscience* **21**(7)**:** 2425-2433.

Croci T, Manara L, Aureggi G, Guagnini F, Rinaldi-Carmona M, Maffrand JP*, et al.* (1998). In vitro functional evidence of neuronal cannabinoid CB1 receptors in human ileum. *Br J Pharmacol* **125**(7)**:** 1393-1395.

Cudaback E, Marrs W, Moeller T, Stella N (2010). The expression level of CB1 and CB2 receptors determines their efficacy at inducing apoptosis in astrocytomas. *PLoS One* **5**(1)**:** e8702.

Currie KP (2010). G protein modulation of CaV2 voltage-gated calcium channels. *Channels* **4**(6)**:** 497-509.

Curtis A, Mitchell I, Patel S, Ives N, Rickards H (2009). A pilot study using nabilone for symptomatic treatment in Huntington's disease. *Movement Disorders* **24**(15)**:** 2254-2259.

Daaka Y, Luttrell LM, Lefkowitz RJ (1997). Switching of the coupling of the [beta]2-adrenergic receptor to different G proteins by protein kinase A. *Nature* **390**(6655)**:** 88-91.

Daigle TL, Kwok ML, Mackie K (2008). Regulation of CB1 cannabinoid receptor internalization by a promiscuous phosphorylation-dependent mechanism. *Journal of Neurochemistry* **106**(1)**:** 70-82.

Damian M, Marie J, Leyris J-P, Fehrentz J-A, Verdié P, Martinez J*, et al.* (2012). High Constitutive Activity Is an Intrinsic Feature of Ghrelin Receptor Protein: A study with a functional monomeric GHS-R1a receptor reconsituted in lipid discs. *Journal of Biological Chemistry* **287**(6)**:** 3630-3641.

Daniel H, Rancillac A, Crepel F (2004). Mechanisms underlying cannabinoid inhibition of presynaptic Ca2+ influx at parallel fibre synapses of the rat cerebellum. *J Physiol* **557**(Pt 1)**:** 159-174.

de Jong APH, Verhage M (2009). Presynaptic signal transduction pathways that modulate synaptic transmission. *Current Opinion in Neurobiology* **19**(3)**:** 245-253.

de Lago E, Fernandez-Ruiz J, Ortega-Gutierrez S, Cabranes A, Pryce G, Baker D*, et al.* (2006). UCM707, an inhibitor of the anandamide uptake, behaves as a symptom control agent in models of Huntington's disease and multiple sclerosis, but fails to delay/arrest the progression of different motor-related disorders. *European neuropsychopharmacology : the journal of the European College of Neuropsychopharmacology* **16**(1)**:** 7-18.

De Mei C, Ramos M, Iitaka C, Borrelli E (2009). Getting specialized: presynaptic and postsynaptic dopamine D2 receptors. *Current Opinion in Pharmacology* **9**(1)**:** 53-58.

de Vries M, van Rijckevorsel DCM, Wilder-Smith OHG, van Goor H (2014). Dronabinol and chronic pain: importance of mechanistic considerations. *Expert Opinion on Pharmacotherapy* **15**(11)**:** 1525-1534.

Dean B, Sundram S, Bradbury R, Scarr E, Copolov D (2001). Studies on [3H]CP-55940 binding in the human central nervous system: regional specific changes in density of cannabinoid-1 receptors associated with schizophrenia and cannabis use. *Neuroscience* **103**(1)**:** 9-15.

Demidov VV, Dokholyan NV, Witte-Hoffmann C, Chalasani P, Yiu H-W, Ding F*, et al.* (2006). Fast complementation of split fluorescent protein triggered by DNA hybridization. *Proceedings of the National Academy of Sciences of the United States of America* **103**(7)**:** 2052-2056.

Derkinderen P, Valjent E, Toutant M, Corvol JC, Enslen H, Ledent C*, et al.* (2003). Regulation of extracellular signal-regulated kinase by cannabinoids in hippocampus. *J Neurosci* **23**(6)**:** 2371-2382.

Di Marzo V, Hill MP, Bisogno T, Crossman AR, Brotchie JM (2000). Enhanced levels of endogenous cannabinoids in the globus pallidus are associated with a reduction in movement in an animal model of Parkinson's disease. *FASEB journal : official publication of the Federation of American Societies for Experimental Biology* **14**(10)**:** 1432-1438.

Diana MA, Levenes C, Mackie K, Marty A (2002). Short-term retrograde inhibition of GABAergic synaptic currents in rat Purkinje cells is mediated by endogenous cannabinoids. *J Neurosci* **22**(1)**:** 200-208.

Díaz-Asensio C, Setién R, Echevarría E, Casis L, Casis E, Garrido A*, et al.* (2008). Type 1 Diabetes Alters Brain Cannabinoid Receptor Expression and Phosphorylation Status in Rats. *Horm Metab Res* **40**(07)**:** 454-458.

Dittman AH, Weber JP, Hinds TR, Choi EJ, Migeon JC, Nathanson NM*, et al.* (1994). A novel mechanism for coupling of m4 muscarinic acetylcholine receptors to calmodulin-sensitive adenylyl cyclases: crossover from G protein-coupled inhibition to stimulation. *Biochemistry* **33**(4)**:** 943-951.

Dolado I, Nebreda A (2008). Regulation of Tumorigenesis by p38α MAP Kinase. In: Posas F, Nebreda A (ed)^(eds). *Stress-Activated Protein Kinases*, edn, Vol. 20: Springer Berlin Heidelberg. p^pp 99-128.

Doupnik CA (2008). GPCR-Kir Channel Signaling Complexes: Defining Rules of Engagement. *Journal of Receptors and Signal Transduction* **28**(1-2)**:** 83-91.

Dowie MJ, Howard ML, Nicholson LF, Faull RL, Hannan AJ, Glass M (2010). Behavioural and molecular consequences of chronic cannabinoid treatment in Huntington's disease transgenic mice. *Neuroscience* **170**(1)**:** 324-336.

Dragavon J, Sinow C, Holland AD, Rekiki A, Theodorou I, Samson C*, et al.* (2014). A Step Beyond BRET: Fluorescence by Unbound Excitation from Luminescence (FUEL). *Journal of Visualized Experiments : JoVE*(87)**:** 51549.

Drinnan SL, Hope BT, Snutch TP, Vincent SR (1991). G(olf) in the basal ganglia. *Molecular and cellular neurosciences* **2**(1)**:** 66-70.

Dupré DJ, Robitaille M, Rebois RV, Hébert TE (2009). The role of Gβγ subunits in the organization, assembly, and function of GPCR signaling complexes. *Annu Rev Pharmacol Toxicol* **49:** 31-56.

Duthey B, Caudron S, Perroy J, Bettler B, Fagni L, Pin J-P*, et al.* (2002). A Single Subunit (GB2) Is Required for G-protein Activation by the Heterodimeric GABAB Receptor. *Journal of Biological Chemistry* **277**(5)**:** 3236-3241.

Dziedzicka-Wasylewska M, Faron-Górecka A, Andrecka J, Polit A, Kuśmider M, Wasylewski Z (2006). Fluorescence studies reveal heterodimerization of dopamine D1 and D2 receptors in the plasma membrane. *Biochemistry* **45**(29)**:** 8751-8759.

Eilam D, Golani I, Szechtman H (1989a). D2-agonist quinpirole induces perseveration of routes and hyperactivity but no perseveration of movements. *Brain research* **490**(2)**:** 255-267.

Eilam D, Szechtman H (1989b). Biphasic effect of D-2 agonist quinpirole on locomotion and movements. *European Journal of Pharmacology* **161**(2–3)**:** 151-157.

Ellis J, Pediani JD, Canals M, Milasta S, Milligan G (2006). Orexin-1 receptor-cannabinoid CB1 receptor heterodimerization results in both ligand-dependent and -independent coordinated alterations of receptor localization and function. *J Biol Chem* **281**(50)**:** 38812-38824.

Emrich HM, Leweke FM, Schneider U (1997). Towards a cannabinoid hypothesis of schizophrenia: cognitive impairments due to dysregulation of the endogenous cannabinoid system. *Pharmacology, biochemistry, and behavior* **56**(4)**:** 803-807.

Endoh T (2006). Pharmacological characterization of inhibitory effects of postsynaptic opioid and cannabinoid receptors on calcium currents in neonatal rat nucleus tractus solitarius. *Br J Pharmacol* **147**(4)**:** 391-401.

Faure M, Voyno-Yasenetskaya TA, Bourne HR (1994). cAMP and beta gamma subunits of heterotrimeric G proteins stimulate the mitogen-activated protein kinase pathway in COS-7 cells. *Journal of Biological Chemistry* **269**(11)**:** 7851-7854.

Felce JH, Davis SJ (2012). Unraveling Receptor Stoichiometry Using Bret. *Frontiers in Endocrinology* **3:** 86.

Felce James H, Knox Rachel G, Davis Simon J (2014). Type-3 BRET, an Improved Competition-Based Bioluminescence Resonance Energy Transfer Assay. *Biophysical Journal* **106**(12)**:** L41-L43.

Felder CC, Joyce KE, Briley EM, Glass M, Mackie KP, Fahey KJ*, et al.* (1998). LY320135, a novel cannabinoid CB1 receptor antagonist, unmasks coupling of the CB1 receptor to stimulation of cAMP accumulation. *J Pharmacol Exp Ther* **284**(1)**:** 291-297.

Felder CC, Joyce KE, Briley EM, Mansouri J, Mackie K, Blond O*, et al.* (1995). Comparison of the pharmacology and signal transduction of the human cannabinoid CB1 and CB2 receptors. *Molecular Pharmacology* **48**(3)**:** 443-450.

Ferré S, Casadó V, Devi LA, Filizola M, Jockers R, Lohse MJ*, et al.* (2014). G Protein–Coupled Receptor Oligomerization Revisited: Functional and Pharmacological Perspectives. *Pharmacological Reviews* **66**(2)**:** 413-434.

Ferre S, Goldberg SR, Lluis C, Franco R (2009). Looking for the role of cannabinoid receptor heteromers in striatal function. *Neuropharmacol* **56**(1)**:** 226-234.

Fieger CB, Huang M-C, Van Brocklyn JR, Goetzl EJ (2005). Type 1 sphingosine 1-phosphate G protein-coupled receptor signaling of lymphocyte functions requires sulfation of its extracellular amino-terminal tyrosines. *The FASEB journal : official publication of the Federation of American Societies for Experimental Biology* **19**(13)**:** 1926-1928.

Filipek S, Krzysko KA, Fotiadis D, Liang Y, Saperstein DA, Engel A*, et al.* (2004). A concept for G protein activation by G protein-coupled receptor dimers: the transducin/rhodopsin interface. *Photochemical & Photobiological Sciences* **3**(6)**:** 628-638.

Fisyunov A, Tsintsadze V, Min R, Burnashev N, Lozovaya N (2006). Cannabinoids modulate the P-type high-voltage-activated calcium currents in purkinje neurons. *Journal of neurophysiology* **96**(3)**:** 1267-1277.

Fitzgerald ML, Mackie K, Pickel VM (2013). The impact of adolescent social isolation on dopamine D2 and cannabinoid CB1 receptors in the adult rat prefrontal cortex. *Neuroscience* **235**(0)**:** 40-50.

Fox P, Bain PG, Glickman S, Carroll C, Zajicek J (2004). The effect of cannabis on tremor in patients with multiple sclerosis. *Neurology* **62**(7)**:** 1105-1109.

Fox SH, Kellett M, Moore AP, Crossman AR, Brotchie JM (2002). Randomised, double-blind, placebo-controlled trial to assess the potential of cannabinoid receptor stimulation in the treatment of dystonia. *Movement Disorders* **17**(1)**:** 145-149.

Frederick AL, Yano H, Trifilieff P, Vishwasrao HD, Biezonski D, Meszaros J*, et al.* (2015). Evidence against dopamine D1/D2 receptor heteromers. *Mol Psychiatry*.

Fukuhara S, Marinissen MJ, Chiariello M, Gutkind JS (2000). Signaling from G protein-coupled receptors to ERK5/Big MAPK 1 involves Galpha q and Galpha 12/13 families of heterotrimeric G proteins. Evidence for the existence of a novel Ras AND Rho-independent pathway. *J Biol Chem* **275**(28)**:** 21730-21736.

Fuxe K, Ferré S, Canals M, Torvinen M, Terasmaa A, Marcellino D*, et al.* (2005). Adenosine A2A and dopamine D2 heteromeric receptor complexes and their function. *Journal of molecular neuroscience* **26**(2-3)**:** 209-220.

Fuxe K, Marcellino D, Guidolin D, Woods AS, Agnati LF (2008). *Heterodimers and Receptor Mosaics of Different Types of G-Protein-Coupled Receptors*. edn, vol. 23.

Fuxe K, Marcellino D, Woods AS, Giuseppina L, Antonelli T, Ferraro L*, et al.* (2009). Integrated signaling in heterodimers and receptor mosaics of different types of GPCRs of the forebrain: relevance for schizophrenia. *Journal of neural transmission* **116**(8)**:** 923-939.

Fuxe K, O. Borroto-Escuela D, Marcellino D, Romero-Fernandez W, Frankowska M, Guidolin D*, et al.* (2012). GPCR Heteromers and their Allosteric Receptor-Receptor Interactions. *Current Medicinal Chemistry* **19**(3)**:** 356-363.

Galve-Roperh I, Rueda D, Gómez del Pulgar T, Velasco G, Guzmán M (2002). Mechanism of Extracellular Signal-Regulated Kinase Activation by the CB1 Cannabinoid Receptor. *Molecular Pharmacology* **62**(6)**:** 1385-1392.

Gandía J, Lluís C, Ferre S, Franco R, Ciruela F (2008). Light resonance energy transfer-based methods in the study of G protein-coupled receptor oligomerization. *Bioessays* **30**(1)**:** 82-89.

Gaoni Y, Mechoulam R (1964). Isolation, structure, and partial synthesis of an active constituent of hashish. *J Am Chem Soc* **86**(8)**:** 1646-1647.

Garcia-Arencibia M, Ferraro L, Tanganelli S, Fernandez-Ruiz J (2008). Enhanced striatal glutamate release after the administration of rimonabant to 6-hydroxydopamine-lesioned rats. *Neurosci Lett* **438**(1)**:** 10-13.

Gary-Bobo M, Elachouri G, Scatton B, Le Fur G, Oury-Donat F, Bensaid M (2006). The Cannabinoid CB1 Receptor Antagonist Rimonabant (SR141716) Inhibits Cell Proliferation and Increases Markers of Adipocyte Maturation in Cultured Mouse 3T3 F442A Preadipocytes. *Molecular Pharmacology* **69**(2)**:** 471-478.

Garzon J, de la Torre-Madrid E, Rodriguez-Munoz M, Vicente-Sanchez A, Sanchez-Blazquez P (2009). Gz mediates the long-lasting desensitization of brain CB1 receptors and is essential for cross-tolerance with morphine. *Mol Pain* **5:** 11.

Gazi L, López-Giménez JF, Rüdiger MP, Strange PG (2003). Constitutive oligomerization of human D2 dopamine receptors expressed in Spodoptera frugiperda 9 (Sf9) and in HEK293 cells. *European Journal of Biochemistry* **270**(19)**:** 3928-3938.

Gebremedhin D, Lange AR, Campbell WB, Hillard CJ, Harder DR (1999). Cannabinoid CB1 receptor of cat cerebral arterial muscle functions to inhibit L-type Ca2+ channel current. *The American journal of physiology* **276**(6 Pt 2)**:** H2085-2093.

Genedani S, Guidolin D, Leo G, Filaferro M, Torvinen M, Woods AS*, et al.* (2005). Computer-assisted image analysis of caveolin-1 involvement in the internalization process of adenosine A2A-dopamine D2 receptor heterodimers. *Journal of Molecular Neuroscience* **26**(2-3)**:** 177-184.

George SR, O'Dowd BF (2007). A novel dopamine receptor signaling unit in brain: heterooligomers of D1 and D2 dopamine receptors. *The Scientific World Journal* **7:** 58-63.

Geyer MA, Wilkinson LS, Humby T, Robbins TW (1993). Isolation rearing of rats produces a deficit in prepulse inhibition of acoustic startle similar to that in schizophrenia. *Biological Psychiatry* **34**(6)**:** 361-372.

Giuffrida A, Parsons LH, Kerr TM, Rodríguez-de-Fonseca F, Navarro M, Piomelli D (1999). Dopamine activation of endogenous cannabinoid signaling in dorsal striatum. *Nat Neurosci* **2:** 358-363.

Glass M, Draganow M, Faull RLM (2000). The pattern of neurodegeneration in Huntington's disease: a comparative study of cannabinoid, dopamine, adenosine and GABAA receptor alterations in the human basal ganglia in Huntington's disease. *Neurosci* **97**(3)**:** 505-519.

Glass M, Felder CC (1997). Concurrent stimulation of cannabinoid CB1 and dopamine D2 receptors augments cAMP accumulation in striatal neurons: evidence for a Gs linkage to the CB1 receptor. *J Neurosci* **17**(14)**:** 5327-5333.

Glass M, Northup JK (1999). Agonist Selective Regulation of G Proteins by Cannabinoid CB1 and CB2 Receptors. *Molecular Pharmacology* **56**(6)**:** 1362-1369.

Gloerich M, Bos JL (2010). Epac: Defining a New Mechanism for cAMP Action. *Annual Review of Pharmacology and Toxicology* **50**(1)**:** 355-375.

Gomes I, Gupta A, Bushlin I, Devi LA (2014). Antibodies to probe endogenous G protein-coupled receptor heteromer expression, regulation, and function. *Frontiers in Pharmacology* **5:** 268.

Gómez dPT, Velasco G, Guzman M (2000). The CB1 cannabinoid receptor is coupled to the activation of protein kinase B/Akt. *Biochem. J* **347:** 369-373.

Gonzalez B, Paz F, Florán L, Aceves J, Erlij D, Florán B (2009). Cannabinoid Agonists Stimulate [3H]GABA Release in the Globus Pallidus of the Rat When Gi Protein-Receptor Coupling Is Restricted: Role of Dopamine D2 Receptors. *Journal of Pharmacology and Experimental Therapeutics* **328**(3)**:** 822-828.

Gray LJ, Cooper N, Dunkley A, Warren FC, Ara R, Abrams K*, et al.* (2012). A systematic review and mixed treatment comparison of pharmacological interventions for the treatment of obesity. *Obesity Reviews* **13**(6)**:** 483-498.

Grimsey NL, Goodfellow CE, Dragunow M, Glass M (2011). Cannabinoid receptor 2 undergoes Rab5-mediated internalization and recycles via a Rab11-dependent pathway. *Biochimica et Biophysica Acta (BBA) - Molecular Cell Research* **1813**(8)**:** 1554-1560.

Grimsey NL, Goodfellow CE, Scotter EL, Dowie MJ, Glass M, Graham ES (2008a). Specific detection of CB 1 receptors; cannabinoid CB 1 receptor antibodies are not all created equal! *Journal of neuroscience methods* **171**(1)**:** 78-86.

Grimsey NL, Graham ES, Dragunow M, Glass M (2010). Cannabinoid receptor 1 trafficking and the role of the intercellular pool: Implications for therapeutics. *Biochemical Pharmacology* **80:** 1050-1062.

Grimsey NL, Narayan PJ, Dragunow M, Glass M (2008b). A novel high-throughput assay for the quantitative assessment of receptor trafficking. *Clinical and Experimental Pharmacology and Physiology* **35**(11)**:** 1377-1382.

Guo N, Guo W, Kralikova M, Jiang M, Schieren I, Narendran R*, et al.* (2010). Impact of D2 receptor internalization on binding affinity of neuroimaging radiotracers. *Neuropsychopharmacology* **35**(3)**:** 806-817.

Guo W, Shi L, Filizola M, Weinstein H, Javitch JA (2005). Crosstalk in G protein-coupled receptors: Changes at the transmembrane homodimer interface determine activation. *Proceedings of the National Academy of Sciences of the United States of America* **102**(48)**:** 17495-17500.

Guo W, Shi L, Javitch JA (2003). The fourth transmembrane segment forms the interface of the dopamine D2 receptor homodimer. *J Biol Chem* **278:** 4385-4388.

Guo W, Urizar E, Kralikova M, Mobarec JC, Shi L, Filizola M*, et al.* (2008). Dopamine D2 receptors form higher order oligomers at physiological expression levels. *EMBO J* **27:** 2293-2304.

Gustafsson SB, Palmqvist R, Henriksson ML, Dahlin AM, Edin S, Jacobsson SOP*, et al.* (2011). High tumour cannabinoid CB 1 receptor immunoreactivity negatively impacts disease-specific survival in stage II microsatellite stable colorectal cancer. *PLoS ONE* **6**(8).

Gye MC, Kang HH, Kang HJ (2005). Expression of cannabinoid receptor 1 in mouse testes. *Systems Biology in Reproductive Medicine* **51**(3)**:** 247-255.

Gyombolai P, Boros E, Hunyady L, Turu G (2013). Differential beta-arrestin2 requirements for constitutive and agonist-induced internalization of the CB1 cannabinoid receptor. *Mol Cell Endocrinol* **372**(1-2)**:** 116-127.

Hague C, Uberti MA, Chen Z, Hall RA, Minneman KP (2004). Cell surface expression of alpha1D-adrenergic receptors is controlled by heterodimerization with alpha1B-adrenergic receptors. *J Biol Chem* **279**(15)**:** 15541-15549.

Hall RA (2005). Co-immunoprecipitation as a strategy to evaluate receptor-receptor or receptor-protein interactions. *G protein coupled receptor–protein interactions. Wiley, New Jersey, USA***:** 165-178.

Han Y, Moreira IS, Urizar E, Weinstein H, Javitch JA (2009). Allosteric communication between protomers of dopamine class A GPCR dimers modulates activation. *Nat Chem Biol* **5**(9)**:** 688-695.

Hanoune J, Defer N (2001). Regulation and role of adenylyl cyclase isoforms. *Annu Rev Pharmacol Toxicol* **41:** 145-174.

Hanson MA, Roth CB, Jo E, Griffith MT, Scott FL, Reinhart G*, et al.* (2012). Crystal Structure of a Lipid G Protein–Coupled Receptor. *Science* **335**(6070)**:** 851-855.

Hanyaloglu AC, Seeber RM, Kohout TA, Lefkowitz RJ, Eidne KA (2002). Homo- and Hetero-oligomerization of Thyrotropin-releasing Hormone (TRH) Receptor Subtypes: Differential regulation of β-arrestins 1 and 2. *Journal of Biological Chemistry* **277**(52)**:** 50422-50430.

Hart RC, Matthews JC, Hori K, Cormier MJ (1979). Renilla reniformis bioluminescence: luciferase-catalyzed production of nonradiating excited states from luciferin analogs and elucidation of the excited state species involved in energy transfer to Renilla green fluorescent protein. *Biochemistry* **18**(11)**:** 2204-2210.

He JC, Gomes I, Nguyen T, Jayaram G, Ram PT, Devi LA*, et al.* (2005). The Gαo/i-coupled Cannabinoid Receptor-mediated Neurite Outgrowth Involves Rap Regulation of Src and Stat3. *Journal of Biological Chemistry* **280**(39)**:** 33426-33434.

Hebert TE, Moffett S, Morello J-P, Loisel TP, Bichet DG, Barret C*, et al.* (1996). A Peptide Derived from a β2-Adrenergic Receptor Transmembrane Domain Inhibits Both Receptor Dimerization and Activation. *Journal of Biological Chemistry* **271**(27)**:** 16384-16392.

Hernández-López S, Tkatch T, Perez-Garci E, Galarraga E, Bargas J, Hamm H*, et al.* (2000). D2 dopamine receptors in striatal medium spiny neurons reduce L-Type Ca2+ currents and excitability vía a novel PLCβ1–IP3–calcineurin-signaling cascade. *The Journal of Neuroscience* **20**(24)**:** 8987-8995.

Herrlich A, Kühn B, Grosse R, Schmid A, Schultz G, Gudermann T (1996). Involvement of Gs and Gi Proteins in Dual Coupling of the Luteinizing Hormone Receptor to Adenylyl Cyclase and Phospholipase C. *Journal of Biological Chemistry* **271**(28)**:** 16764-16772.

Herve D, Levi-Strauss M, Marey-Semper I, Verney C, Tassin JP, Glowinski J*, et al.* (1993). G(olf) and Gs in rat basal ganglia: possible involvement of G(olf) in the coupling of dopamine D1 receptor with adenylyl cyclase. *J Neurosci* **13**(5)**:** 2237-2248.

Hietala J, Syvälahti E, Vuorio K, et al. (1994). STriatal d2 dopamine receptor characteristics in neuroleptic-naive schizophrenic patients studied with positron emission tomography. *Archives of General Psychiatry* **51**(2)**:** 116-123.

Higashijima T, Ferguson KM, Sternweis PC, Smigel MD, Gilman AG (1987). Effects of Mg2+ and the beta gamma-subunit complex on the interactions of guanine nucleotides with G proteins. *J Biol Chem* **262**(2)**:** 762-766.

Hillion J, Canals M, Torvinen M, Casado V, Scott R, Terasmaa A*, et al.* (2002). Coaggregation, cointernalization, and codesensitization of adenosine A2A receptors and dopamine D2 receptors. *J Biol Chem* **277**(20)**:** 18091-18097.

Ho BY, Uezono Y, Takada S, Takase I, Izumi F (1999). Coupling of the expressed cannabinoid CB1 and CB2 receptors to phospholipase C and G protein-coupled inwardly rectifying K+ channels. *Receptors & channels* **6**(5)**:** 363-374.

Hojo M, Sudo Y, Ando Y, Minami K, Takada M, Matsubara T*, et al.* (2008). . MU.-Opioid Receptor Forms a Functional Heterodimer With Cannabinoid CB1 Receptor: Electrophysiological and FRET Assay Analysis. *Journal of pharmacological sciences* **108**(3)**:** 308-319.

Holland AD, Rückerl F, Dragavon JM, Rekiki A, Tinevez J-Y, Tournebize R*, et al.* (2014). In vitro characterization of fluorescence by unbound excitation from luminescence: Broadening the scope of energy transfer. *Methods* **66**(2)**:** 353-361.

Horne AW, Phillips Iii JA, Kane N, Lourenco PC, McDonald SE, Williams ARW*, et al.* (2008). CB1 expression is attenuated in Fallopian tube and decidua of women with ectopic pregnancy. *PLoS One* **3**(12)**:** e3969.

Hounsou C, Margathe JF, Oueslati N, Belhocine A, Dupuis E, Thomas C*, et al.* (2015). Time-resolved FRET binding assay to investigate hetero-oligomer binding properties: proof of concept with dopamine D1/D3 heterodimer. *ACS chemical biology* **10**(2)**:** 466-474.

Howlett AC, Breivogel CS, Childers SR, Deadwyler SA, Hampson RE, Porrino LJ (2004). Cannabinoid physiology and pharmacology: 30 years of progress. *Neuropharmacology* **47 Suppl 1:** 345-358.

Howlett AC, Qualy JM, Khachatrian LL (1986). Involvement of Gi in the inhibition of adenylate cyclase by cannabimimetic drugs. *Mol Pharmacol* **29**(3)**:** 307-313.

Hsieh C, Brown S, Derleth C, Mackie K (1999). Internalization and Recycling of the CB1 Cannabinoid Receptor. *Journal of Neurochemistry* **73**(2)**:** 493-501.

Hu J, Thor D, Zhou Y, Liu T, Wang Y, McMillin SM*, et al.* (2012). Structural aspects of M3 muscarinic acetylcholine receptor dimer formation and activation. *The FASEB Journal* **26**(2)**:** 604-616.

Huang CL, Slesinger PA, Casey PJ, Jan YN, Jan LY (1995). Evidence that direct binding of G beta gamma to the GIRK1 G protein-gated inwardly rectifying K+ channel is important for channel activation. *Neuron* **15**(5)**:** 1133-1143.

Huang J, Chen S, Zhang JJ, Huang X-Y (2013). Crystal structure of oligomeric β1-adrenergic G protein–coupled receptors in ligand-free basal state. *Nature structural & molecular biology* **20**(4)**:** 419-425.

Hudson BD, Hebert TE, Kelly MEM (2010a). Ligand- and heterodimer-directed signaling of the CB1 cannabinoid receptor. *Mol Pharmacol* **77**(1)**:** 1-9.

Hudson BD, Hébert TE, Kelly MEM (2010b). Physical and functional interaction between CB1 cannabinoid receptors and β2-adrenoceptors. *British journal of pharmacology* **160**(3)**:** 627-642.

Hungund BL, Vinod KY, Kassir SA, Basavarajappa BS, Yalamanchili R, Cooper TB*, et al.* (2004). Upregulation of CB1 receptors and agonist-stimulated [lsqb]35S[rsqb]GTP[gamma]S binding in the prefrontal cortex of depressed suicide victims. *Mol Psychiatry* **9**(2)**:** 184-190.

Hunter MR Using a bivalent ligand to target CB1-D2 receptor dimers. Bachelor of Science Honours, University of Auckland, Auckland, New Zealand, 2010.

Hurley MJ, Mash DC, Jenner P (2003). Expression of cannabinoid CB1 receptor mRNA in basal ganglia of normal and parkinsonian human brain. *Journal of neural transmission (Vienna, Austria : 1996)* **110**(11)**:** 1279-1288.

Hurst D, Umejiego U, Lynch D, Seltzman H, Hyatt S, Roche M*, et al.* (2006). Biarylpyrazole inverse agonists at the cannabinoid CB1 receptor: importance of the C-3 carboxamide oxygen/lysine3.28(192) interaction. *Journal of medicinal chemistry* **49**(20)**:** 5969-5987.

Hurst DP, Schmeisser M, Reggio PH (2013). Endogenous lipid activated G protein-coupled receptors: Emerging structural features from crystallography and molecular dynamics simulations. *Chemistry and Physics of Lipids* **169**(0)**:** 46-56.

Iizuka Y, Sei Y, Weinberger DR, Straub RE (2007). Evidence that the BLOC-1 protein dysbindin modulates dopamine D2 receptor internalization and signaling but not D1 internalization. *J Neurosci* **27**(45)**:** 12390-12395.

Insel PA, Zhang L, Murray F, Yokouchi H, Zambon AC (2012). Cyclic AMP is both a pro-apoptotic and anti-apoptotic second messenger. *Acta Physiologica* **204**(2)**:** 277-287.

Irannejad R, Tomshine JC, Tomshine JR, Chevalier M, Mahoney JP, Steyaert J*, et al.* (2013). Conformational biosensors reveal GPCR signalling from endosomes. *Nature* **495**(7442)**:** 534-538.

Irannejad R, von Zastrow M (2014). GPCR signaling along the endocytic pathway. *Current Opinion in Cell Biology* **27**(0)**:** 109-116.

Ishii I, Chun J (2002). Anandamide-induced neuroblastoma cell rounding via the CB1 cannabinoid receptors. *Neuroreport* **13**(5)**:** 593-596.

Ito K, Haga T, Lameh J, Sadée W (1999). Sequestration of dopamine D2 receptors depends on coexpression of G-protein-coupled receptor kinases 2 or 5. *European Journal of Biochemistry* **260**(1)**:** 112-119.

Iwata K, Ito K, Fukuzaki A, Inaki K, Haga T (1999). Dynamin and Rab5 regulate GRK2-dependent internalization of dopamine D2 receptors. *European Journal of Biochemistry* **263**(2)**:** 596-602.

James JR, Oliveira MI, Carmo AM, Iaboni A, Davis SJ (2006). A rigorous experimental framework for detecting protein oligomerization using bioluminescence resonance energy transfer. *Nat Meth* **3**(12)**:** 1001-1006.

Janetopoulos C, Devreotes P (2002). Monitoring receptor-mediated activation of heterotrimeric G-proteins by fluorescence resonance energy transfer. *Methods* **27**(4)**:** 366-373.

Jäntti MH, Mandrika I, Kukkonen JP (2014). Human orexin/hypocretin receptors form constitutive homo- and heteromeric complexes with each other and with human CB1 cannabinoid receptors. *Biochemical and Biophysical Research Communications* **445**(2)**:** 486-490.

Jarrahian A, Watts VJ, Barker EL (2004). D2 dopamine receptors modulate Gα-subunit coupling of the CB1 cannabinoid receptor. *J Pharmacol Exp Ther* **308**(3)**:** 880-886.

Jean-Alphonse F, Hanyaloglu AC (2011). Regulation of GPCR signal networks via membrane trafficking. *Molecular and Cellular Endocrinology* **331**(2)**:** 205-214.

Ji Y, Yang F, Papaleo F, Wang H-X, Gao W-J, Weinberger DR*, et al.* (2009). Role of dysbindin in dopamine receptor trafficking and cortical GABA function. *Proceedings of the National Academy of Sciences* **106**(46)**:** 19593-19598.

Jiang LI, Collins J, Davis R, Lin K-M, DeCamp D, Roach T*, et al.* (2007). Use of a cAMP BRET Sensor to Characterize a Novel Regulation of cAMP by the Sphingosine 1-Phosphate/G13 Pathway. *Journal of Biological Chemistry* **282**(14)**:** 10576-10584.

Jiang M, Spicher K, Boulay G, Wang Y, Birnbaumer L (2001). Most central nervous system D2 dopamine receptors are coupled to their effectors by Go. *Proceedings of the National Academy of Sciences* **98**(6)**:** 3577-3582.

Jin W, Brown S, Roche JP, Hsieh C, Celver JP, Kovoor A*, et al.* (1999). Distinct Domains of the CB1 Cannabinoid Receptor Mediate Desensitization and Internalization. *The Journal of Neuroscience* **19**(10)**:** 3773-3780.

Jonas KC, Fanelli F, Huhtaniemi IT, Hanyaloglu AC (2015). Single Molecule Analysis of Functionally Asymmetric G Protein-coupled Receptor (GPCR) Oligomers Reveals Diverse Spatial and Structural Assemblies. *Journal of Biological Chemistry* **290**(7)**:** 3875-3892.

Jones D (2008). End of the line for cannabinoid receptor 1 as an anti-obesity target? *Nat Rev Drug Discov* **7**(12)**:** 961-962.

Jörg M, May LT, Mak FS, Lee KCK, Miller ND, Scammells PJ*, et al.* (2014a). Synthesis and Pharmacological Evaluation of Dual Acting Ligands Targeting the Adenosine A2A and Dopamine D2 Receptors for the Potential Treatment of Parkinson's Disease. *Journal of Medicinal Chemistry* **58**(2)**:** 718-738.

Jörg M, Scammells PJ, Capuano B (2014b). The Dopamine D2 and Adenosine A2A Receptors: Past, Present and Future Trends for the Treatment of Parkinson's Disease. *Current Medicinal Chemistry* **21**(27)**:** 3188-3210.

Juhasz JR, Hasbi A, Rashid AJ, So CH, George SR, O'Dowd BF (2008). Mu-opioid receptor heterooligomer formation with the dopamine D1 receptor as directly visualized in living cells. *European Journal of Pharmacology* **581**(3)**:** 235-243.

Jung CK, Kang WK, Park JM, Ahn HJ, Kim SW, Oh ST*, et al.* (2013). Expression of the cannabinoid type I receptor and prognosis following surgery in colorectal cancer. *Oncology Letters* **5**(3)**:** 870-876.

Kabbani N, Negyessy L, Lin R, Goldman-Rakic P, Levenson R (2002). Interaction with Neuronal Calcium Sensor NCS-1 Mediates Desensitization of the D2 Dopamine Receptor. *The Journal of Neuroscience* **22**(19)**:** 8476-8486.

Kai H, Fukui T, Lassègue B, Shah A, Minieri CA, Griendling KK (1996). Prolonged exposure to agonist results in a reduction in the levels of the Gq/G11 alpha subunits in cultured vascular smooth muscle cells. *Molecular Pharmacology* **49**(1)**:** 96-104.

Kamenetsky M, Middelhaufe S, Bank EM, Levin LR, Buck J, Steegborn C (2006). Molecular Details of cAMP Generation in Mammalian Cells: A Tale of Two Systems. *Journal of Molecular Biology* **362**(4)**:** 623-639.

Kamiya T, Saitoh O, Yoshioka K, Nakata H (2003). Oligomerization of adenosine A2A and dopamine D2 receptors in living cells. *Biochemical and Biophysical Research Communications* **306**(2)**:** 544-549.

Kanterman RY, Mahan LC, Briley EM, Monsma FJ, Sibley DR, Axelrod J*, et al.* (1991). Transfected D2 dopamine receptors mediate the potentiation of arachidonic acid release in Chinese hamster ovary cells. *Molecular pharmacology* **39**(3)**:** 364-369.

Kapur A, Hurst DP, Fleischer D, Whitnell R, Thakur GA, Makriyannis A*, et al.* (2007). Mutation studies of Ser7. 39 and Ser2. 60 in the human CB1 cannabinoid receptor: evidence for a serine-induced bend in CB1 transmembrane helix 7. *Molecular pharmacology* **71**(6)**:** 1512-1524.

Katona I, Sperlágh B, Sík A, Käfalvi A, Vizi ES, Mackie K*, et al.* (1999). Presynaptically Located CB1 Cannabinoid Receptors Regulate GABA Release from Axon Terminals of Specific Hippocampal Interneurons. *The Journal of Neuroscience* **19**(11)**:** 4544-4558.

Katritch V, Cherezov V, Stevens RC (2012). Diversity and modularity of G protein-coupled receptor structures. *Trends in Pharmacological Sciences* **33**(1)**:** 17-27.

Kearn CS, Blake-Palmer K, Daniel E, Mackie K, Glass M (2005). Concurrent stimulation of cannabinoid CB1 and dopamine D2 receptors enhances heterodimer formation: a mechanism for receptor cross-talk? *Mol Pharmacol* **67**(5)**:** 1697-1704.

Keravis T, Lugnier C (2010). Cyclic nucleotide phosphodiesterases (PDE) and peptide motifs. *Current pharmaceutical design* **16**(9)**:** 1114-1125.

Kerppola TK (2006). Design and implementation of bimolecular fluorescence complementation (BiFC) assays for the visualization of protein interactions in living cells. *Nat. Protocols* **1**(3)**:** 1278-1286.

Khan SS, Lee FJS (2014). Delineation of Domains Within the Cannabinoid CB1 and Dopamine D2 Receptors That Mediate the Formation of the Heterodimer Complex. *Journal of Molecular Neuroscience* **53**(1)**:** 10-21.

Kim SJ, Kim MY, Lee EJ, Ahn YS, Baik J-H (2004). Distinct regulation of internalization and mitogen-activated protein kinase activation by two isoforms of the dopamine D2 receptor. *Molecular Endocrinology* **18**(3)**:** 640-652.

Klein TW, Newton C, Larsen K, Lu L, Perkins I, Nong L*, et al.* (2003). The cannabinoid system and immune modulation. *Journal of Leukocyte Biology* **74**(4)**:** 486-496.

Kniazeff J, Prézeau L, Rondard P, Pin J-P, Goudet C (2011). Dimers and beyond: The functional puzzles of class C GPCRs. *Pharmacology & Therapeutics* **130**(1)**:** 9-25.

Knight A, Misra A, Quirk K, Benwell K, Revell D, Kennett G*, et al.* (2004). Pharmacological characterisation of the agonist radioligand binding site of 5-HT2A, 5-HT2B and 5-HT2C receptors. *Naunyn-Schmiedeberg's Archives of Pharmacology* **370**(2)**:** 114-123.

Kocan M, Pfleger KG (2011). Study of GPCR–Protein Interactions by BRET. In: Willars GB, Challiss RAJ (ed)^(eds). *Receptor Signal Transduction Protocols*, edn, Vol. 746: Humana Press. p^pp 357-371.

Koenig JA (2004). Assessment of receptor internalization and recycling. *Methods in molecular biology (Clifton, N.J.)* **259:** 249-273.

Kolch W (2005). Coordinating ERK/MAPK signalling through scaffolds and inhibitors. *Nat Rev Mol Cell Biol* **6**(11)**:** 827-837.

Kouznetsova M, Kelley B, Shen M, Thayer SA (2002). Desensitization of Cannabinoid-Mediated Presynaptic Inhibition of Neurotransmission Between Rat Hippocampal Neurons in Culture. *Molecular Pharmacology* **61**(3)**:** 477-485.

Kreitzer AC, Regehr WG (2001). Retrograde inhibition of presynaptic calcium influx by endogenous cannabinoids at excitatory synapses onto Purkinje cells. *Neuron* **29**(3)**:** 717-727.

Kull B, Svenningsson P, Fredholm BB (2000). Adenosine A2A Receptors are Colocalized with and Activate Golf in Rat Striatum. *Molecular Pharmacology* **58**(4)**:** 771-777.

Kuszak AJ, Pitchiaya S, Anand JP, Mosberg HI, Walter NG, Sunahara RK (2009). Purification and Functional Reconstitution of Monomeric μ-Opioid Receptors: ALLOSTERIC MODULATION OF AGONIST BINDING BY Gi2. *Journal of Biological Chemistry* **284**(39)**:** 26732-26741.

Kyriakis JM, Avruch J (2012). Mammalian MAPK signal transduction pathways activated by stress and inflammation: a 10-year update. *Physiological reviews* **92**(2)**:** 689-737.

Lastres-Becker I, Bizat N, Boyer F, Hantraye P, Brouillet E, Fernandez-Ruiz J (2003). Effects of cannabinoids in the rat model of Huntington's disease generated by an intrastriatal injection of malonate. *Neuroreport* **14**(6)**:** 813-816.

Lastres-Becker I, Cebeira M, L. de Ceballos M, Zeng BY, Jenner P, Ramos JA*, et al.* (2001). Increased cannabinoid CB1 receptor binding and activation of GTP-binding proteins in the basal ganglia of patients with Parkinson's syndrome and of MPTP-treated marmosets. *European Journal of Neuroscience* **14**(11)**:** 1827-1832.

Lastres-Becker I, Hansen HH, Berrendero F, De Miguel R, Pérez-Rosado A, Manzanares J*, et al.* (2002). Alleviation of motor hyperactivity and neurochemical deficits by endocannabinoid uptake inhibition in a rat model of Huntington's disease. *Synapse* **44**(1)**:** 23-35.

Lastres-Becker I, Molina-Holgado F, Ramos JA, Mechoulam R, Fernandez-Ruiz J (2005). Cannabinoids provide neuroprotection against 6-hydroxydopamine toxicity in vivo and in vitro: relevance to Parkinson's disease. *Neurobiology of disease* **19**(1-2)**:** 96-107.

Lauckner JE, Hille B, Mackie K (2005). The cannabinoid agonist WIN55,212-2 increases intracellular calcium via CB1 receptor coupling to Gq/11 G proteins. *Proc Natl Acad Sci U S A* **102**(52)**:** 19144-19149.

Le Foll B, Gorelick D, Goldberg S (2009). The future of endocannabinoid-oriented clinical research after CB1 antagonists. *Psychopharmacology* **205**(1)**:** 171-174.

Le Naour M, Akgün E, Yekkirala A, Lunzer MM, Powers MD, Kalyuzhny AE*, et al.* (2013). Bivalent Ligands That Target μ Opioid (MOP) and Cannabinoid1 (CB1) Receptors Are Potent Analgesics Devoid of Tolerance. *Journal of Medicinal Chemistry* **56**(13)**:** 5505-5513.

Lee SP, So CH, Rashid AJ, Varghese G, Cheng R, Lança AJ*, et al.* (2004). Dopamine D1 and D2 Receptor Co-activation Generates a Novel Phospholipase C-mediated Calcium Signal. *Journal of Biological Chemistry* **279**(34)**:** 35671-35678.

Leterrier C, Lainé J, Darmon M, Boudin H, Rossier J, Lenkei Z (2006). Constitutive Activation Drives Compartment-Selective Endocytosis and Axonal Targeting of Type 1 Cannabinoid Receptors. *The Journal of Neuroscience* **26**(12)**:** 3141-3153.

Levoye A, Balabanian K, Baleux F, Bachelerie F, Lagane B (2009). *CXCR7 heterodimerizes with CXCR4 and regulates CXCL12-mediated G protein signaling*. edn, vol. 113.

Leweke FM, Giuffrida A, Wurster U, Emrich HM, Piomelli D (1999a). Elevated endogenous cannabinoids in schizophrenia. *Neuroreport* **10**(8)**:** 1665-1669.

Leweke FM, Schneider U, Thies M, Münte TF, Emrich HM (1999b). Effects of synthetic Δ9-tetrahydrocannabinol on binocular depth inversion of natural and artificial objects in man. *Psychopharmacology* **142**(3)**:** 230-235.

Li Y, Roy BD, Wang W, Zhang L, Zhang L, Sampson SB*, et al.* (2012). Identification of Two Functionally Distinct Endosomal Recycling Pathways for Dopamine D2 Receptor. *The Journal of Neuroscience* **32**(21)**:** 7178-7190.

Lim G, Sung B, Ji R-R, Mao J (2003). Upregulation of spinal cannabinoid-1-receptors following nerve injury enhances the effects of Win 55,212-2 on neuropathic pain behaviors in rats. *Pain* **105**(1–2)**:** 275-283.

Liu Z-j, Yang Y-j, Jiang L, Xu Y-c, Wang A-x, Du G-h*, et al.* (2011). Tyrosine sulfation in N-terminal domain of human C5a receptor is necessary for binding of chemotaxis inhibitory protein of Staphylococcus aureus. *Acta Pharmacol Sin* **32**(8)**:** 1038-1044.

Loening AM, Fenn TD, Wu AM, Gambhir SS (2006). Consensus guided mutagenesis of Renilla luciferase yields enhanced stability and light output. *Protein Engineering Design and Selection* **19**(9)**:** 391-400.

Logue JS, Scott JD (2010). Organizing signal transduction through A-kinase anchoring proteins (AKAPs). *FEBS Journal* **277**(21)**:** 4370-4375.

Luo Y, Kokkonen GC, Wang X, Neve KA, Roth GS (1998). D2 dopamine receptors stimulate mitogenesis through pertussis toxin-sensitive G proteins and ras-involved ERK and SAP/JNK pathways in rat C6-D2L glioma cells. *Journal of neurochemistry* **71**(3)**:** 980-990.

Lutge EE, Gray A, Siegfried N (2012). Medical use of cannabis in patients with HIV/AIDS. *Health*.

Luttrell LM, Lefkowitz RJ (2002). The role of β-arrestins in the termination and transduction of G-protein-coupled receptor signals. *Journal of Cell Science* **115**(3)**:** 455-465.

Machado Rocha FC, StÉFano SC, De CÁSsia Haiek R, Rosa Oliveira LMQ, Da Silveira DX (2008). Therapeutic use of Cannabis sativa on chemotherapy-induced nausea and vomiting among cancer patients: systematic review and meta-analysis. *European Journal of Cancer Care* **17**(5)**:** 431-443.

Mackie K, Hille B (1992). Cannabinoids inhibit N-type calcium channels in neuroblastoma-glioma cells. *Proc Natl Acad Sci U S A* **89:** 3825-3829.

Mackie K, Lai Y, Westenbroek R, Mitchell R (1995). Cannabinoids activate an inwardly rectifying potassium conductance and inhibit Q-type calcium currents in AtT20 cells transfected with rat brain cannabinoid receptor. *J Neurosci* **15**(10)**:** 6552-6561.

Magalhaes AC, Dunn H, Ferguson SS (2012). Regulation of GPCR activity, trafficking and localization by GPCR-interacting proteins. *Br J Pharmacol* **165**(6)**:** 1717-1736.

Mahavadi S, Sriwai W, Huang J, Grider JR, Murthy KS (2014). *Inhibitory signaling by CB1 receptors in smooth muscle mediated by GRK5/β-arrestin activation of ERK1/2 and Src kinase*. edn, vol. 306.

Malone DT, Taylor DA (2006). The effect of Δ9-tetrahydrocannabinol on sensorimotor gating in socially isolated rats. *Behavioural Brain Research* **166**(1)**:** 101-109.

Mancia F, Assur Z, Herman AG, Siegel R, Hendrickson WA (2008). Ligand sensitivity in dimeric associations of the serotonin 5HT2c receptor. *EMBO Rep* **9:** 363-369.

Maneuf YP, Brotchie JM (1997). Paradoxical action of the cannabinoid WIN 55,212-2 in stimulated and basal cyclic AMP accumulation in rat globus pallidus slices. *Br J Pharmacol* **120:** 1397-1398.

Manglik A, Kruse AC, Kobilka TS, Thian FS, Mathiesen JM, Sunahara RK*, et al.* (2012). Crystal structure of the [micro]-opioid receptor bound to a morphinan antagonist. *Nature* **485**(7398)**:** 321-326.

Marcellino D, Carriba P, Filip M, Borgkvist A, Frankowska M, Bellido I*, et al.* (2008). Antagonistic cannabinoid CB1/dopamine D2 receptor interactions in striatal CB1/D2 heteromers. A combined neurochemical and behavioral analysis. *Neuropharmacol* **54:** 815-823.

Marchese A, Paing MM, Temple BRS, Trejo J (2008). G protein-coupled receptor sorting to endosomes and lysosomes. *Annual Review of Pharmacology and Toxicology* **48:** 601-629.

Margeta-Mitrovic M, Jan YN, Jan LY (2000). A trafficking checkpoint controls GABA(B) receptor heterodimerization. *Neuron* **27**(1)**:** 97-106.

Marley A, von Zastrow M (2010). Dysbindin promotes the post-endocytic sorting of G protein-coupled receptors to lysosomes. *PloS one* **5**(2)**:** e9325.

Marshall AD, Lagutina I, Grosveld GC (2011). PAX3-FOXO1 Induces Cannabinoid Receptor 1 to Enhance Cell Invasion and Metastasis. *Cancer Research* **71**(24)**:** 7471-7480.

Martín AB, Fernandez-Espejo E, Ferrer B, Gorriti MA, Bilbao A, Navarro M*, et al.* (2008). Expression and function of CB1 receptor in the rat striatum: localization and effects on D1 and D2 dopamine receptor-mediated motor behaviours. *Neuropsychopharmacol* **33:** 1667-1679.

Massa F, Storr M, Lutz B (2005). The endocannabinoid system in the physiology and pathophysiology of the gastrointestinal tract. *Journal of molecular medicine* **83**(12)**:** 944-954.

Matsuda LA, Lolait SJ, Brownstein MJ, Young AC, Bonner TI (1990). Structure of a cannabinoid receptor and functional expression of the cloned cDNA. *Nature* **346**(6284)**:** 561-564.

Maurice P, Benleulmi-Chaachoua A, Jockers R (2012). Differential Assembly of GPCR Signaling Complexes Determines Signaling Specificity. In: Dupré DJ, Hébert TE, Jockers R (ed)^(eds). *GPCR Signalling Complexes – Synthesis, Assembly, Trafficking and Specificity*, edn, Vol. 63: Springer Netherlands. p^pp 225-240.

Maurice P, Kamal M, Jockers R (2011). Asymmetry of GPCR oligomers supports their functional relevance. *Trends in Pharmacological Sciences* **32**(9)**:** 514-520.

McAllister G, Knowles MR, Ward-Booth SM, Sinclair HA, Patel S, Marwood R*, et al.* (1995). Functional coupling of human D2, D3, and D4 dopamine receptors in HEK293 cells. *Journal of receptor and signal transduction research* **15**(1-4)**:** 267-281.

McAllister SD, Griffin G, Satin LS, Abood ME (1999). Cannabinoid receptors can activate and inhibit G protein-coupled inwardly rectifying potassium channels in a xenopus oocyte expression system. *J Pharmacol Exp Ther* **291**(2)**:** 618-626.

McAllister SD, Hurst DP, Barnett-Norris J, Lynch D, Reggio PH, Abood ME (2004). Structural Mimicry in Class AG Protein-coupled Receptor Rotamer Toggle Switches: The importance of the F3. 36 (201)/W6. 48 (357) interaction in cannabinoid CB1 recepter activation. *Journal of Biological Chemistry* **279**(46)**:** 48024-48037.

McAllister SD, Rizvi G, Anavi-Goffer S, Hurst DP, Barnett-Norris J, Lynch DL*, et al.* (2003). An Aromatic Microdomain at the Cannabinoid CB1 Receptor Constitutes an Agonist/Inverse Agonist Binding Region. *J. Med. Chem* **46:** 5139-5152.

McIntosh BT, Hudson B, Yegorova S, Jollimore CAB, Kelly MEM (2007). Agonist-dependent cannabinoid receptor signalling in human trabecular meshwork cells. *British Journal of Pharmacology* **152**(7)**:** 1111-1120.

Mesnage V, Houeto JL, Bonnet AM, Clavier I, Arnulf I, Cattelin F*, et al.* (2004). Neurokinin B, neurotensin, and cannabinoid receptor antagonists and Parkinson disease. *Clinical neuropharmacology* **27**(3)**:** 108-110.

Messalli EM, Grauso F, Luise R, Angelini A, Rossiello R (2014). Cannabinoid receptor type 1 immunoreactivity and disease severity in human epithelial ovarian tumors. *American Journal of Obstetrics and Gynecology* **211**(3)**:** 234.e231-234.e236.

Michael G, Haydar A, Philippe J, Brian C, Ujendra K (2008). Cell Growth Inhibition and Functioning of Human Somatostatin Receptor Type 2 Are Modulated by Receptor Heterodimerization. *Molecular Endocrinology* **22**(10)**:** 2278-2292.

Michal P, Lysíková M, Tuček S (2001). Dual effects of muscarinic M2 acetylcholine receptors on the synthesis of cyclic AMP in CHO cells: dependence on time, receptor density and receptor agonists. *British Journal of Pharmacology* **132**(6)**:** 1217-1228.

Michel MC, Wieland T, Tsujimoto G (2009). How reliable are G-protein-coupled receptor antibodies? *Naunyn-Schmiedeberg's archives of pharmacology* **379**(4)**:** 385-388.

Mievis S, Blum D, Ledent C (2011). Worsening of Huntington disease phenotype in CB1 receptor knockout mice. *Neurobiology of disease* **42**(3)**:** 524-529.

Milligan G (1988). Techniques used in the identification and analysis of function of pertussis toxin-sensitive guanine nucleotide binding proteins. *Biochemical Journal* **255**(1)**:** 1-13.

Milligan G, Green A (1991). Agonist control of G-protein levels. *Trends in Pharmacological Sciences* **12**(0)**:** 207-209.

Minneman KP (2007). Heterodimerization and surface localization of G protein coupled receptors. *Biochemical Pharmacology* **73**(8)**:** 1043-1050.

Moravcová Z, Rudajev Vr, Stöhr J, Novotný J, Černý J, Parenti M*, et al.* (2004). Long-term agonist stimulation of IP prostanoid receptor depletes the cognate Gsα protein in membrane domains but does not change the receptor level. *Biochimica et Biophysica Acta (BBA) - Molecular Cell Research* **1691**(1)**:** 51-65.

Morgese MG, Cassano T, Gaetani S, Macheda T, Laconca L, Dipasquale P*, et al.* (2009). Neurochemical changes in the striatum of dyskinetic rats after administration of the cannabinoid agonist WIN55,212-2. *Neurochemistry International* **54**(1)**:** 56-64.

Morin JG, Hastings JW (1971). Energy transfer in a bioluminescent system. *Journal of cellular physiology* **77**(3)**:** 313-318.

Mullaney I, Dodd MW, Buckley N, Milligan G (1993). Agonist activation of transfected human M1 muscarinic acetylcholine receptors in CHO cells results in down-regulation of both the receptor and the alpha subunit of the G-protein Gq. *Biochem. J* **289:** 125-131.

Müller-Vahl KR, Kolbe H, Schneider U, Emrich HM (1998). Cannabinoids: possible role in patho-physiology and therapy of Gilles de la Tourette syndrome. *Acta Psychiatrica Scandinavica* **98**(6)**:** 502-506.

Müller-Vahl KR, Schneider U, Koblenz A, Jöbges M, Kolbe H, Daldrup T*, et al.* (2002). Treatment of Tourette's Syndrome with Δ9-Tetrahydrocannabinol (THC): A Randomized Crossover Trial. *Pharmacopsychiatry* **35**(02)**:** 57-61.

Müller-Vahl KR, Schneider U, Prevedel H, Theloe K, Kolbe H, Daldrup T*, et al.* (2003). the Treatment of Tics in Tourette Syndrome: a 6-Week Randomized Trial. *J Clin Psychiatry* **64:** 00-00.

Munro S, Thomas KL, Abu-Shaar M (1993). Molecular characterization of a peripheral receptor for cannabinoids. *Nature* **365**(6441)**:** 61-65.

Murphy JE, Padilla BE, Hasdemir B, Cottrell GS, Bunnett NW (2009). Endosomes: A legitimate platform for the signaling train. *Proceedings of the National Academy of Sciences* **106**(42)**:** 17615-17622.

Nagai T, Ibata K, Park ES, Kubota M, Mikoshiba K, Miyawaki A (2002). A variant of yellow fluorescent protein with fast and efficient maturation for cell-biological applications. *Nature biotechnology* **20**(1)**:** 87-90.

Namkung Y, Dipace C, Javitch JA, Sibley DR (2009). G Protein-coupled Receptor Kinase-mediated Phosphorylation Regulates Post-endocytic Trafficking of the D2 Dopamine *The Journal of Biological Chemistry* **284:** 15038-15051.

Namkung Y, Sibley DR (2004). Protein Kinase C Mediates Phosphorylation, Desensitization, and Trafficking of the D2 Dopamine Receptor. *Journal of Biological Chemistry* **279**(47)**:** 49533-49541.

Nava F, Carta G, Battasi AM, Gessa GL (2000). D2 dopamine receptors enable D9-tetrahydrocannabinol induced memory impairment and reduction of hippocampal extracellular acetylcholine concentration. *Br J Pharmacol* **130:** 1201-1210.

Navarro G, Carriba P, Gandí J, Ciruela F, Casadó V, Cortés A*, et al.* (2008a). Detection of Heteromers Formed by Cannabinoid CB1, Dopamine D2, and Adenosine A2A G-Protein-Coupled Receptors by Combining Bimolecular Fluorescence Complementation and Bioluminescence Energy Transfer. *TheScientificWorldJOURNAL* **8**.

Navarro G, Carriba P, Gandía J, Ciruela F, Casadó V, Cortés A*, et al.* (2008b). Detection of heteromers formed by cannabinoid CB1, dopamine D2, and adenosine A2A G-protein-coupled receptors by combining bimolecular fluorescence complementation and bioluminescence energy transfer. *ScientificWorldJournal* **11**(8)**:** 1088-1097.

Navarro G, Ferré S, Cordomi A, Moreno E, Mallol J, Casadó V*, et al.* (2010). Interactions between intracellular domains as key determinants of the quaternary structure and function of receptor heteromers. *J Biol Chem* **285**.

Neve KA, Seamans JK, Trantham-Davidson H (2004). Dopamine Receptor Signaling. *Journal of Receptors and Signal Transduction* **24**(3)**:** 165-205.

Neves SR, Ram PT, Iyengar R (2002). G protein pathways. *Science* **296**(5573)**:** 1636-1639.

Nguyen PT, Schmid CL, Raehal KM, Selley DE, Bohn LM, Sim-Selley LJ (2012). β-Arrestin2 Regulates Cannabinoid CB1 Receptor Signaling and Adaptation in a Central Nervous System Region–Dependent Manner. *Biological Psychiatry* **71**(8)**:** 714-724.

Nie J, Lewis DL (2001). Structural Domains of the CB1 Cannabinoid Receptor That Contribute to Constitutive Activity and G-Protein Sequestration. *The Journal of Neuroscience* **21**(22)**:** 8758-8764.

Novotna A, Mares J, Ratcliffe S, Novakova I, Vachova M, Zapletalova O*, et al.* (2011). A randomized, double-blind, placebo-controlled, parallel-group, enriched-design study of nabiximols* (Sativex®), as add-on therapy, in subjects with refractory spasticity caused by multiple sclerosis. *European Journal of Neurology* **18**(9)**:** 1122-1131.

Nurmikko TJ, Serpell MG, Hoggart B, Toomey PJ, Morlion BJ, Haines D (2007). Sativex successfully treats neuropathic pain characterised by allodynia: A randomised, double-blind, placebo-controlled clinical trial. *PAIN*® **133**(1–3)**:** 210-220.

O'Dowd BF, Ji X, Nguyen T, George SR (2012). Two amino acids in each of D1 and D2 dopamine receptor cytoplasmic regions are involved in D1–D2 heteromer formation. *Biochemical and Biophysical Research Communications* **417**(1)**:** 23-28.

O'Dowd BF, Nguyen T, Ji X, George SR (2013). D5 dopamine receptor carboxyl tail involved in D5–D2 heteromer formation. *Biochemical and Biophysical Research Communications* **431**(3)**:** 586-589.

Octeau JC, Schrader JM, Masuho I, Sharma M, Aiudi C, Chen C-K*, et al.* (2014). G Protein Beta 5 Is Targeted to D2-Dopamine Receptor-Containing Biochemical Compartments and Blocks Dopamine-Dependent Receptor Internalization. *PloS one* **9**(8)**:** e105791.

Ohno-Shosaku T, Maejima T, Kano M (2001). Endogenous cannabinoids mediate retrograde signals from depolarized postsynaptic neurons to presynaptic terminals. *Neuron* **29**(3)**:** 729-738.

Okamoto T, Nishimoto I (1992). Detection of G protein-activator regions in M4 subtype muscarinic, cholinergic, and alpha 2-adrenergic receptors based upon characteristics in primary structure. *Journal of Biological Chemistry* **267**(12)**:** 8342-8346.

Olah ME (1997). Identification of A2a adenosine receptor domains involved in selective coupling to Gs. Analysis of chimeric A1/A2a adenosine receptors. *J Biol Chem* **272**(1)**:** 337-344.

Oldham WM, Hamm HE (2008). Heterotrimeric G protein activation by G-protein-coupled receptors. *Nat Rev Mol Cell Biol* **9:** 60-71.

Orcel H, Albizu L, Perkovska S, Durroux T, Mendre C, Ansanay H*, et al.* (2009). Differential Coupling of the Vasopressin V1b Receptor through Compartmentalization within the Plasma Membrane. *Molecular Pharmacology* **75**(3)**:** 637-647.

Orru M, Bakešová J, Brugarolas M, Quiroz C, Beaumont V, Goldberg SR*, et al.* (2011). Striatal pre-and postsynaptic profile of adenosine A2A receptor antagonists. *PLoS One* **6**(1)**:** e16088.

Padilla-Parra S, Tramier M (2012). FRET microscopy in the living cell: Different approaches, strengths and weaknesses. *BioEssays* **34**(5)**:** 369-376.

Pan X, Ikeda SR, Lewis DL (1996). Rat brain cannabinoid receptor modulates N-type Ca2+ channels in a neuronal expression system. *Mol Pharmacol* **49**(4)**:** 707-714.

Pan X, Ikeda SR, Lewis DL (1998). SR 141716A acts as an inverse agonist to increase neuronal voltage-dependent Ca2+ currents by reversal of tonic CB1 cannabinoid receptor activity. *Mol Pharmacol* **54**(6)**:** 1064-1072.

Park B, Gibbons HM, Mitchell MD, Glass M (2003). Identification of the CB1 Cannabinoid Receptor and Fatty Acid Amide Hydrolase (FAAH) in the Human Placenta. *Placenta* **24**(10)**:** 990-995.

Pellissier LP, Barthet G, Gaven F, Cassier E, Trinquet E, Pin J-P*, et al.* (2011). G Protein Activation by Serotonin Type 4 Receptor Dimers: Evidence that turning on two protomers is more efficient. *Journal of Biological Chemistry* **286**(12)**:** 9985-9997.

Pertwee RG, Howlett AC, Abood ME, Alexander SPH, Di Marzo V, Elphick MR*, et al.* (2010). International Union of Basic and Clinical Pharmacology. LXXIX. Cannabinoid receptors and their ligands: beyond CB1 and CB2. *Pharmacological reviews* **62**(4)**:** 588-631.

Pfeiffer M, Kirscht S, Stumm R, Koch T, Wu D, Laugsch M*, et al.* (2003). Heterodimerization of Substance P and μ-Opioid Receptors Regulates Receptor Trafficking and Resensitization. *The Journal of Biological Chemistry* **278:** 51630-51637.

Pfleger KDG, Eidne KA (2006a). Illuminating insights into protein-protein interactions using bioluminescence resonance energy transfer (BRET). *Nat Meth* **3**(3)**:** 165-174.

Pfleger KDG, Eidne KA (2003). New technologies: bioluminescence resonance energy transfer (BRET) for the detection of real time interactions involving G-protein coupled receptors. *Pituitary* **6**(3)**:** 141-151.

Pfleger KDG, Seeber RM, Eidne KA (2006b). Bioluminescence resonance energy transfer (BRET) for the real-time detection of protein-protein interactions. *Nat. Protocols* **1**(1)**:** 337-345.

Pickel VA, Chan J, Kearn CS, Mackie K (2006). Targeting dopamine D2 and cannabinoid-1 (CB1) receptors in rat nucleus accumbens. *J Comp Neurol* **495**(2)**:** 299-313.

Picone RP, Khanolkar AD, Xu W, Ayotte LA, Thakur GA, Hurst DP*, et al.* (2005). (-)-7′-Isothiocyanato-11-hydroxy-1′, 1′-dimethylheptylhexahydrocannabinol (AM841), a high-affinity electrophilic ligand, interacts covalently with a cysteine in helix six and activates the CB1 cannabinoid receptor. *Molecular pharmacology* **68**(6)**:** 1623-1635.

Pike LJ (2003). Lipid rafts: bringing order to chaos. *Journal of Lipid Research* **44**(4)**:** 655-667.

Pin J, Neubig R, Bouvier M, Devi L, Filizola M, Javitch JA*, et al.* (2007). International Union of Basic and Clinical Pharmacology. LXVII. Recommendations for the recognition and nomenclature of G protein-coupled receptor heteromultimers. *Pharmacol Rev* **59**(1)**:** 5-13.

Pindon A, van Hecke G, van Gompel P, Lesage AS, Leysen JE, Jurzak M (2002). Differences in Signal Transduction of Two 5-HT4Receptor Splice Variants: Compound Specificity and Dual Coupling with Gαs- and Gαi/o-Proteins. *Molecular Pharmacology* **61**(1)**:** 85-96.

Pintor A, Tebano MT, Martire A, Grieco R, Galluzzo M, Scattoni ML*, et al.* (2006). The cannabinoid receptor agonist WIN 55,212-2 attenuates the effects induced by quinolinic acid in the rat striatum. *Neuropharmacology* **51**(5)**:** 1004-1012.

Pontier SM, Percherancier Y, Galandrin S, Breit A, Galés C, Bouvier M (2008). Cholesterol-dependent Separation of the β2-Adrenergic Receptor from Its Partners Determines Signaling Efficacy: Insight into nanoscale organisation of signal transduction. *Journal of Biological Chemistry* **283**(36)**:** 24659-24672.

Price DA, Martinez AA, Seillier A, Koek W, Acosta Y, Fernandez E*, et al.* (2009). WIN55,212-2, a cannabinoid receptor agonist, protects against nigrostriatal cell loss in the 1-methyl-4-phenyl-1,2,3,6-tetrahydropyridine mouse model of Parkinson's disease. *European Journal of Neuroscience* **29**(11)**:** 2177-2186.

Przybyla JA, Watts VJ (2010). Ligand-induced regulation and localization of cannabinoid CB1 and dopamine D2L receptor heterodimers. *J Pharmacol Exp Ther* **332**(3)**:** 710-719.

Qian J, Yao B, Wu C (2014). Fluorescence resonance energy transfer detection methods: Sensitized emission and acceptor bleaching. *Experimental and therapeutic medicine* **8**(5)**:** 1375-1380.

Raaijmakers JH, Bos JL (2009). Specificity in Ras and Rap Signaling. *Journal of Biological Chemistry* **284**(17)**:** 10995-10999.

Ramsay D, Kellett E, McVey M, Rees S, Milligan G (2002). Homo-and hetero-oligomeric interactions between G-protein-coupled receptors in living cells monitored by two variants of bioluminescence resonance energy transfer (BRET): hetero-oligomers between receptor subtypes form more efficiently than between less closely related sequences. *Biochem. J* **365:** 429-440.

Rapoport TA, Jungnickel B, Kutay U (1996). Protein transport across the eukaryotic endoplasmic reticulum and bacterial inner membranes. *Annual review of biochemistry* **65:** 271-303.

Rasmussen SGF, Choi H-J, Rosenbaum DM, Kobilka TS, Thian FS, Edwards PC*, et al.* (2007). Crystal structure of the human beta-2 adrenergic G-protein-coupled receptor. *Nature* **450**(7168)**:** 383-387.

Rasmussen SGF, DeVree BT, Zou Y, Kruse AC, Chung KY, Kobilka TS*, et al.* (2011). Crystal structure of the [bgr]2 adrenergic receptor-Gs protein complex. *Nature* **477**(7366)**:** 549-555.

Rebois RV, Warner DR, Basi NS (1997). Does subunit dissociation necessarily accompany the activation of all heterotrimeric G proteins? *Cellular signalling* **9**(2)**:** 141-151.

Reggio PH, Barnett-Norris J, Hurst DP, Guarnieri F (2002). Global positioning of TMH 3 extracellular end in CB1 receptor is controlled by interplay of two small, polar residues. *Biophysical journal* **82:** 533A-533A.

Reid BG, Flynn GC (1997). Chromophore Formation in Green Fluorescent Protein. *Biochemistry* **36**(22)**:** 6786-6791.

Reiter E, Lefkowitz RJ (2006). GRKs and β-arrestins: roles in receptor silencing, trafficking and signaling. *Trends in Endocrinology & Metabolism* **17**(4)**:** 159-165.

Rhee M-H, Bayewitch M, Avidor-Reiss T, Levy R, Vogel Z (1998). Cannabinoid Receptor Activation Differentially Regulates the Various Adenylyl Cyclase Isozymes. *Journal of Neurochemistry* **71**(4)**:** 1525-1534.

Richter A, Loscher W (2002). Effects of pharmacological manipulations of cannabinoid receptors on severity of dystonia in a genetic model of paroxysmal dyskinesia. *Eur J Pharmacol* **454**(2-3)**:** 145-151.

Richter A, Loscher W (1994). (+)-WIN 55,212-2, a novel cannabinoid receptor agonist, exerts antidystonic effects in mutant dystonic hamsters. *Eur J Pharmacol* **264**(3)**:** 371-377.

Rinaldi-Carmona M, Le Duigou A, Oustric D, Barth F, Bouaboula M, Carayon P*, et al.* (1998). Modulation of CB1 Cannabinoid Receptor Functions after a Long-Term Exposure to Agonist or Inverse Agonist in the Chinese Hamster Ovary Cell Expression System. *Journal of Pharmacology and Experimental Therapeutics* **287**(3)**:** 1038-1047.

Rios C, Gomes I, Devi LA (2006). μ opioid and CB1 cannabinoid receptor interactions: reciprocal inhibition of receptor signaling and neuritogenesis. *British journal of pharmacology* **148**(4)**:** 387-395.

Robbe D, Alonso G, Duchamp F, Bockaert J, Manzoni OJ (2001). Localization and mechanisms of action of cannabinoid receptors at the glutamatergic synapses of the mouse nucleus accumbens. *J Neurosci* **21**(1)**:** 109-116.

Robbe D, Kopf M, Remaury A, Bockaert J, Manzoni OJ (2002). Endogenous cannabinoids mediate long-term synaptic depression in the nucleus accumbens. *Proceedings of the National Academy of Sciences* **99**(12)**:** 8384-8388.

Rodriguez de Fonseca F, Del Arco I, Martin-Calderon JL, Gorriti MA, Navarro M (1998). Role of the endogenous cannabinoid system in the regulation of motor activity. *Neurobiology of disease* **5**(6 Pt B)**:** 483-501.

Romero J, Berrendero F, Perez-Rosado A, Manzanares J, Rojo A, Fernandez-Ruiz JJ*, et al.* (2000). Unilateral 6-hydroxydopamine lesions of nigrostriatal dopaminergic neurons increased CB1 receptor mRNA levels in the caudate-putamen. *Life Sci* **66**(6)**:** 485-494.

Ronesi J, Lovinger DM (2005). Induction of striatal long-term synaptic depression by moderate frequency activation of cortical afferents in rat. *The Journal of Physiology* **562**(1)**:** 245-256.

Rothbauer U, Zolghadr K, Tillib S, Nowak D, Schermelleh L, Gahl A*, et al.* (2006). Targeting and tracing antigens in live cells with fluorescent nanobodies. *Nat Meth* **3**(11)**:** 887-889.

Rozenfeld R, Devi LA (2008). Regulation of CB1 cannabinoid receptor trafficking by the adaptor protein AP-3. *The FASEB Journal* **22**(7)**:** 2311-2322.

Rozenfeld R, Gupta A, Gagnidze K, Lim MP, Gomes I, Less-Ramos D*, et al.* (2011). AT1R-CB1R heteromerization reveals a new mechanism for the pathogenic properties of angiotensin II. *The EMBO Journal***:** 1-14.

Rubino T, Viganò D, Premoli F, Castiglioni C, Bianchessi S, Zippel R*, et al.* (2006). Changes in the expression of G protein-coupled receptor kinases and β-arrestins in mouse brain during cannabinoid tolerance. *Mol Neurobiol* **33**(3)**:** 199-213.

Rubovitch V, Gafni M, Sarne Y (2004). The involvement of VEGF receptors and MAPK in the cannabinoid potentiation of Ca2+ flux into N18TG2 neuroblastoma cells. *Brain Res Mol Brain Res* **120**(2)**:** 138-144.

Rueda D, Galve-Roperh I, Haro A, Guzmán M (2000). The CB1 Cannabinoid Receptor Is Coupled to the Activation of c-Jun N-Terminal Kinase. *Molecular Pharmacology* **58**(4)**:** 814-820.

Ruiz-Llorente L, Sánchez MG, Carmena MJ, Prieto JC, Sánchez-Chapado M, Izquierdo A*, et al.* (2003). Expression of functionally active cannabinoid receptor CB1 in the human prostate gland. *The Prostate* **54**(2)**:** 95-102.

Salahpour A, Barak LS (2011). Visualizing receptor endocytosis and trafficking. *Methods in molecular biology (Clifton, N.J.)* **756:** 311-323.

Salahpour A, Espinoza S, Masri B, Lam V, Barak LS, Gainetdinov RR (2012). BRET biosensors to study GPCR biology, pharmacology, and signal transduction. *Frontiers in Endocrinology* **3:** 105.

Salim K, Fenton T, Bacha J, Urien-Rodriguez H, Bonnert T, Skynner HA*, et al.* (2002). Oligomerization of G-protein-coupled Receptors Shown by Selective Co-immunoprecipitation. *Journal of Biological Chemistry* **277**(18)**:** 15482-15485.

Sanudo-Pena MC, Force M, Tsou K, Miller AS, Walker JM (1998). Effects of intrastriatal cannabinoids on rotational behaviour in rats: interactions with the dopaminergic system. *Synapse* **30:** 221-226.

Sapsford KE, Berti L, Medintz IL (2006). Materials for Fluorescence Resonance Energy Transfer Analysis: Beyond Traditional Donor–Acceptor Combinations. *Angewandte Chemie International Edition* **45**(28)**:** 4562-4589.

Sarfaraz S, Afaq F, Adhami VM, Mukhtar H (2005). Cannabinoid Receptor as a Novel Target for the Treatment of Prostate Cancer. *Cancer Research* **65**(5)**:** 1635-1641.

Schmidt PM, Sparrow LG, Attwood RM, Xiao X, Adams TE, McKimm-Breschkin JL (2012). Taking down the FLAG! How Insect Cell Expression Challenges an Established Tag-System. *PLoS ONE* **7**(6)**:** e37779.

Schneider M, Koch M (2003). Chronic Pubertal, but not Adult Chronic Cannabinoid Treatment Impairs Sensorimotor Gating, Recognition Memory, and the Performance in a Progressive Ratio Task in Adult Rats. *Neuropsychopharmacology* **28**(10)**:** 1760-1769.

Schneider U, Leweke FM, Mueller-Vahl KR, Emrich HM (1998). Cannabinoid/anandamide system and schizophrenia: is there evidence for association? *Pharmacopsychiatry* **31:** 110-113.

Scotter EL, Goodfellow CE, Graham ES, Dragunow M, Glass M (2010). Neuroprotective potential of CB1 receptor agonists in an in vitro model of Huntington's disease. *British Journal of Pharmacology* **160**(3)**:** 747-761.

Seabrook GR, Knowles M, Brown N, Myers J, Sinclair H, Patel S*, et al.* (1994). Pharmacology of high-threshold calcium currents in GH4C1 pituitary cells and their regulation by activation of human D2 and D4 dopamine receptors. *British Journal of Pharmacology* **112**(3)**:** 728-734.

Seeman P, Bzowej NH, Guan HC, Bergeron C, Reynolds GP, Bird ED*, et al.* (1987). Human brain D_1 and D_2 dopamine receptors in schizophrenia, Alzheimer's, Parkinson's, and Huntington's diseases. *Neuropsychopharmacology*.

Seeman P, Van Tol HHM (1994). Dopamine receptor pharmacology. *Trends in Pharmacological Sciences* **15**(7)**:** 264-270.

Sharma M, Celver J, Octeau JC, Kovoor A (2013). Plasma Membrane Compartmentalization of D2 Dopamine Receptors. *Journal of Biological Chemistry* **288**(18)**:** 12554-12568.

Shi C, Szczesniak A, Mao L, Jollimore C, Coca-Prados M, Hung O*, et al.* (2003). A3 adenosine and CB1 receptors activate a PKC-sensitive Cl- current in human nonpigmented ciliary epithelial cells via a G beta gamma-coupled MAPK signaling pathway. *Br J Pharmacol* **139**(3)**:** 475-486.

Shi L, Simpson MM, Ballesteros JA, Javitch JA (2001). The first transmembrane segment of the dopamine D2 receptor: accessibility in the binding-site crevice and position in the transmembrane bundle. *Biochemistry* **40**(41)**:** 12339.

Shonberg J, Scammells PJ, Capuano B (2011). Design Strategies for Bivalent Ligands Targeting GPCRs. *ChemMedChem* **6**(6)**:** 963-974.

Sidhu A, Niznik HB (2000). Coupling of dopamine receptor subtypes to multiple and diverse G proteins. *International Journal of Developmental Neuroscience* **18**(7)**:** 669-677.

Siegling A, Hofmann HA, Denzer D, Mauler F, De Vry J (2001). Cannabinoid CB1 receptor upregulation in a rat model of chronic neuropathic pain. *European Journal of Pharmacology* **415**(1)**:** R5-R7.

Sieradzan KA, Fox SH, Hill M, Dick JP, Crossman AR, Brotchie JM (2001). Cannabinoids reduce levodopa-induced dyskinesia in Parkinson's disease: a pilot study. *Neurology* **57**(11)**:** 2108-2111.

Skinbjerg M, Ariano MA, Thorsell A, Heilig M, Halldin C, Innis RB*, et al.* (2009). Arrestin3 Mediates D(2) Dopamine Receptor Internalization. *Synapse (New York, N.Y.)* **63**(7)**:** 621-624.

Skosnik PD, Spatz-Glenn L, Park S (2001). Cannabis use is associated with schizotypy and attentional disinhibition. *Schizophrenia research* **48**(1)**:** 83-92.

So CH, Varghese G, Curley KJ, Kong MMC, Alijaniaram M, Ji X*, et al.* (2005). D1 and D2 dopamine receptors form heterooligomers and cointernalize after selective activation of either receptor. *Molecular pharmacology* **68**(3)**:** 568-578.

Song Z-H, Bonner TI (1996). A lysine residue of the cannabinoid receptor is critical for receptor recognition by several agonists but not WIN55212-2. *Molecular pharmacology* **49**(5)**:** 891-896.

Stryer L (1978). Fluorescence energy transfer as a spectroscopic ruler. *Annual review of biochemistry* **47:** 819-846.

Surmeier DJ, Kitai ST (1993). D 1 and D 2 dopamine receptor modulation of sodium and potassium currents in rat neostriatal neurons. *Progress in brain research* **99:** 309-324.

Suzuki N, Nakamura S, Mano H, Kozasa T (2003). Galpha 12 activates Rho GTPase through tyrosine-phosphorylated leukemia-associated RhoGEF. *Proc Natl Acad Sci U S A* **100**(2)**:** 733-738.

Svenningsson P, Fredholm BB, Bloch B, Le Moine C (2000). Co-stimulation of D(1)/D(5) and D(2) dopamine receptors leads to an increase in c-fos messenger RNA in cholinergic interneurons and a redistribution of c-fos messenger RNA in striatal projection neurons. *Neuroscience* **98**(4)**:** 749-757.

Szabo B, Nordheim U, Niederhoffer N (2001). Effects of cannabinoids on sympathetic and parasympathetic neuroeffector transmission in the rabbit heart. *J Pharmacol Exp Ther* **297**(2)**:** 819-826.

Szalai B, Hoffmann P, Prokop S, Erdélyi L, Várnai P, Hunyady L (2014). Improved Methodical Approach for Quantitative BRET Analysis of G Protein Coupled Receptor Dimerization. *PloS one* **9**(10)**:** e109503.

Takahashi H, Higuchi M, Suhara T (2006). The Role of Extrastriatal Dopamine D2 Receptors in Schizophrenia. *Biological Psychiatry* **59**(10)**:** 919-928.

Tan JHY, Ludeman JP, Wedderburn J, Canals M, Hall P, Butler SJ*, et al.* (2013). Tyrosine Sulfation of Chemokine Receptor CCR2 Enhances Interactions with Both Monomeric and Dimeric Forms of the Chemokine Monocyte Chemoattractant Protein-1 (MCP-1). *Journal of Biological Chemistry* **288**(14)**:** 10024-10034.

Tan S, Hermann B, Borrelli E (2003). Dopaminergic mouse mutants: investigating the roles of the different dopamine receptor subtypes and the dopamine transporter. *International review of neurobiology***:** 146-199.

Tappe-Theodor A, Agarwal N, Katona I, Rubino T, Martini L, Swiercz J*, et al.* (2007). A Molecular Basis of Analgesic Tolerance to Cannabinoids. *The Journal of Neuroscience* **27**(15)**:** 4165-4177.

Tatake RJ, O'Neill MM, Kennedy CA, Wayne AL, Jakes S, Wu D*, et al.* (2008). Identification of pharmacological inhibitors of the MEK5/ERK5 pathway. *Biochemical and Biophysical Research Communications* **377**(1)**:** 120-125.

Taylor SS, Yang J, Wu J, Haste NM, Radzio-Andzelm E, Anand G (2004). PKA: a portrait of protein kinase dynamics. *Biochimica et Biophysica Acta (BBA) - Proteins and Proteomics* **1697**(1–2)**:** 259-269.

Tena-Campos M, Ramon E, Rivera D, O Borroto-Escuela D, Romero-Fernandez W, Fuxe K*, et al.* (2014). G-Protein-Coupled Receptors Oligomerization: Emerging Signaling Units and New Opportunities for Drug Design. *Current Protein and Peptide Science* **15**(7)**:** 648-658.

Terrillon S, Barberis C, Bouvier M (2004). Heterodimerization of V1a and V2 vasopressin receptors determines the interaction with β-arrestin and their trafficking patterns. *PNAS* **101**(6)**:** 1548-1553.

Terrillon S, Durroux T, Mouillac B, Breit A, Ayoub MA, Taulan M*, et al.* (2003). Oxytocin and Vasopressin V1a and V2 Receptors Form Constitutive Homo- and Heterodimers during Biosynthesis. *Molecular Endocrinology* **17**(4)**:** 677-691.

Thibonnier M, Preston JA, Dulin N, Wilkins PL, Berti-Mattera LN, Mattera R (1997). The Human V3 Pituitary Vasopressin Receptor: Ligand Binding Profile and Density-Dependent Signaling Pathways 1. *Endocrinology* **138**(10)**:** 4109-4122.

Thompson D, Pusch M, Whistler JL (2007). Changes in G Protein-coupled Receptor Sorting Protein Affinity Regulate Postendocytic Targeting of G Protein-coupled Receptors. *Journal of Biological Chemistry* **282**(40)**:** 29178-29185.

Trejo J (2014). Ubiquitin and intracellular signaling by G protein-coupled receptors (354.2). *The FASEB Journal* **28**(1 Supplement).

Trifilieff P, Rives M-L, Urizar E, Piskorowski RA, Vishwasrao HD, Castrillon J*, et al.* (2011). Detection of antigen interactions ex vivo by proximity ligation assay: endogenous dopamine D2-adenosine A2A receptor complexes in the striatum. *BioTechniques* **51**(2)**:** 111-118.

Tucek S, Michal P, Vlachova V (2001). Dual effects of muscarinic M2 receptors on the synthesis of cyclic AMP in CHO cells: Background and model. *Life Sciences* **68**(22–23)**:** 2501-2510.

Turu G, Hunyady L (2010). Signal transduction of the CB1 cannabinoid receptor. *J Mol Endocrinol* **44:** 75-85.

Twitchell W, Brown S, Mackie K (1997). Cannabinoids inhibit N- and P/Q-type calcium channels in cultured rat hippocampal neurons. *Journal of neurophysiology* **78**(1)**:** 43-50.

Tyrrell J, Hurst D, Reggio PH (2008). Modeling studies of the CB1/dopamine D2short heterodimer using correlated mutation analysis. In: *Symposium on the Cannabinoids*. Scotland.

Uhlen M, Oksvold P, Fagerberg L, Lundberg E, Jonasson K, Forsberg M*, et al.* (2010). Towards a knowledge-based Human Protein Atlas. *Nat Biotech* **28**(12)**:** 1248-1250.

Urigüen L, García-Fuster MJ, Callado L, Morentin B, La Harpe R, Casadó V*, et al.* (2009). Immunodensity and mRNA expression of A2A adenosine, D2 dopamine, and CB1 cannabinoid receptors in postmortem frontal cortex of subjects with schizophrenia: effect of antipsychotic treatment. *Psychopharmacology* **206**(2)**:** 313-324.

Valdeolivas S, Satta V, Pertwee RG, Fernandez-Ruiz J, Sagredo O (2012). Sativex-like combination of phytocannabinoids is neuroprotective in malonate-lesioned rats, an inflammatory model of Huntington's disease: role of CB1 and CB2 receptors. *ACS chemical neuroscience* **3**(5)**:** 400-406.

Van Laere K, Casteels C, Dhollander I, Goffin K, Grachev I, Bormans G*, et al.* (2010). Widespread decrease of type 1 cannabinoid receptor availability in Huntington disease in vivo. *Journal of nuclear medicine : official publication, Society of Nuclear Medicine* **51**(9)**:** 1413-1417.

Veatch W, Stryer L (1977). The dimeric nature of the gramicidin A transmembrane channel: Conductance and fluorescence energy transfer studies of hybrid channels. *Journal of Molecular Biology* **113**(1)**:** 89-102.

Venkatakrishnan AJ, Deupi X, Lebon G, Tate CG, Schertler GF, Babu MM (2013). Molecular signatures of G-protein-coupled receptors. *Nature* **494**(7436)**:** 185-194.

Vickery RG, von Zastrow M (1999). Distinct Dynamin-dependent and -independent Mechanisms Target Structurally Homologous Dopamine Receptors to Different Endocytic Membranes. *The Journal of Cell Biology* **144**(1)**:** 31-43.

Vischer HF, Nijmeijer S, Smit MJ, Leurs R (2008). Viral hijacking of human receptors through heterodimerization. *Biochemical and Biophysical Research Communications* **377**(1)**:** 93-97.

Vistein R, Puthenveedu MA (2013). Reprogramming of G protein-coupled receptor recycling and signaling by a kinase switch. *Proceedings of the National Academy of Sciences* **110**(38)**:** 15289-15294.

Voruganti LN, Slomka P, Zabel P, Mattar A, Awad AG (2001). Cannabis induced dopamine release: an in-vivo SPECT study. *Psychiatry research* **107**(3)**:** 173-177.

Wade DT, Collin C, Stott C, Duncombe P (2010). Meta-analysis of the efficacy and safety of Sativex (nabiximols), on spasticity in people with multiple sclerosis. *Multiple Sclerosis* **16**(6)**:** 707-714.

Wager-Miller J, Westenbroek R, Mackie K (2002). Dimerization of G protein-coupled receptors: CB1 cannabinoid receptors as an example. *Chem Phys Lipids* **121**(1-2)**:** 83-89.

Wagner JA, Járai Z, Bátkai S, Kunos G (2001). Hemodynamic effects of cannabinoids: coronary and cerebral vasodilation mediated by cannabinoid CB1 receptors. *European Journal of Pharmacology* **423**(2–3)**:** 203-210.

Wang S, Lim G, Mao J, Sung B, Yang L, Mao J (2007). Central glucocorticoid receptors regulate the upregulation of spinal cannabinoid-1 receptors after peripheral nerve injury in rats. *Pain* **131**(1–2)**:** 96-105.

Wang Y, Xu R, Sasaoka T, Tonegawa S, Kung M-P, Sankoorikal E-B (2000). Dopamine D2 Long Receptor-Deficient Mice Display Alterations in Striatum-Dependent Functions. *The Journal of Neuroscience* **20**(22)**:** 8305-8314.

Ward RJ, Pediani JD, Milligan G (2011). Heteromultimerization of cannabinoid CB1 receptor and orexin OX1 receptor generates a unique complex in which both protomers are regulated by orexin A. *Journal of Biological Chemistry* **286**(43)**:** 37414-37428.

Ware MA, Daeninck P, Maida V (2008). A review of nabilone in the treatment of chemotherapy-induced nausea and vomiting. *Therapeutics and Clinical Risk Management* **4**(1)**:** 99-107.

Watts VJ, Wiens BL, Cumbay MG, Vu MN, Neve RL, Neve KA (1998). Selective Activation of Gαo by D2LDopamine Receptors in NS20Y Neuroblastoma Cells. *The Journal of Neuroscience* **18**(21)**:** 8692-8699.

Whorton MR, Bokoch MP, Rasmussen SGF, Huang B, Zare RN, Kobilka B*, et al.* (2007). A monomeric G protein-coupled receptor isolated in a high-density lipoprotein particle efficiently activates its G protein. *Proceedings of the National Academy of Sciences* **104**(18)**:** 7682-7687.

Whorton MR, Jastrzebska B, Park PSH, Fotiadis D, Engel A, Palczewski K*, et al.* (2008). Efficient Coupling of Transducin to Monomeric Rhodopsin in a Phospholipid Bilayer. *Journal of Biological Chemistry* **283**(7)**:** 4387-4394.

Wiley JL, Kendler SH, Burston JJ, Howard DR, Selley DE, Sim-Selley LJ (2008). Antipsychotic-induced alterations in CB1 receptor-mediated G-protein signaling and in vivo pharmacology in rats. *Neuropharmacology* **55**(7)**:** 1183-1190.

Wilson RI, Nicoll RA (2001). Endogenous cannabinoids mediate retrograde signalling at hippocampal synapses. *Nature* **410**(6828)**:** 588-592.

Wolber PK, Hudson BS (1979). An analytic solution to the Förster energy transfer problem in two dimensions. *Biophysical Journal* **28**(2)**:** 197-210.

Wu B, Chien EYT, Mol CD, Fenalti G, Liu W, Katritch V*, et al.* (2010). Structures of the CXCR4 Chemokine GPCR with Small-Molecule and Cyclic Peptide Antagonists. *Science* **330**(6007)**:** 1066-1071.

Wu H, Wacker D, Mileni M, Katritch V, Han GW, Vardy E*, et al.* (2012). Structure of the human kappa-opioid receptor in complex with JDTic. *Nature* **485**(7398)**:** 327-332.

Wu PG, Brand L (1994). Resonance Energy Transfer: Methods and Applications. *Analytical Biochemistry* **218**(1)**:** 1-13.

Wu Y-C, Lai H-L, Chang W-C, Lin J-T, Liu Y-J, Chern Y (2013). A novel Gαs-binding protein, Gas-2 like 2, facilitates the signaling of the A2A adenosine receptor. *Biochimica et Biophysica Acta (BBA) - Molecular Cell Research* **1833**(12)**:** 3145-3154.

Xia Z, Dickens M, Raingeaud J, Davis RJ, Greenberg ME (1995). Opposing effects of ERK and JNK-p38 MAP kinases on apoptosis. *Science* **270**(5240)**:** 1326-1331.

Xie Z, Bhushan RG, Daniels DJ, Portoghese PS (2005). Interaction of bivalent ligand KDN21 with heterodimeric d-k opioid receptors in human embryonic kidney 293 cells. *Mol Pharmacol* **68**(4)**:** 1079-1086.

Xu C, Peter M, Bouquier N, Ollendorff V, Villamil I, Liu J*, et al.* (2013). REV, a BRET-based sensor of ERK activity. *Frontiers in Endocrinology* **4**.

Xu X, Liu Y, Huang S, Liu G, Xie C, Zhou J*, et al.* (2006). Overexpression of cannabinoid receptors CB1 and CB2 correlates with improved prognosis of patients with hepatocellular carcinoma. *Cancer Genetics and Cytogenetics* **171**(1)**:** 31-38.

Yamada M, Inanobe A, Kurachi Y (1998). G protein regulation of potassium ion channels. *Pharmacol Rev* **50**(4)**:** 723-760.

Yan Z, Song W-J, Surmeier DJ (1997). D2 dopamine receptors reduce N-type Ca2+ currents in rat neostriatal cholinergic interneurons through a membrane-delimited, protein-kinase-C-insensitive pathway. *Journal of neurophysiology* **77**(2)**:** 1003-1015.

Yasuda S-i, Ishida J (2014). GPR39-1b, the 5-transmembrane isoform of GPR39 interacts with neurotensin receptor NTSR1 and modifies its function. *Journal of Receptors and Signal Transduction* **34**(4)**:** 307-312.

Yasuno F, Suhara T, Okubo Y, Sudo Y, Inoue M, Ichimiya T*, et al.* (2014). Low dopamine D2 receptor binding in subregions of the thalamus in schizophrenia.

Yoshida T, Hashimoto K, Zimmer A, Maejima T, Araishi K, Kano M (2002). The cannabinoid CB1 receptor mediates retrograde signals for depolarization-induced suppression of inhibition in cerebellar Purkinje cells. *J Neurosci* **22**(5)**:** 1690-1697.

Zadikoff C, Wadia PM, Miyasaki J, Chen R, Lang AE, So J*, et al.* (2011). Cannabinoid, CB1 agonists in cervical dystonia: Failure in a phase IIa randomized controlled trial. *Basal Ganglia* **1**(2)**:** 91-95.

Zajicek J, Fox P, Sanders H, Wright D, Vickery J, Nunn A*, et al.* (2003). Cannabinoids for treatment of spasticity and other symptoms related to multiple sclerosis (CAMS study): multicentre randomised placebo-controlled trial. *Lancet* **362**(9395)**:** 1517-1526.

Zalduegui A, López de Jesús M, Callado LF, Meana JJ, Sallés J (2011). Levels of Gsα(short and long), Gαolf and Gβ(common) subunits, and calcium-sensitive adenylyl cyclase isoforms (1, 5/6, 8) in post-mortem human brain caudate and cortical membranes: Comparison with rat brain membranes and potential stoichiometric relationships. *Neurochemistry International* **58**(2)**:** 180-189.

Zamberletti E, Viganò D, Guidali C, Rubino T, Parolaro D (2012). *Long-lasting recovery of psychotic-like symptoms in isolation-reared rats after chronic but not acute treatment with the cannabinoid antagonist AM251*. edn, vol. 15.

Zhan X, Kook S, Gurevich E, Gurevich V (2014). Arrestin-Dependent Activation of JNK Family Kinases. In: Gurevich VV (ed)^(eds). *Arrestins - Pharmacology and Therapeutic Potential*, edn, Vol. 219: Springer Berlin Heidelberg. p^pp 259-280.

Zhang X, Liu J, Jiang D (2014). Why is dimerization essential for class-C GPCR function? New insights from mGluR1 crystal structure analysis. *Protein Cell* **5**(7)**:** 492-495.

Zhao Y, Terry D, Shi L, Weinstein H, Blanchard SC, Javitch JA (2010). Single-molecule dynamics of gating in a neurotransmitter transporter homologue. *Nature* **465**(7295)**:** 188-193.

Zhou XB, Lutz S, Steffens F, Korth M, Wieland T (2007). Oxytocin receptors differentially signal via Gq and Gi proteins in pregnant and nonpregnant rat uterine myocytes: implications for myometrial contractility. *Molecular endocrinology (Baltimore, Md.)* **21**(3)**:** 740-752.

Zoppi S, Perez Nievas BG, Madrigal JLM, Manzanares J, Leza JC, Garcia-Bueno B (2011). Regulatory Role of Cannabinoid Receptor 1 in Stress-Induced Excitotoxicity and Neuroinflammation. *Neuropsychopharmacology* **36**(4)**:** 805-818.